



The Abdus Salam
International Centre for Theoretical Physics



2165-3

**International MedCLIVAR-ICTP-ENEA Summer School on the
Mediterranean Climate System and Regional Climate Change**

13 - 22 September 2010

Intro: Introduction to Mediterranean circulation and climate

ARTALE Vincenzo

E.N.E.A.

Cre Casaccia, via Anguillarese 301

Santa Maria di Galeria, 00123

Roma

ITALY



Introduction to Mediterranean circulation and climate

by

Vincenzo Artale *
ENEA

**Unita Tecnica Modellistica Energetica Ambientale
(UTMEA)**

CR Casaccia, Rome (Italy)

<http://clima.casaccia.enea.it/staff/artale>

**in collaboration with V. Rupolo, R. Iacono, E. Napolitano, G.M. Sannino, A. Carillo
ENEA-UTMEA-CLIM.*

**Trieste 13-22 september 2010, International MedCLIVAR-ICTP-ENEA
Summer School on the Mediterranean Climate System and Regional Climate Change**



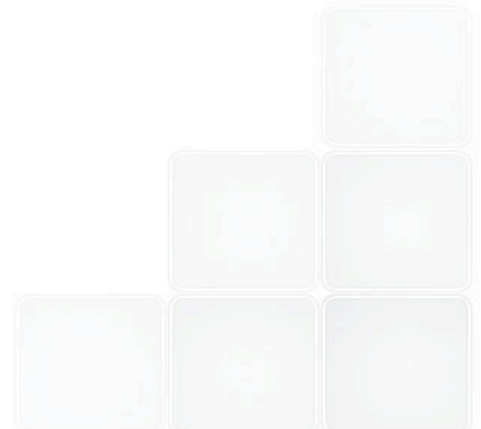
The Abdus Salam
International Centre for Theoretical Physics



Lecture index



- ✓ Ocean variability and its stability
- ✓ Wind circulation of the Mediterranean sea
- ✓ Mediterranean Thermohaline circulation
- ✓ Deep water formation, precondition phase
- ✓ Role of the coherent structures, gyres, fronts and eddies in the Mediterranean Circulation
- ✓ Diffusion, lagrangian diffusion
- ✓ Multiple equilibria, natural variability, and EMT



Role of the ocean in climate

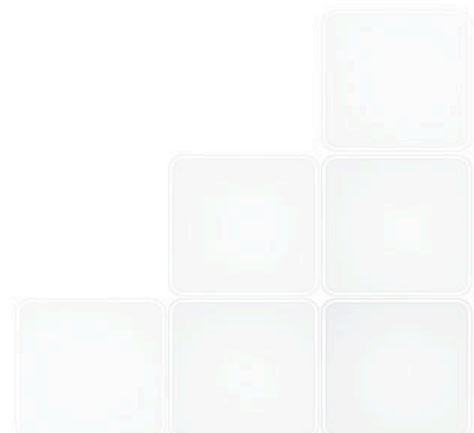


Main roles:

- ✓ Storage and transport of heat
- ✓ Storage and transport of CO₂
- ✓ Production of Cloud Condensation Nuclei
- ✓ Ocean/ice sheet interactions

Other potentially important roles:

- ✓ Methane hydrate release
- ✓ Production of N₂O



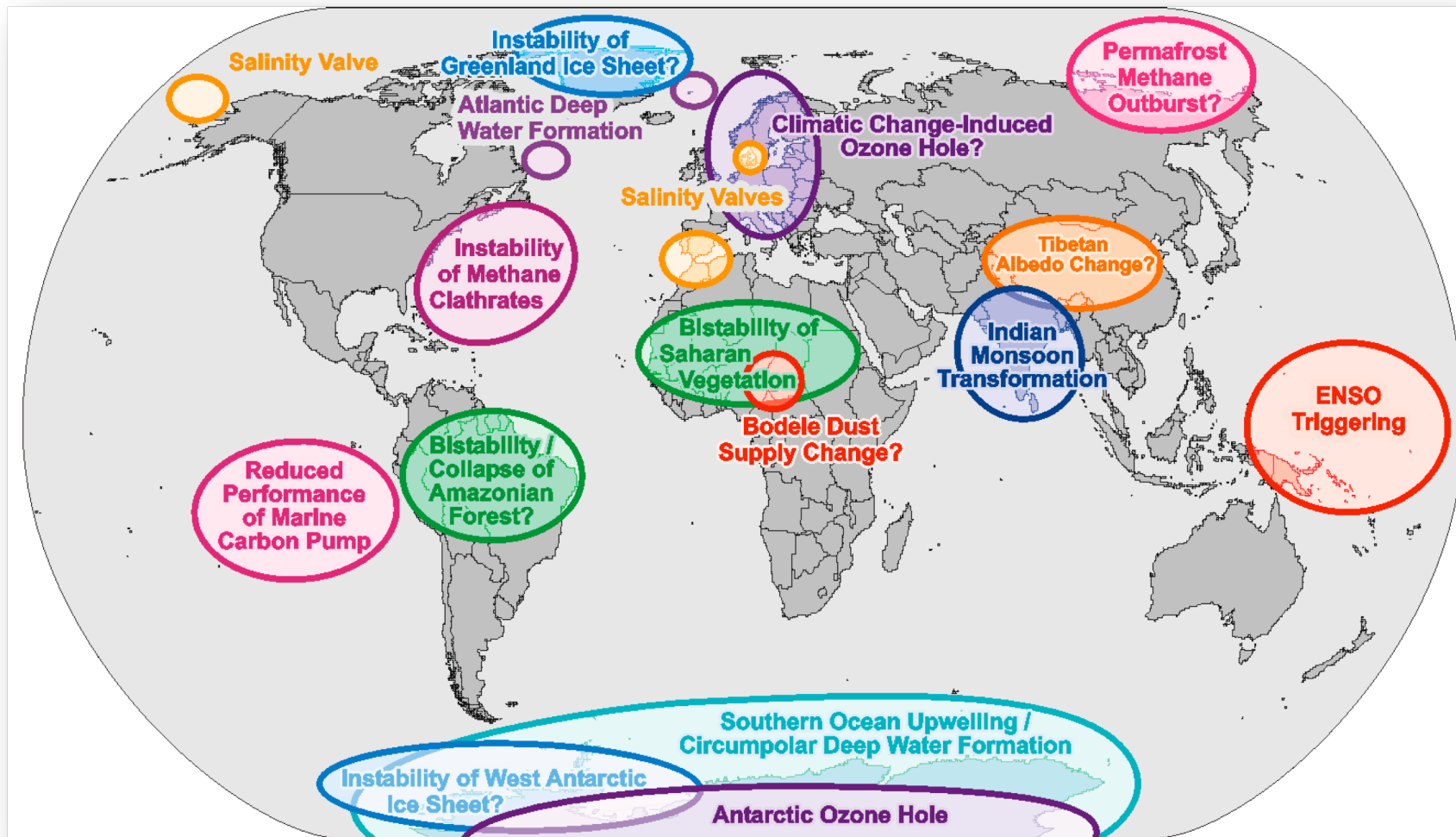
Ocean climate variability



- Instrumental records of increasing duration and spatial coverage document substantial variability in the path and intensity of ocean characteristics on timescales of months to decades: **oscillations or trends?**
- The oceanic variability at interannual, interdecadal, and multi-decadal scale plays a key role in climate variability and climate change.
- Some observed variability can be clearly related to forcing mechanisms, but for many other the mechanism is less clear. In fact, even if the external forcing were constant in time the climate system display variability on many timescales.
- Processes internal to the climate system can thus give rise to spectral peaks that are not related directly to the temporal variability of the forcing

Tipping Points in the Earth System

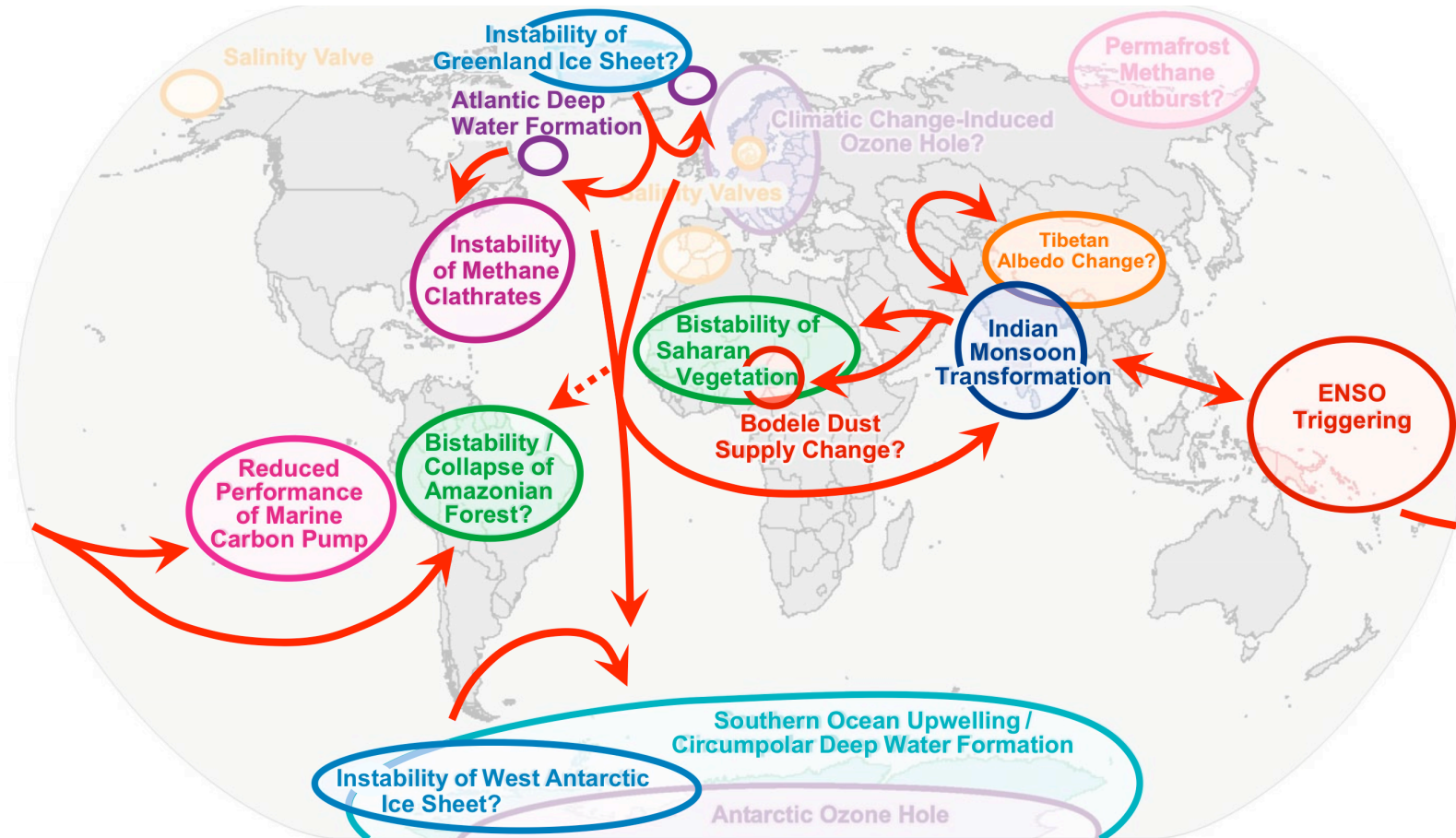
where a small change in forcing causes a qualitative change in their future state



From Schellnhuber et al., PNAS, 2008

See also Lenton, T. M. et al., Tipping Elements in the Earth's Climate System. *Proceedings of the National Academy of Science* **105** (6), 1786 (2008). Kreigler, E. et al., Imprecise probability assessment of tipping points in the climate system. *Proceedings of the National Academy of Science* (2009).

Teleconnections and Feedbacks



Mediterranean climate

(it's relevant for climate studies?)



- The Mediterranean is located in a transitional zone where mid-latitude and tropical variability are both important and compete
- The northern part of the Mediterranean region presents a Maritime west coastal climate while the southern part is characterized by a Subtropical desert climate
- in summer is exposed to South Asian Monsoon and the Siberian high pressure system in winter
- The southern part is mostly under the influence of the descending branch of the Hadley cell, while the northern is more linked to NAO and other mid-latitude teleconnections patterns

The hydrological Mediterranean cycle

(The closure depends on the Gibraltar Strait !!)



- In the Mediterranean P has an annual mean ranging from 331 to 477 mm yr-1, with a maximum of 700 mm yr-1.
 - Evaporation is estimated in the range of 934–1176 mm yr-1 with a maximum of 1000 mm yr-1.
 - The E-P gives an annual mean Mediterranean Sea water loss from 500 to 700 mm yr-1.
- The annual mean river discharge is 100 mm yr-1.
 - **The estimated Mediterranean freshwater deficit of about 500 mm yr-1, consistent with the water flux at the Gibraltar Strait of about 1 Sv**

closure of the Mediterranean hydrological cycle

(from Mariotti et al., 2002)

The main components of the Mediterranean Sea hydrological cycle are shown in the schematic two-box diagram of Fig. 1. The time-varying equation for the vertically integrated atmospheric water budget is

$$\frac{dW}{dt} = E - P - D, \quad (1)$$

where W is the total water vapor content, P is precipitation, E evaporation, and D is the vertically integrated moisture divergence:

$$D = \nabla \cdot \mathbf{Q}, \quad \mathbf{Q} \equiv \int_0^H \mathbf{V} q \, dz.$$

Here \mathbf{Q} is the vertically integrated atmospheric moisture flux (\mathbf{V} is the wind, q is atmospheric specific humidity, and H is the height in meters). On an annual mean basis the lhs of Eq. (1) can be neglected and the atmospheric water budget equation is approximately

$$E - P \approx D. \quad (2)$$

Here we have also neglected the analysis error (Schubert et al. 1993) that for NCEP reanalyses is at most about 25% of the annual mean D . The time-varying equation for the total Mediterranean Sea water content M is

$$\frac{dM}{dt} = G + B + R - D, \quad (3)$$

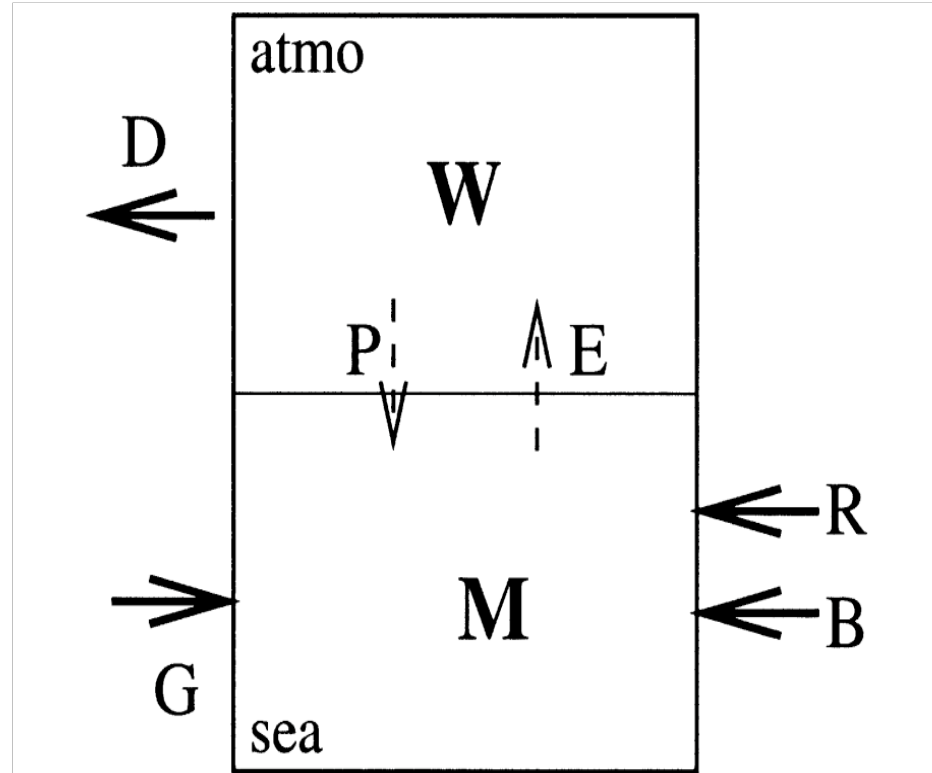
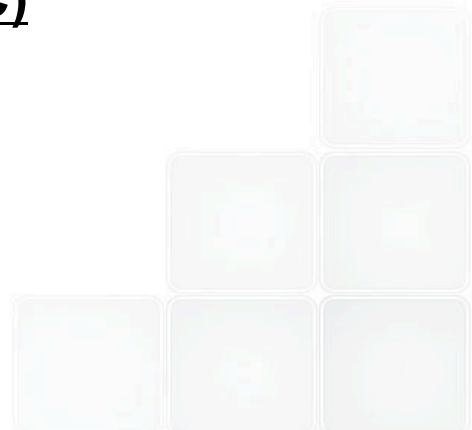


FIG. 1. A schematic two-box diagram illustrating the main components of the Mediterranean Sea hydrological cycle. M and W are the total Mediterranean atmospheric and oceanic water content, respectively. P is precipitation, E evaporation, D the atmospheric moisture divergence, R the Mediterranean river discharge, B and G are the total water fluxes from the Black Sea and the Gibraltar Strait, respectively.

Role of the Mediterranean at global scale



- as heat reservoir and source of moisture for surrounding land areas
- as source of energy and latent heat for cyclone development and its possible effect on remote areas, such as Sahel region
- **on the Atlantic overturning circulation (MOC)**

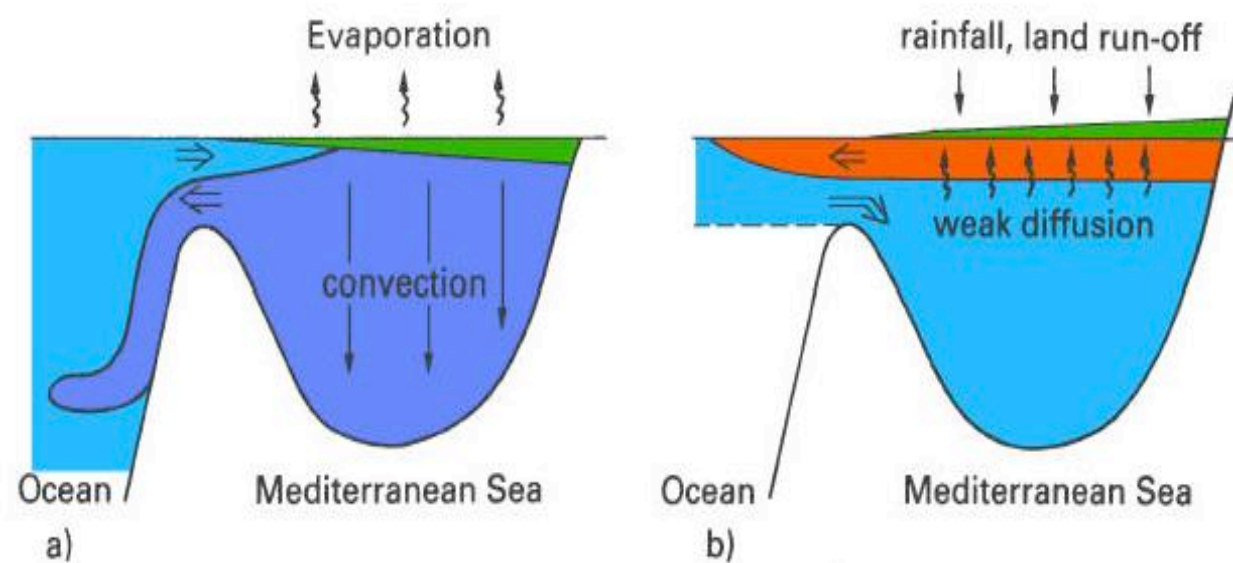


Mediterranean thermohaline circulation



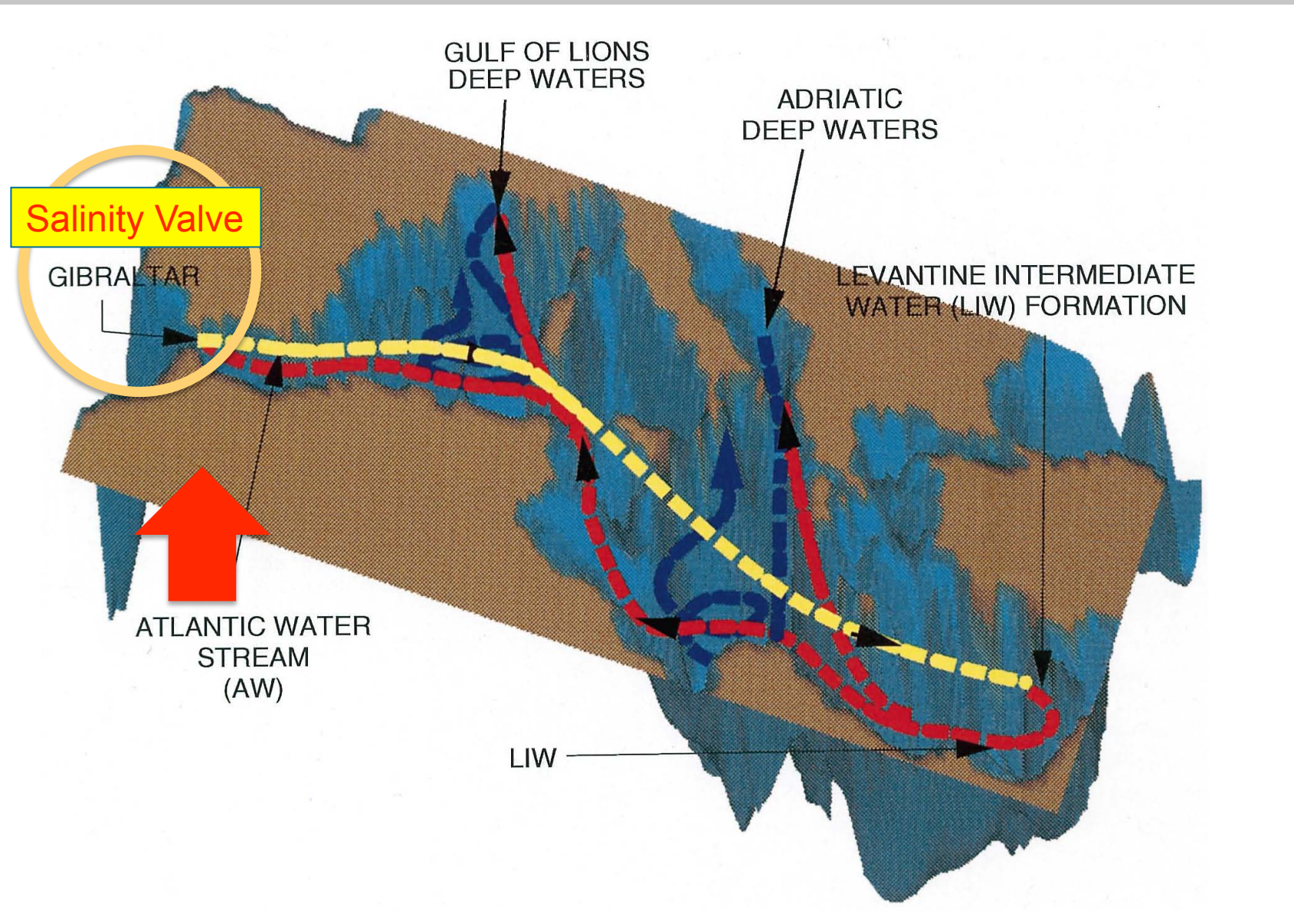
- the basin-scale circulation is composed by three major thermohaline circulation : the first is “open” zonal circulation that connects the western to the eastern part of the basin; the others two are meridional cells confined to the western and eastern basin
- the driving force is derived by air-sea interaction that determines localized convection processes
- the western and eastern sub-basins are disconnected at deep levels and their thermohaline circulation are driven by the respective sources. The eastern is a closed cell endowed with multiple equilibrium (EMT), in the western sub-basin observational and modeling studies are lacking

Functioning of the Mediterranean Sea

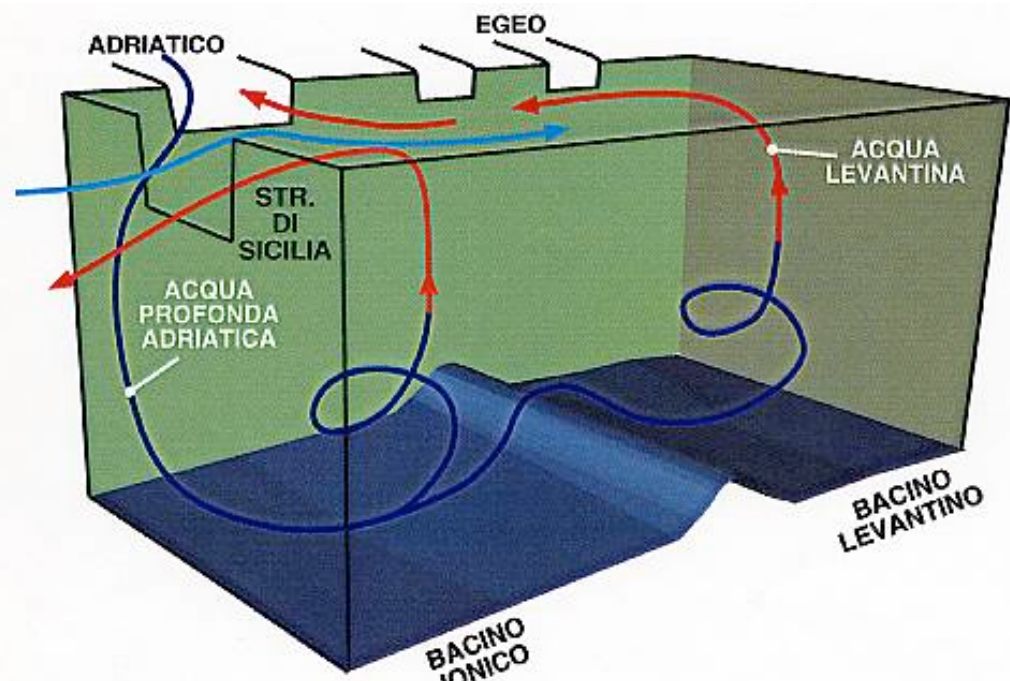
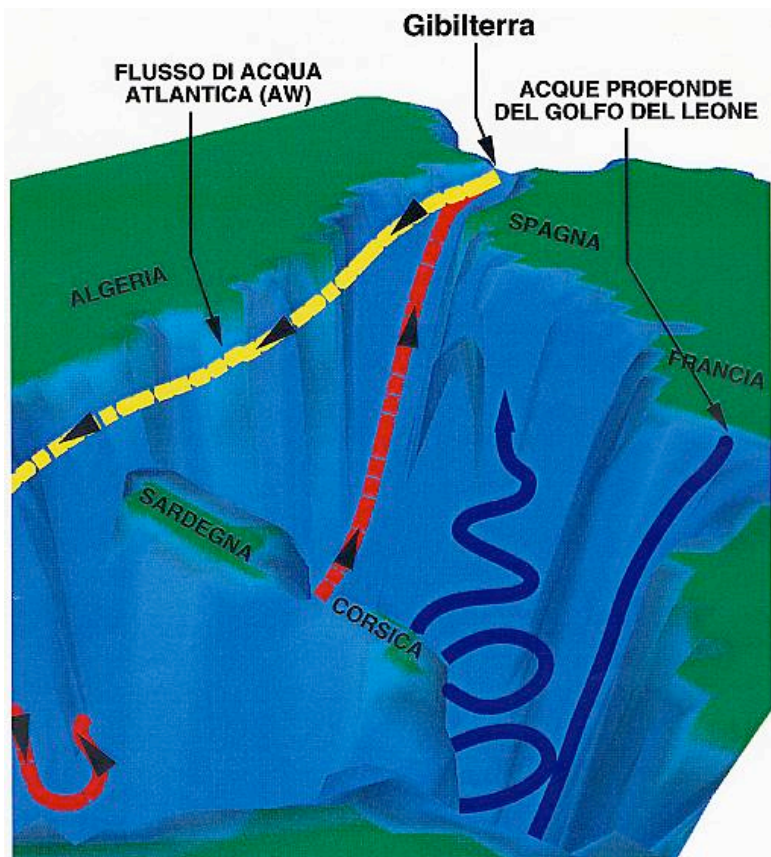


Schematic illustration of the circulation in mediterranean seas; (a) with negative precipitation - evaporation balance, (b) with positive precipitation - evaporation balance.

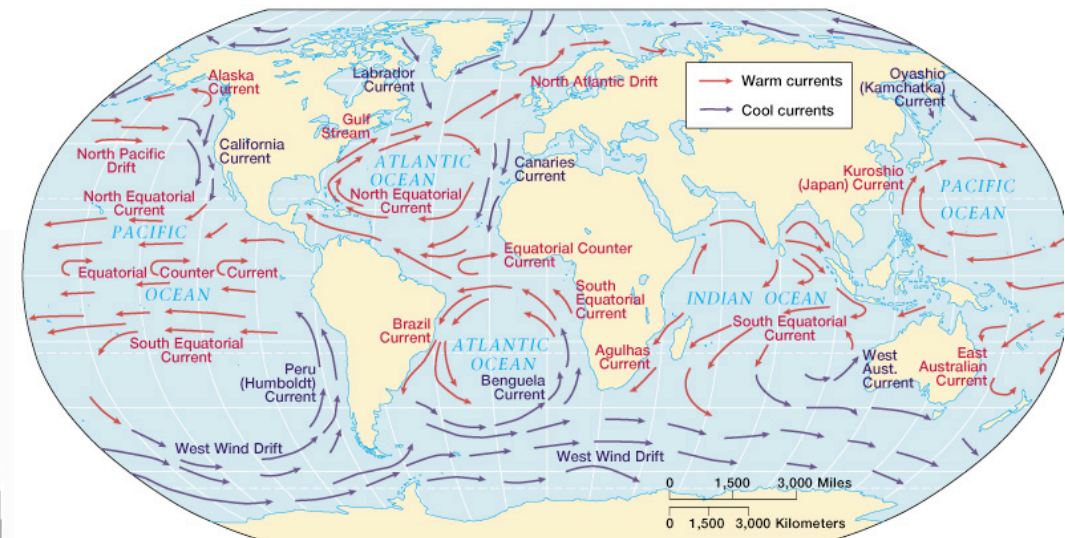
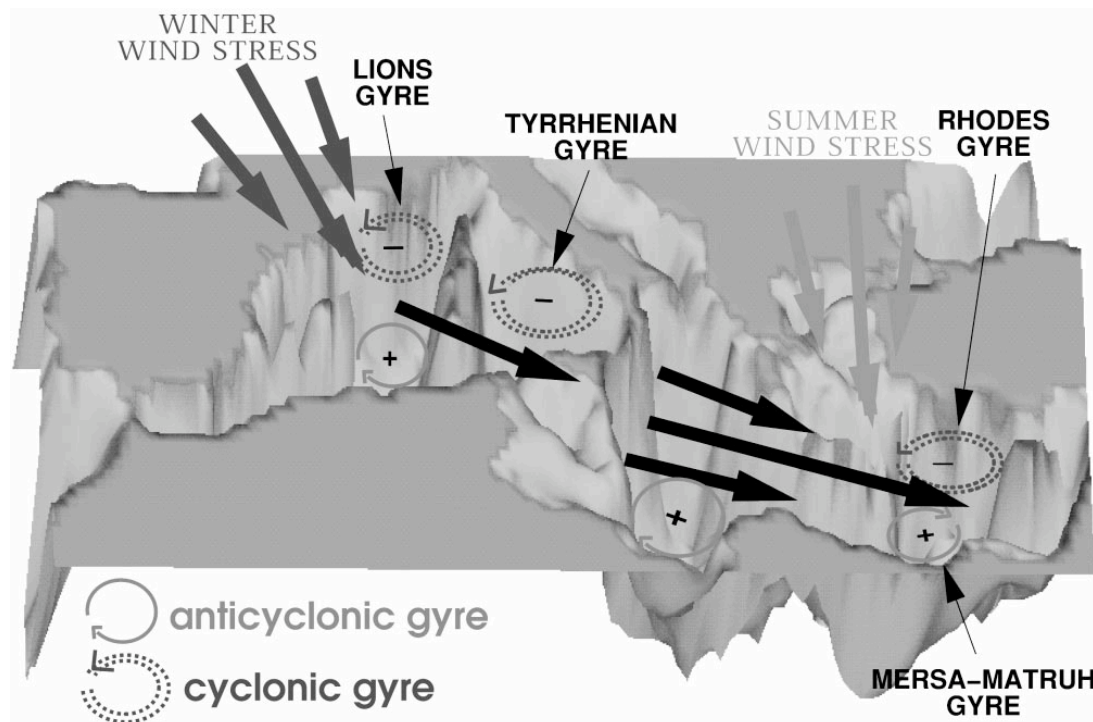
Mediterranean Thermohaline Circulation



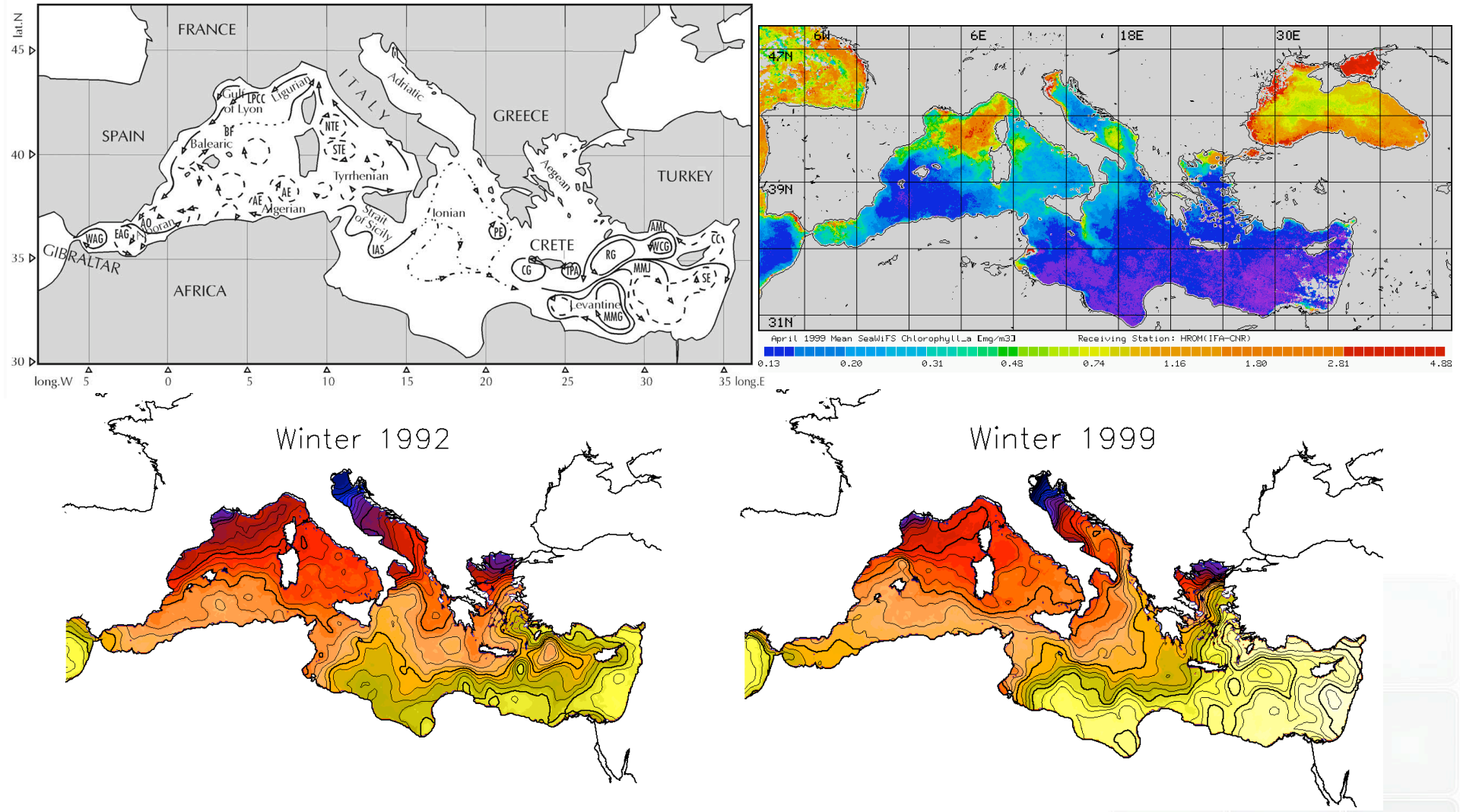
West and east circulation



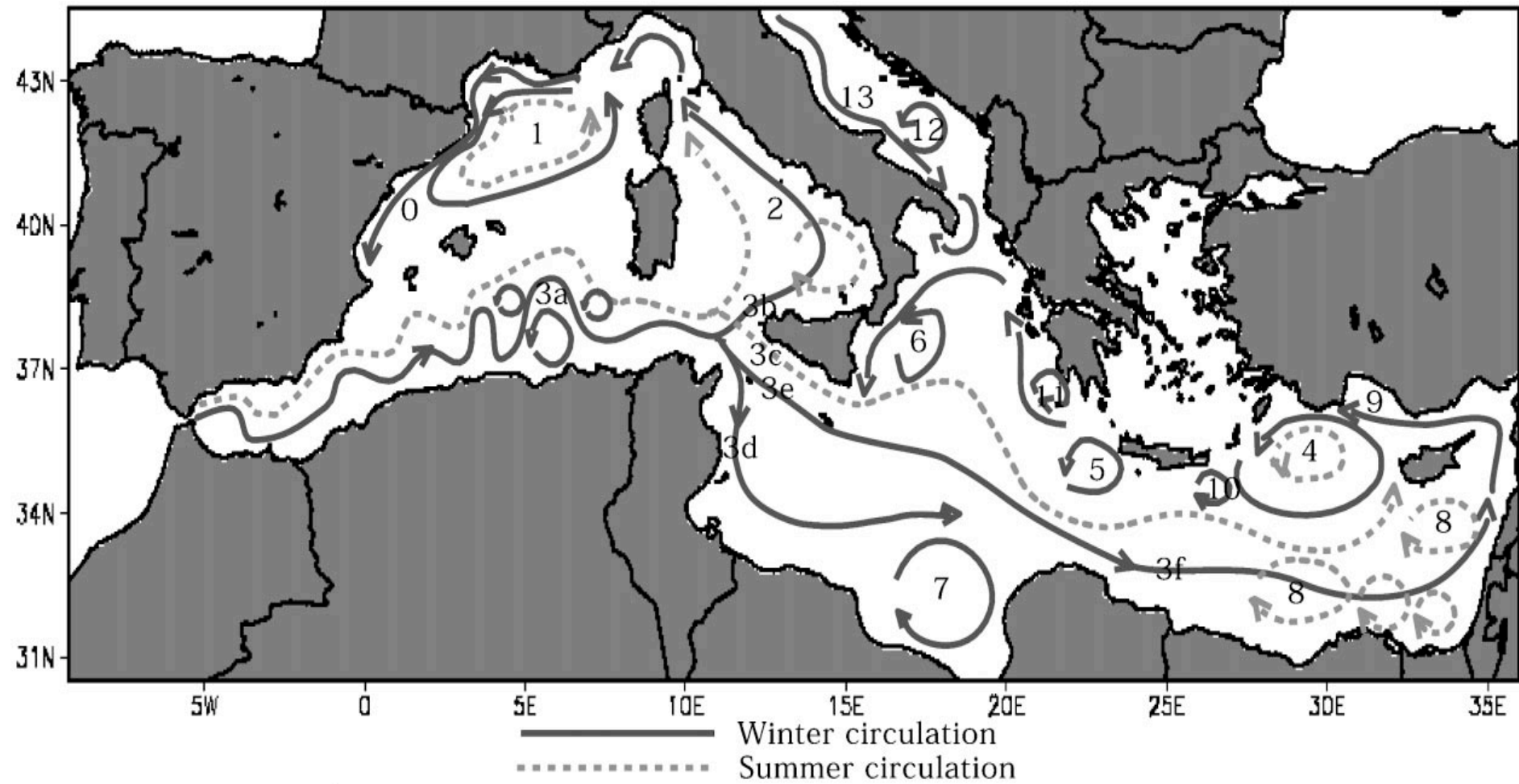
WIND CIRCULATION



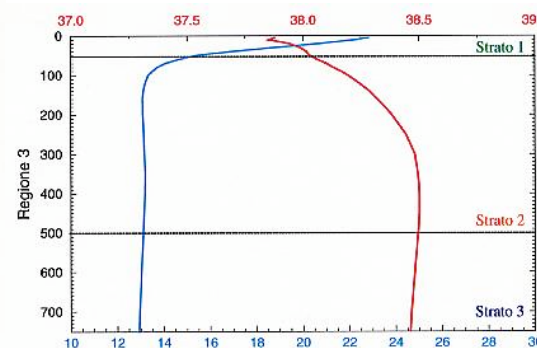
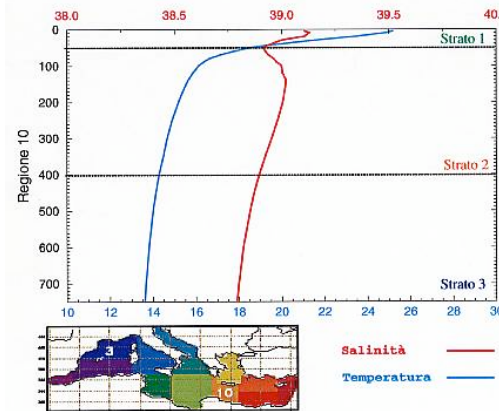
SURFACE CIRCULATION, MESOSCALE, GYRES, FRONTS AND INSTABILITIES (STREAM CURRENT)



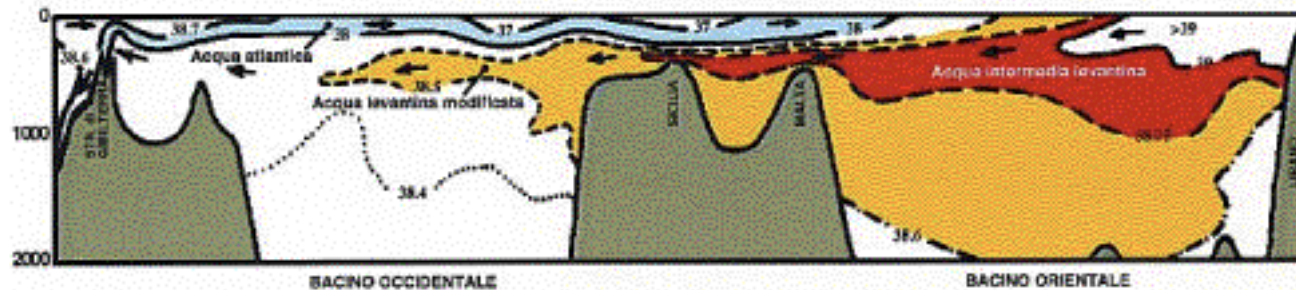
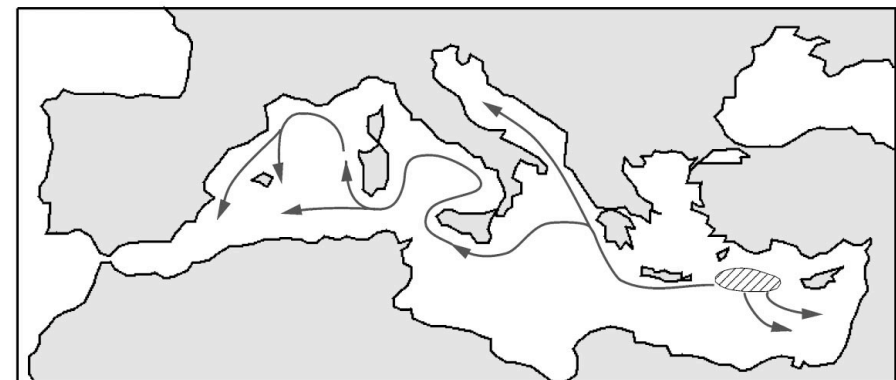
Surface circulation



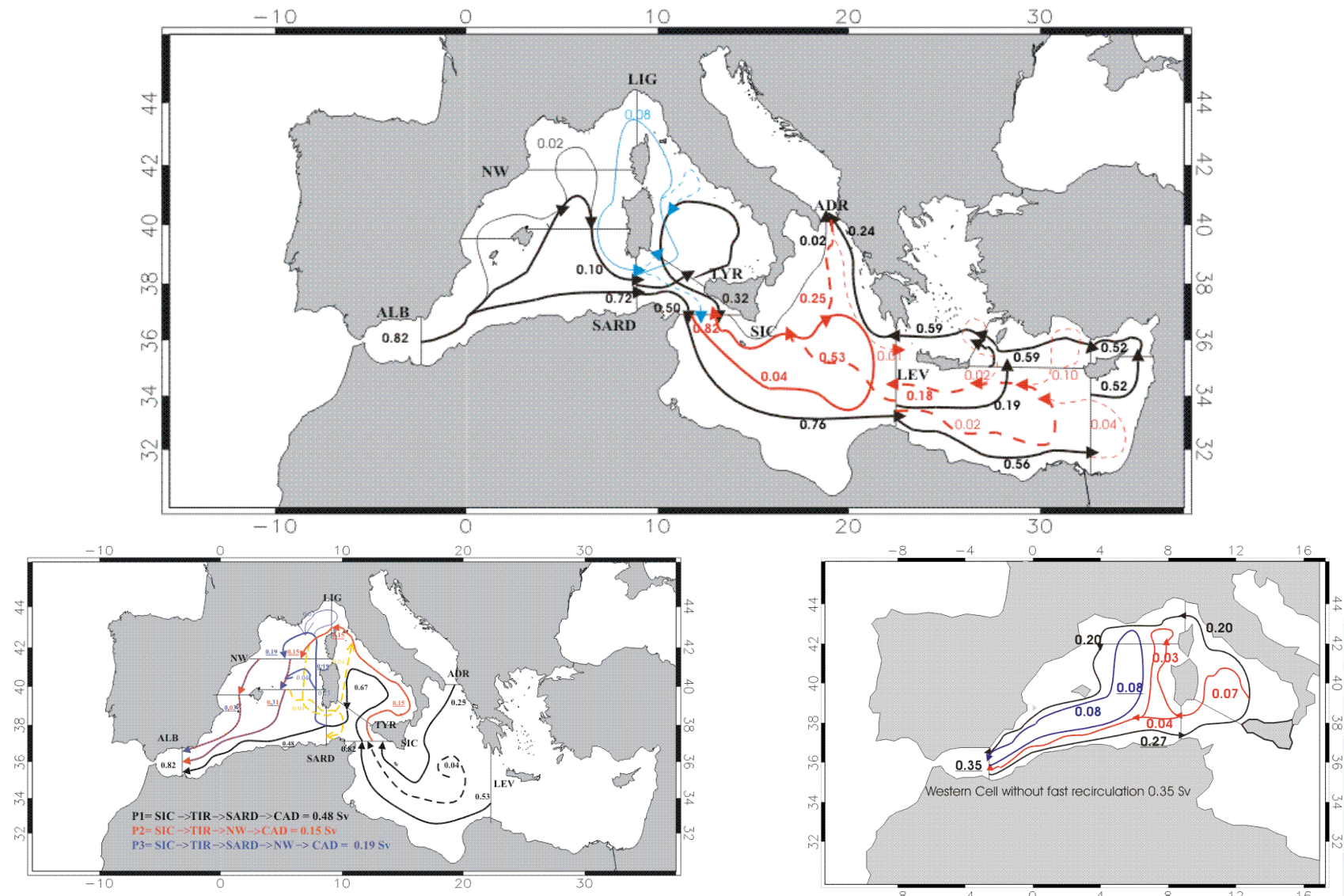
LIW Circulation



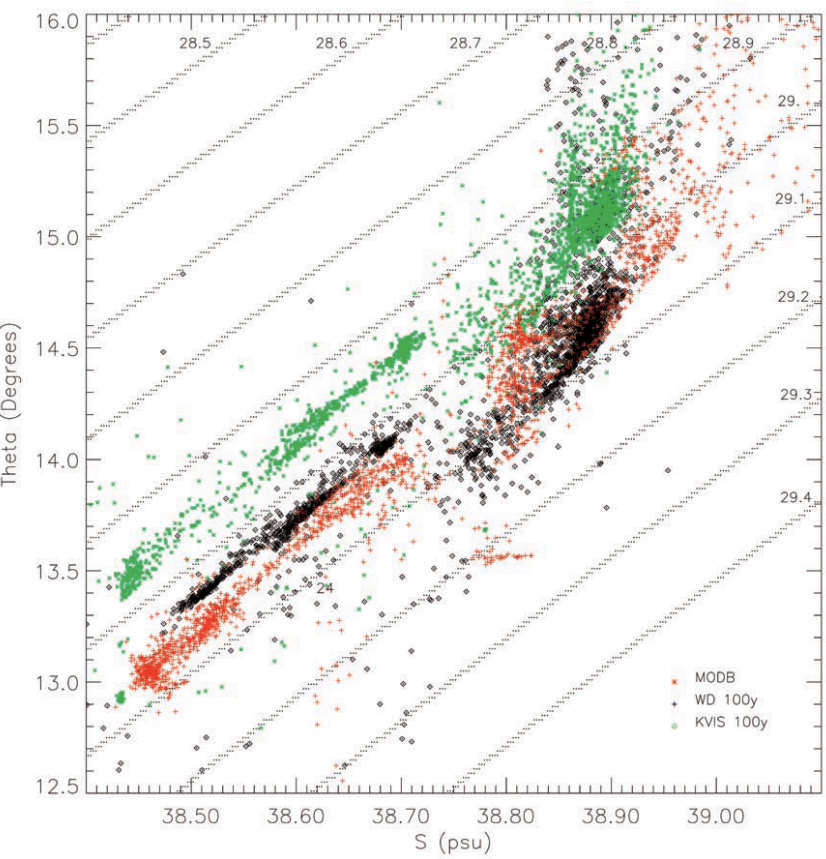
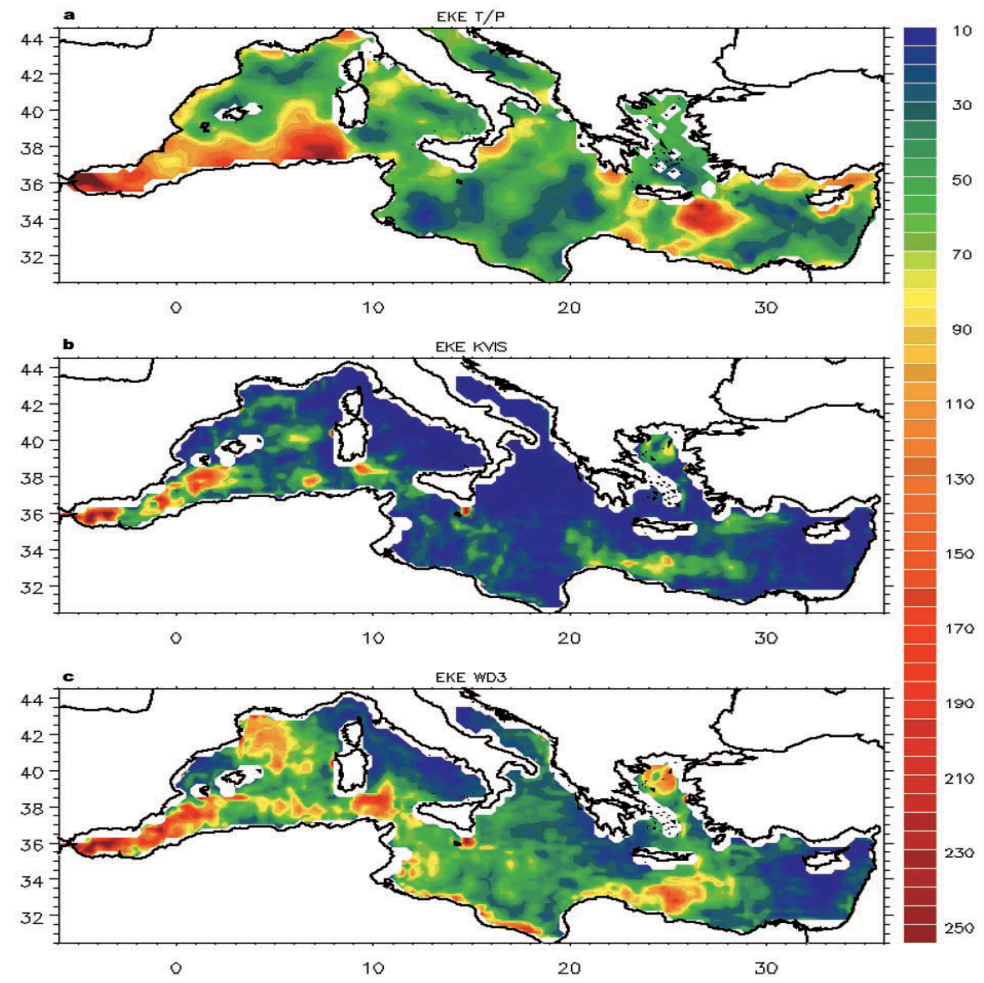
Levantine Intermediate Water (LIW) circulation



Transport computation using a lagrangian approach



KE DISTRIBUTION



SURFACE HEAT FLUXES

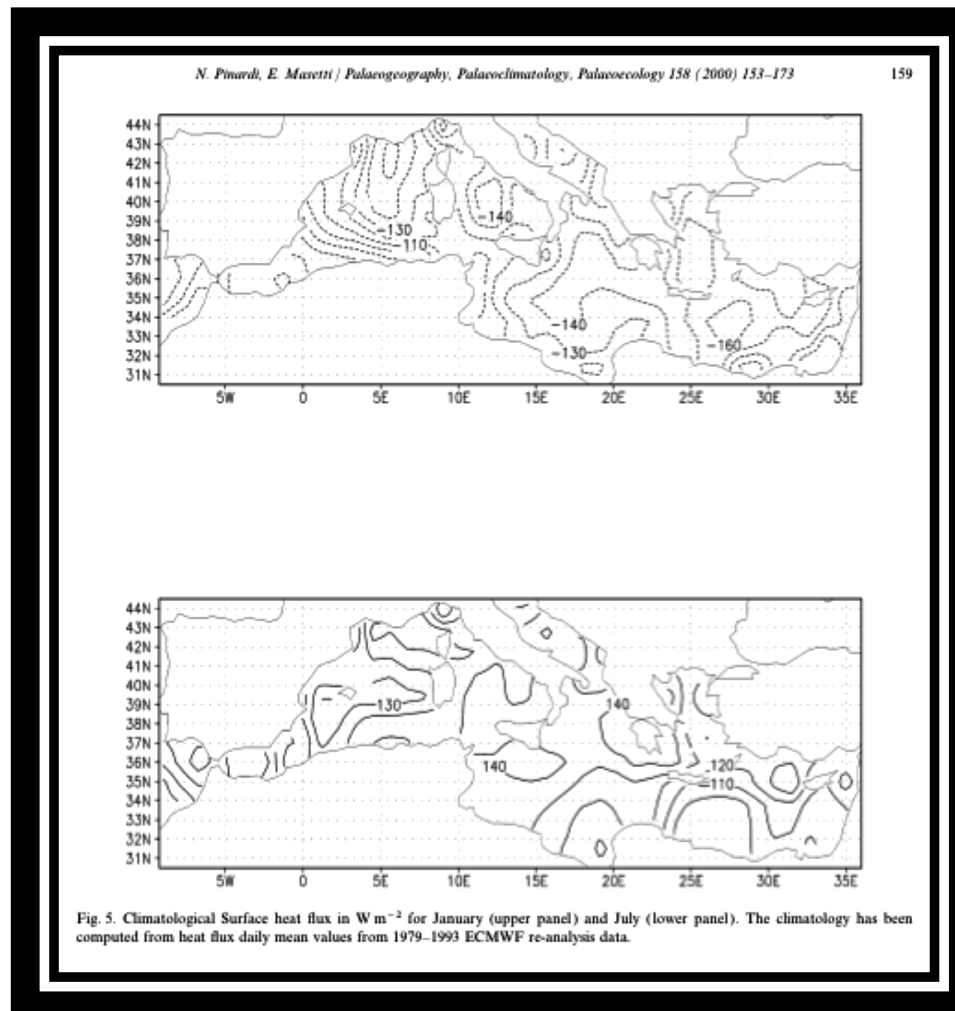
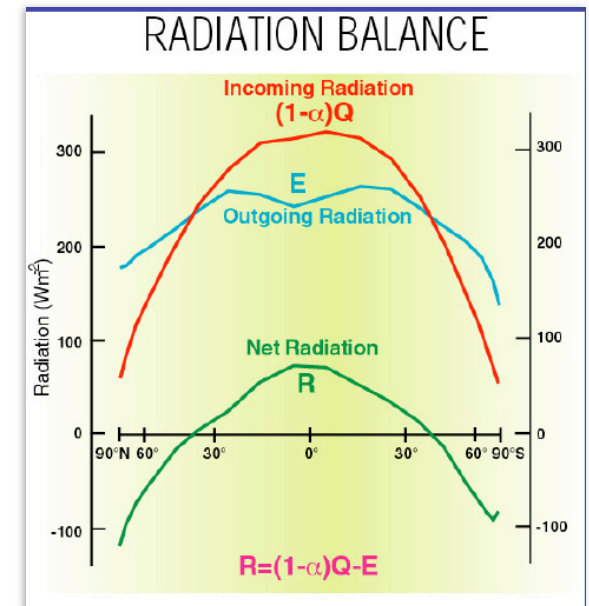


Fig. 5. Climatological Surface heat flux in W m^{-2} for January (upper panel) and July (lower panel). The climatology has been computed from heat flux daily mean values from 1979–1993 ECMWF re-analysis data.



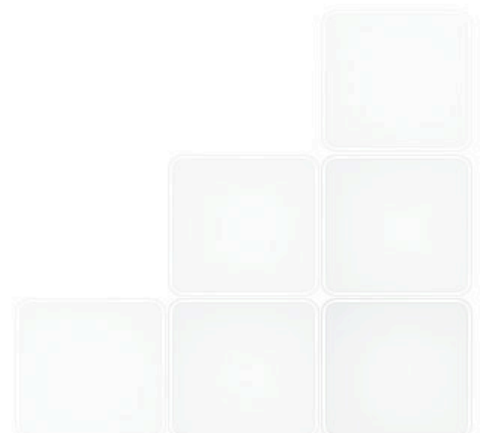
Deep water formation



- In addition to the large-scale hydrostatic TH circulation, relatively intense localized buoyancy-driven (i.e. nonhydrostatic) convective circulation cells induced by unstable vertical gradients of density, particularly in high latitude where strong surface cooling and evaporation can occur
- These areas are located at high latitudes in particular in Greenland sea, Labrador sea and Weddell sea
- Mediterranean sea (Gulf of Lions)
- Red sea

- Deep water is formed by cooling of the upper layer followed by an overturning of the water column

- Adjusts on a larger scale to its neutrally level transported by advection



- Change in the deep water production have a large scale response in the thermohaline circulation
- The physics of the deep-water formation is poorly understood: for example the sensitivity of the amount of deep and intermediate water to changes in the ocean-atmosphere heat flux

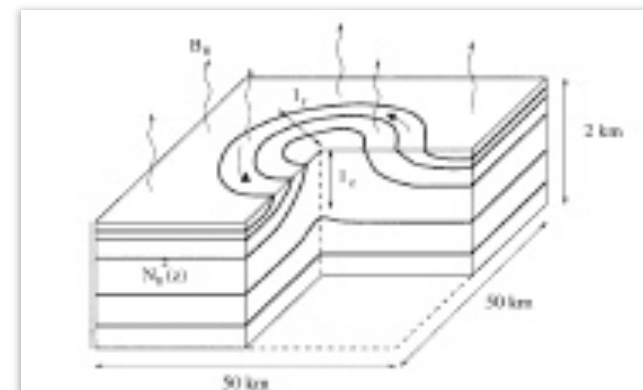
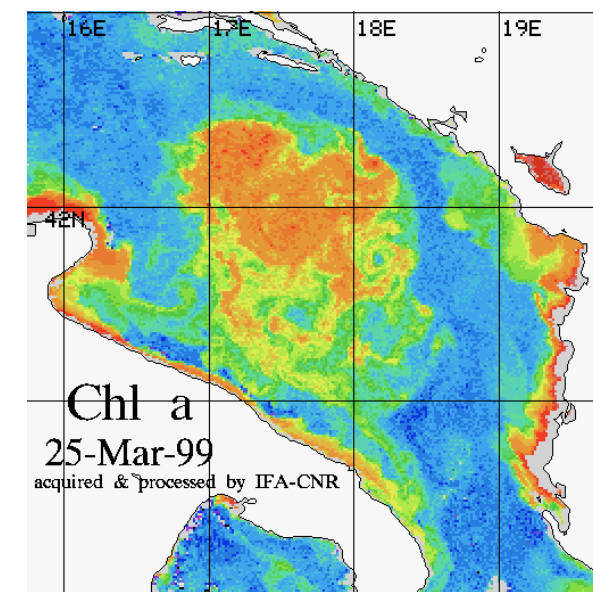
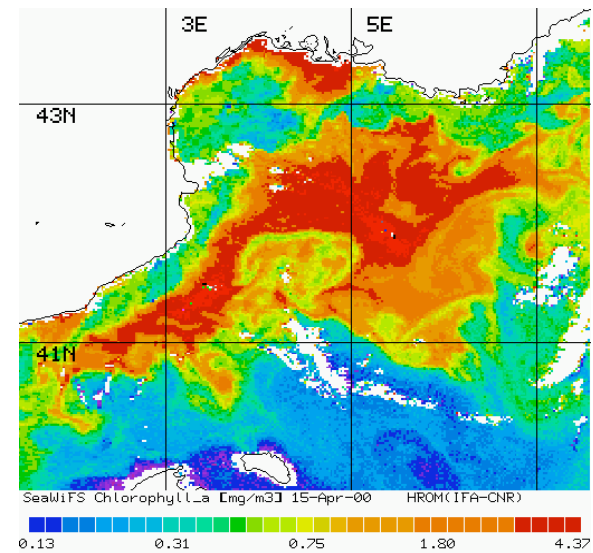
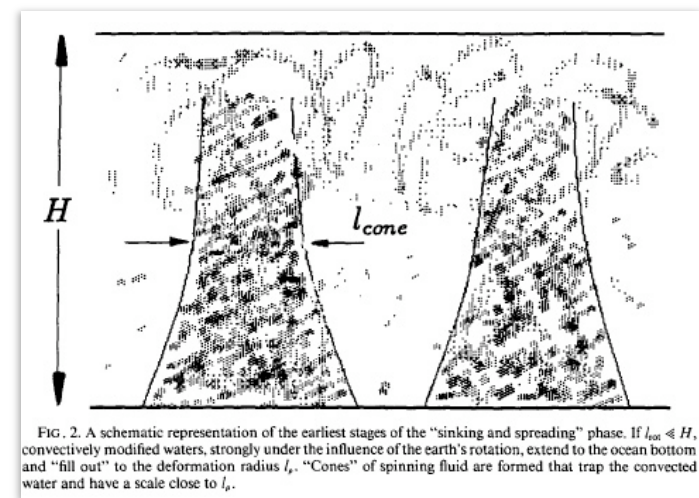
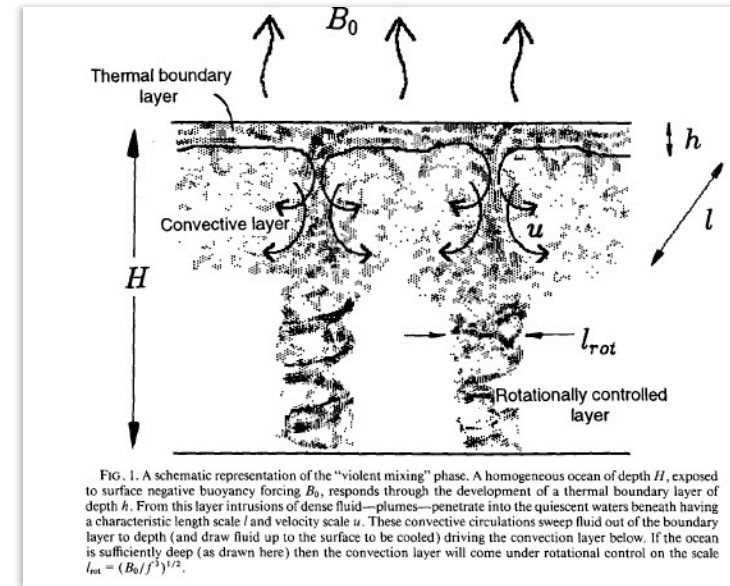
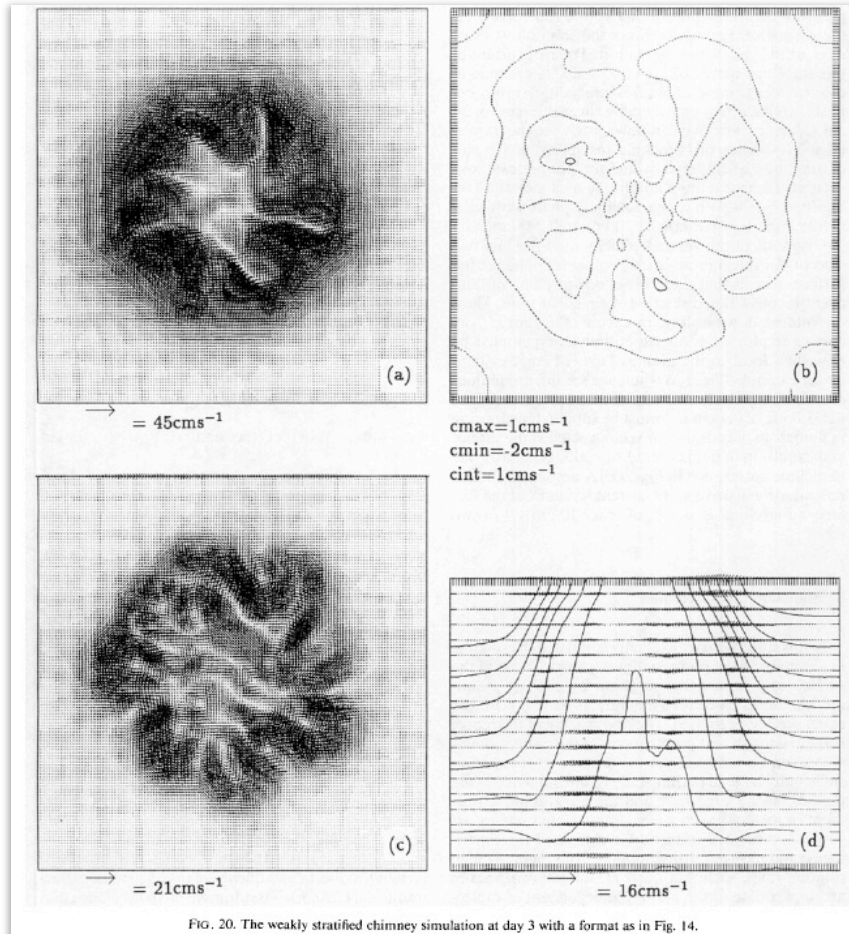


FIG. 1. A schematic diagram showing the simulation volume: an area $50 \text{ km} \times 50 \text{ km}$ across and 2 km deep. Initially the whole domain is stably stratified, with a region of weaker stratification: a cold core eddy associated with a cyclonic shear. The eddy anomaly has a Gaussian form in the horizontal, decaying on a length scale l_x , and decays exponentially in the vertical over a scale l_z . The anomalous stratification in the center of the eddy is $N(z)$ where $N(z) < 0$; the background stratification is $N_0(z)$. A uniform surface buoyancy flux B_s is applied over the whole domain.

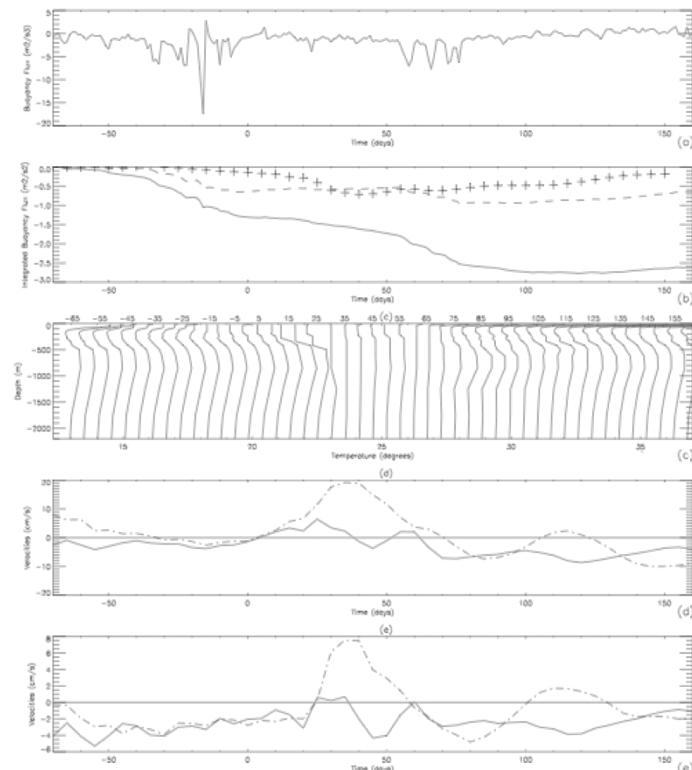


Different phase of the deep water simulation



- “deep mixing is not occurring by simple overturning of surface mixing layer, but rather through a complex hierarchy of mixing scales and dynamical processes” (Gascard, 1983)

The different phase of the DW formation from numerical model



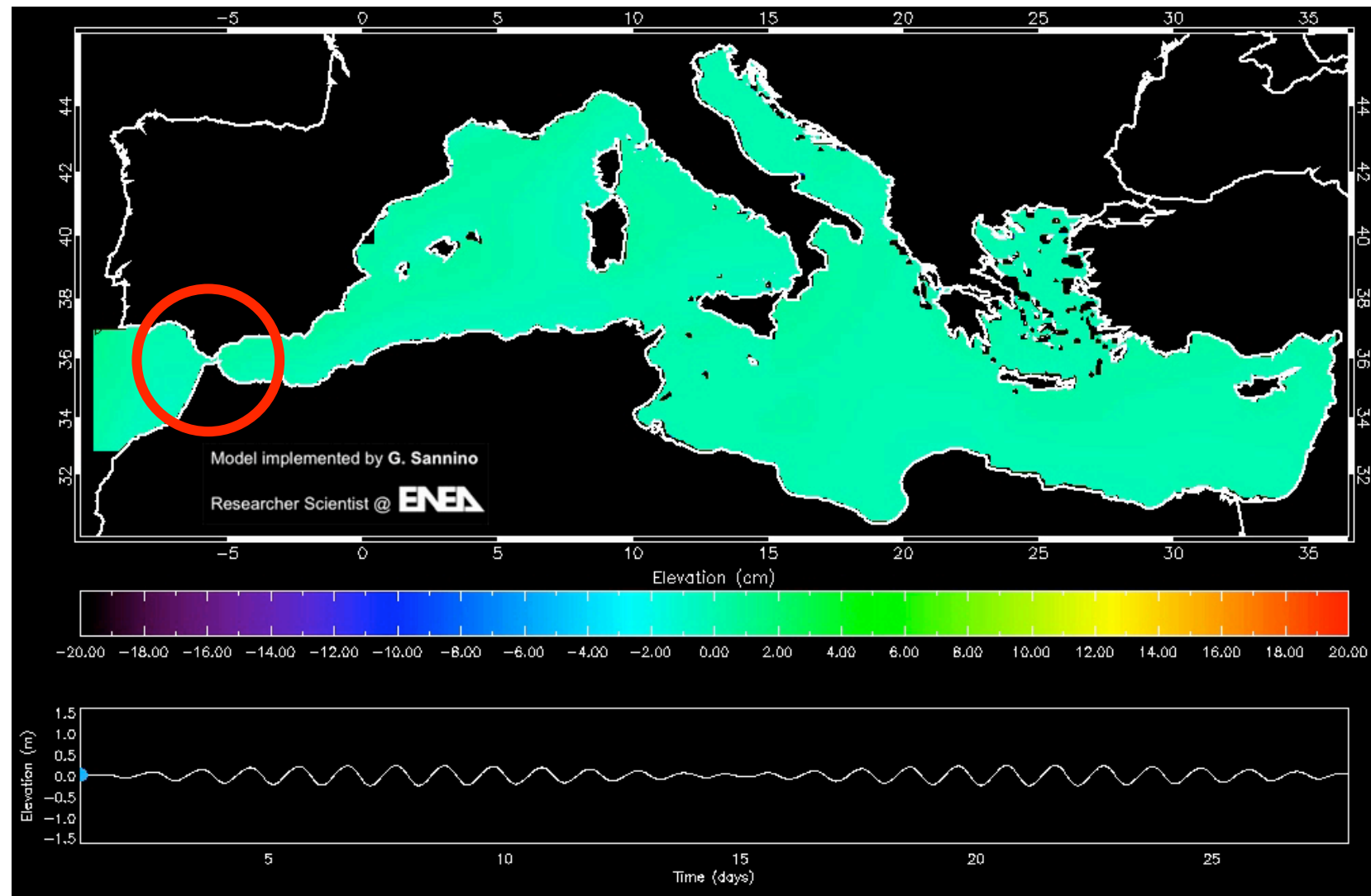
Time evolution of relevant parameters for the deep convection in WD at year 100;

- (a) Daily surface buoyancy fluxes.
- (b) Integrated buoyancy flux: solid line,
- (c) integrated surface buoyancy fluxes; dashed line, heat contribution; dot-dashed line, freshwater contribution; and crosses, integrated columnar buoyancy.
- (c) Vertical profiles of model temperature. Time sampling is 5 days.
In abscissa, on top of the plot, time is in Julian days.
Profiles are shifted by 0.5.
- (d) Model surface velocities: solid line, zonal component; and dot-dashed line, meridional component.
- (e) Model velocities at 500 m: solid line, zonal component; and dot-dashed line, meridional component.

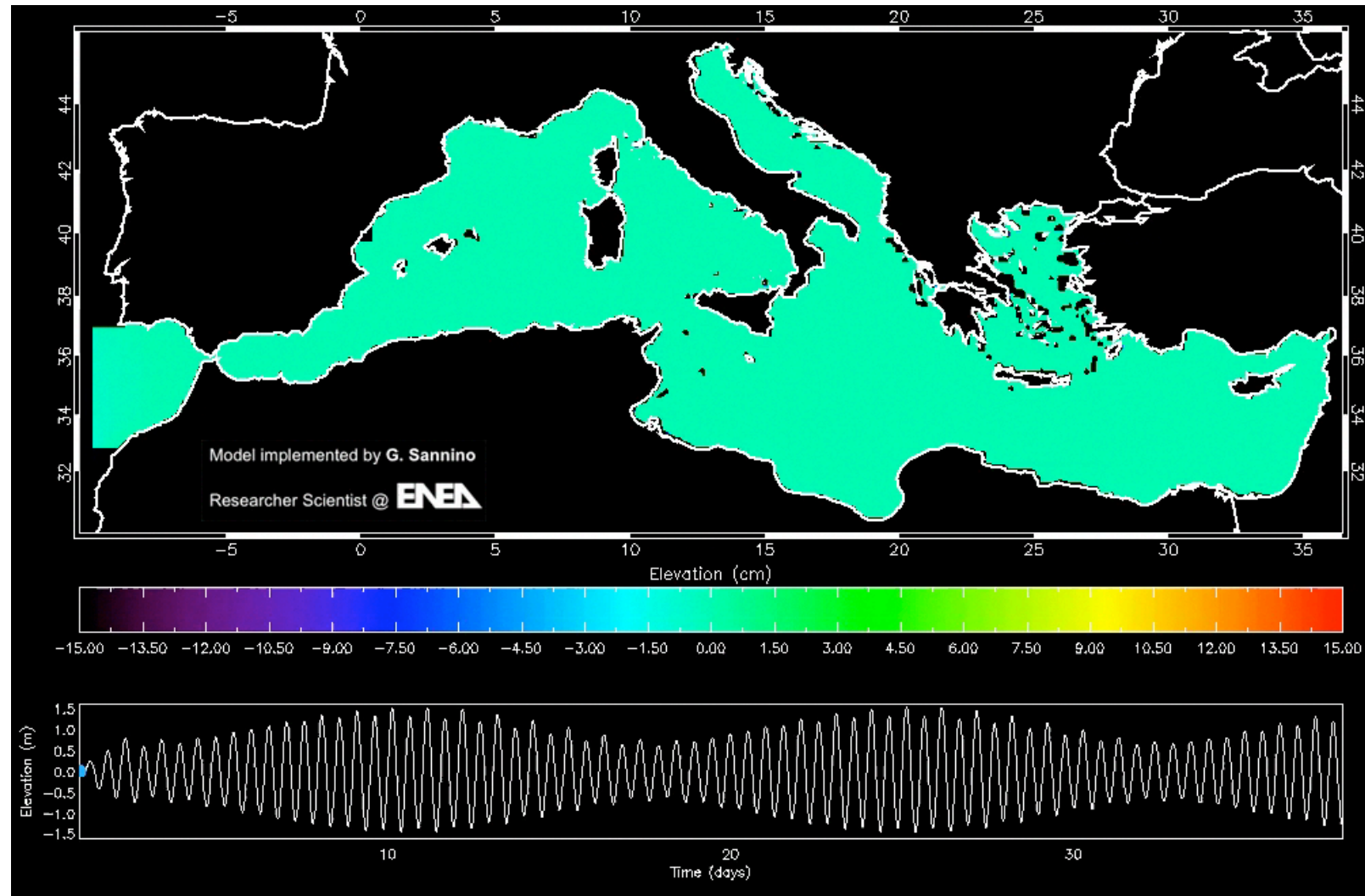
The dynamics of the Gibraltar Strait as one of the limiting factors of the Mediterranean circulation



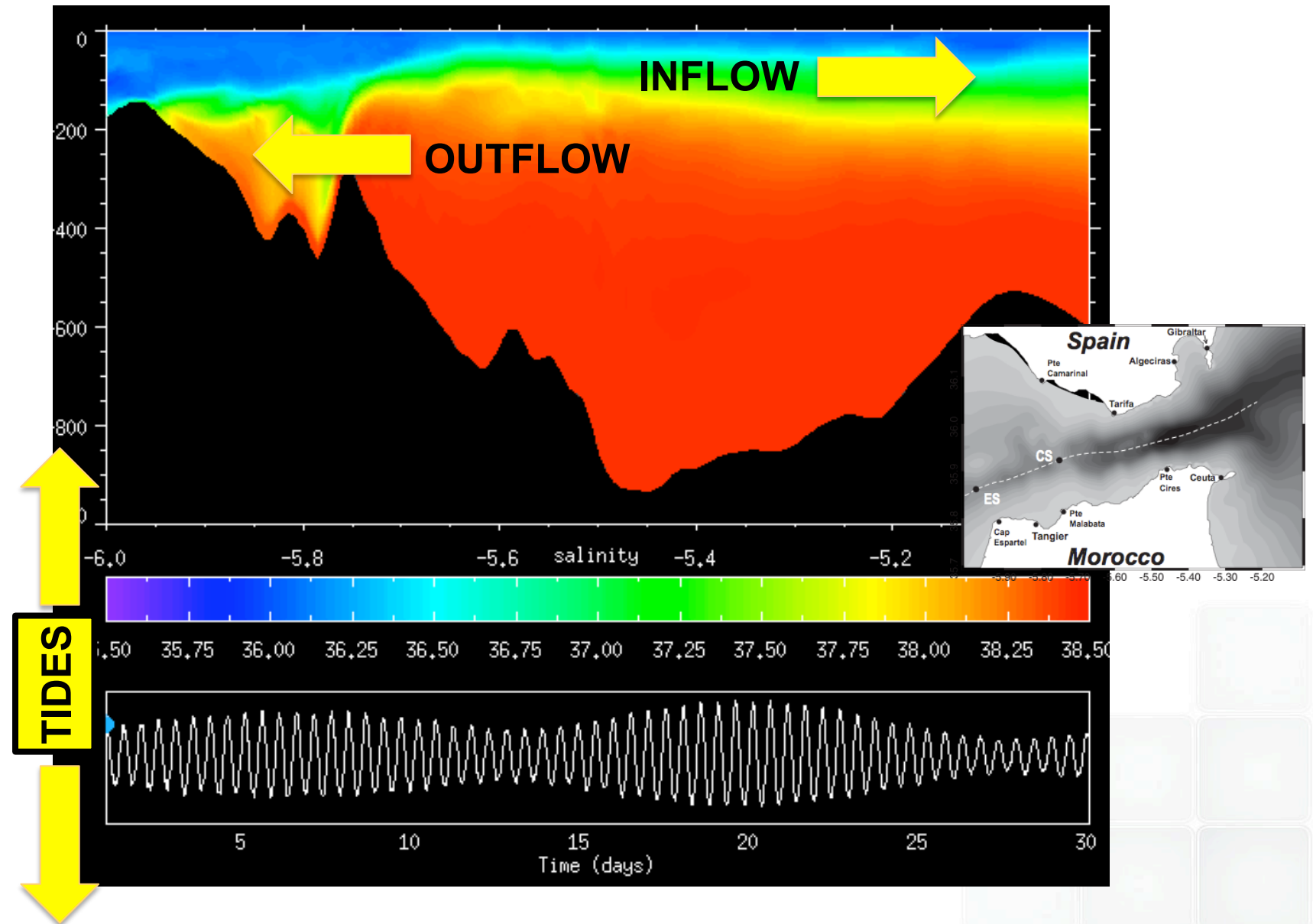
The simulation of barotropic tide



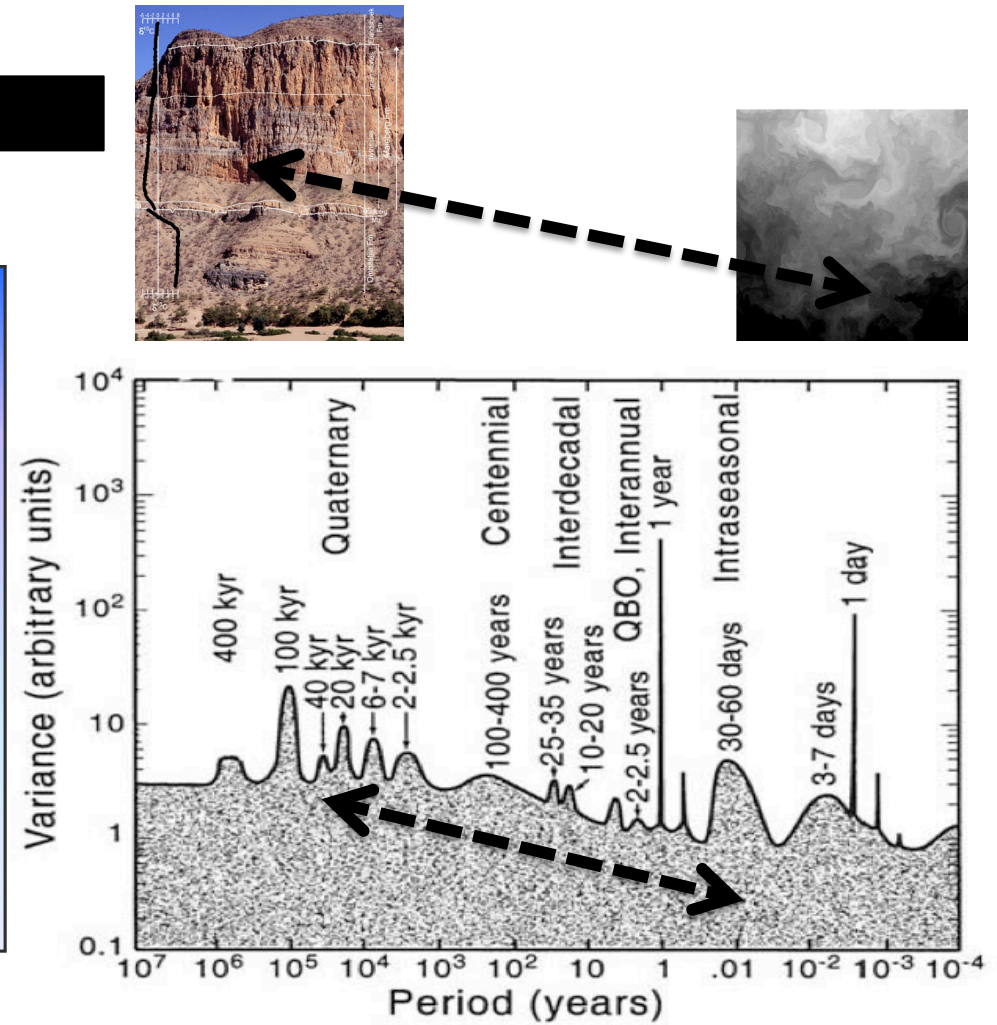
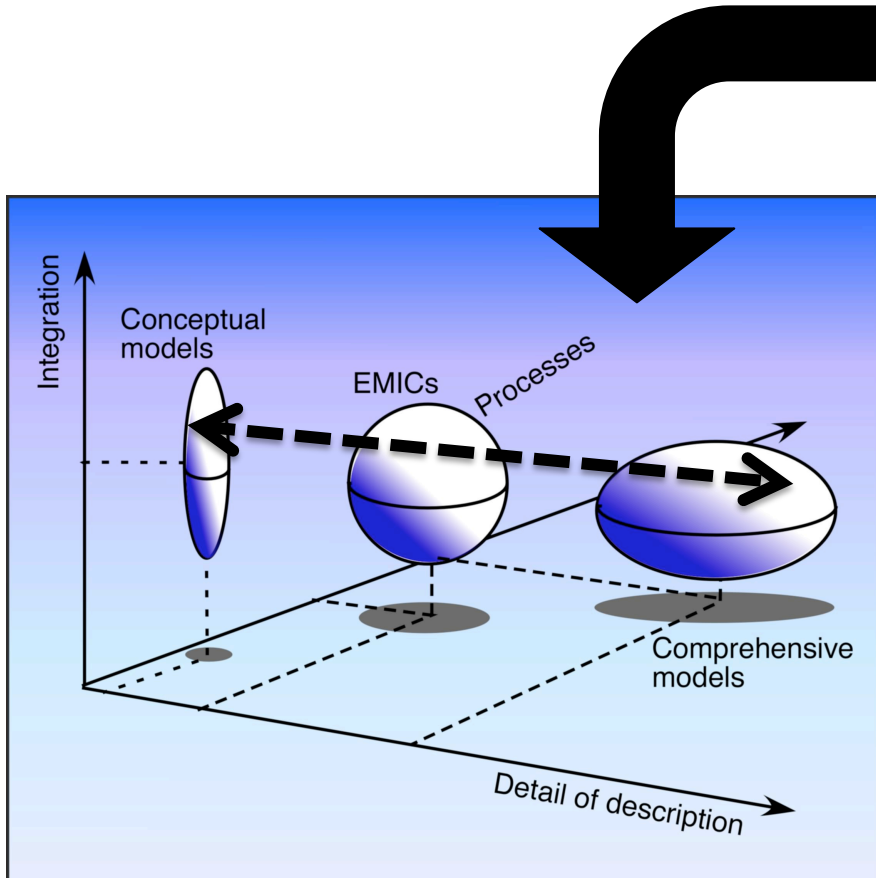
Total



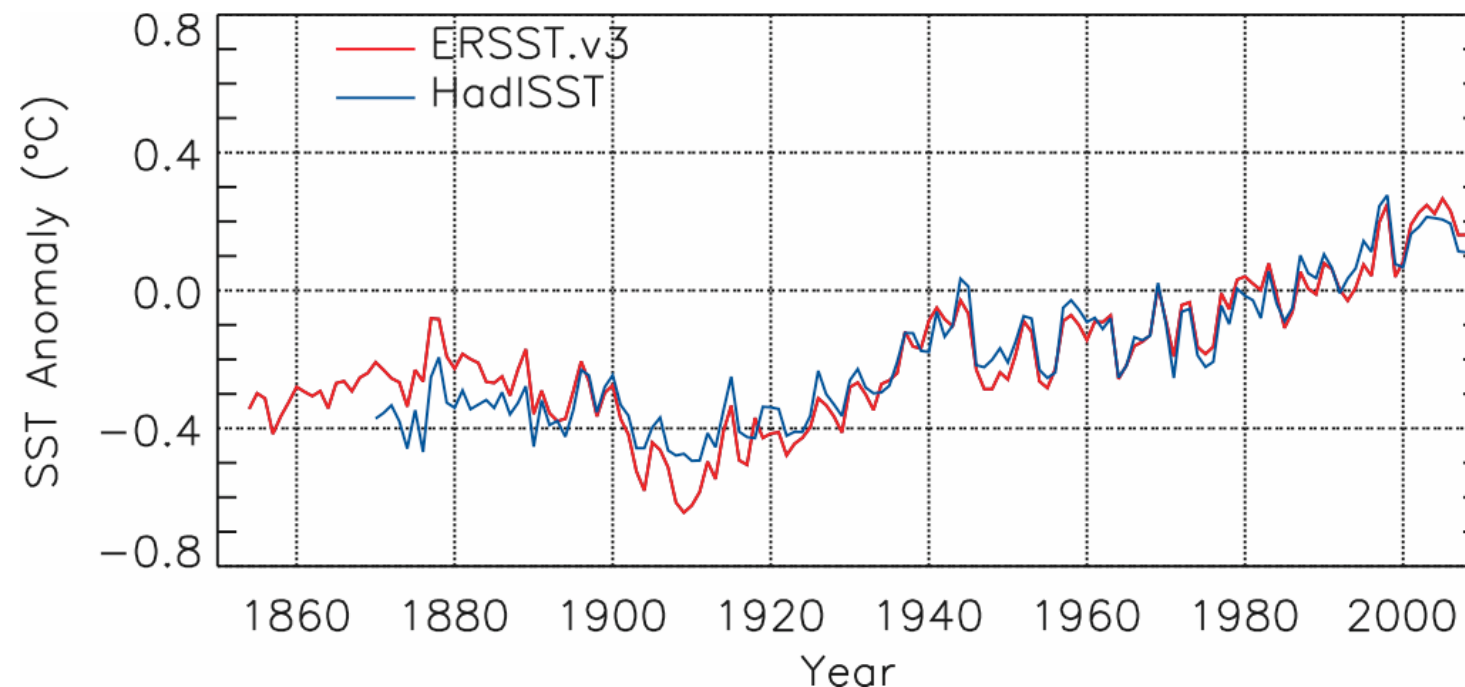
INTERNAL TIDE



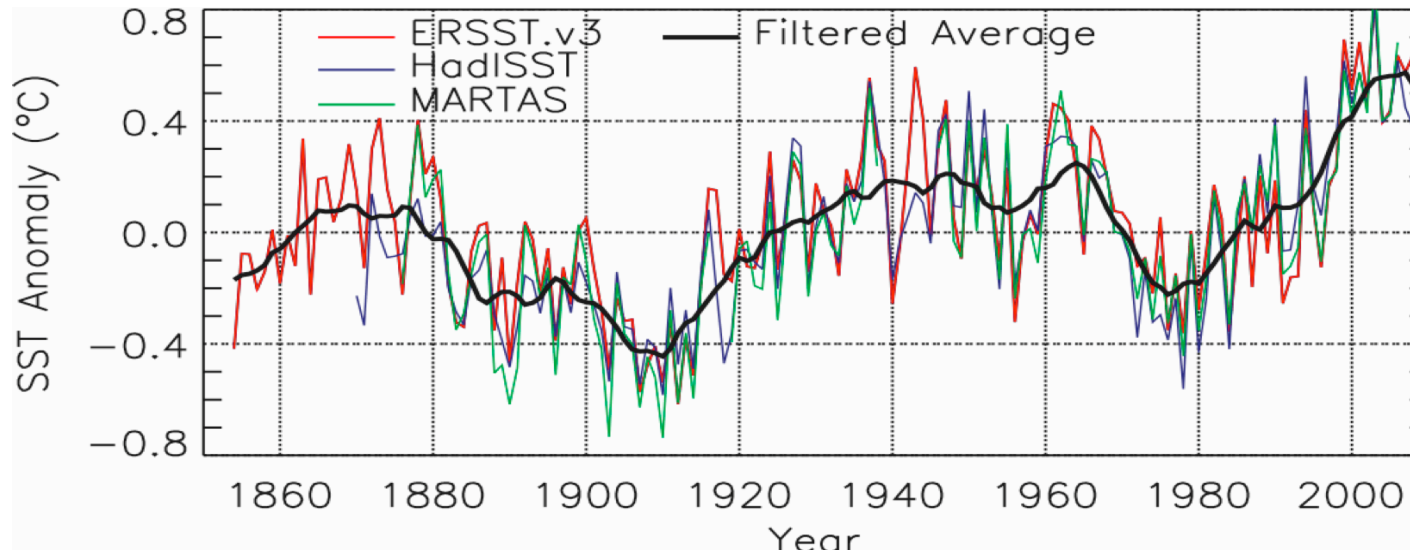
TEMPORAL SCALE INVOLVED IN CLIMATE SYSTEM AND MODELLING SIMULATIONS: THE MEDITERRANEAN CASE



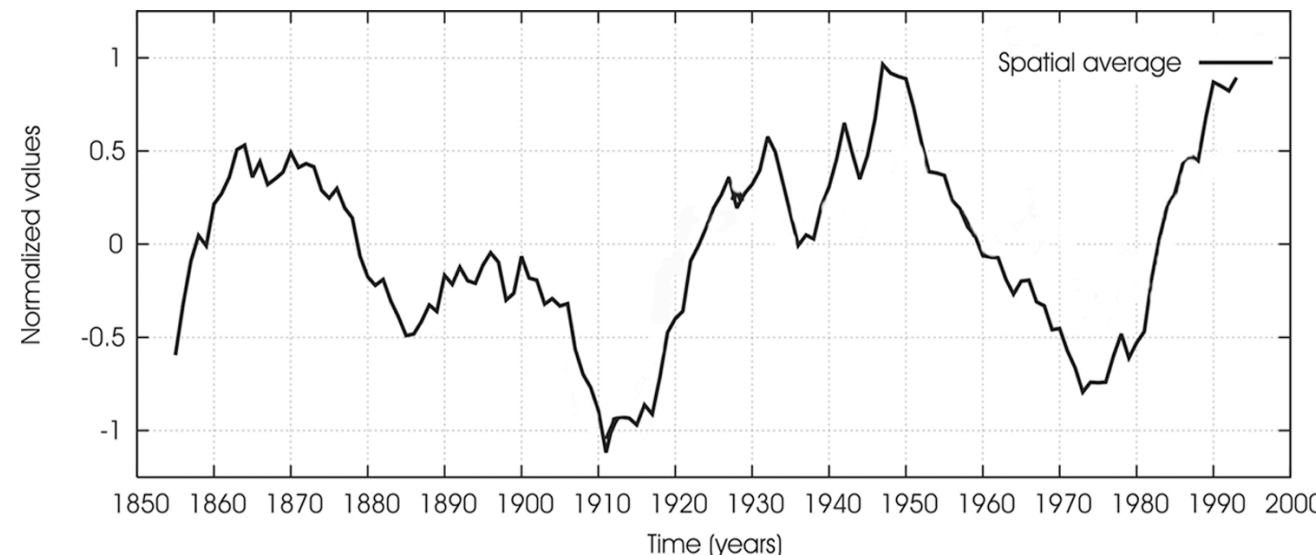
The long time variability of SST at global scale



Hydrological characteristic of the Mediterranean sea at Multidecadal scale: SST (from 1854-today) and Atlantic Multidecadal Oscillation (AMO)



Mediterranean annual
SST anomaly (respect to
the 1971-2000 average)
from 1854 to 2008



The curve corresponds to
standardized values of
the spatial average of
Mediterranean summer
temperatures for the
period 1850–1999.
(Xoplaki et al., 2003)

Warming of the Mediterranean surface layer: sst are increasing since 1860 by 0.4°C

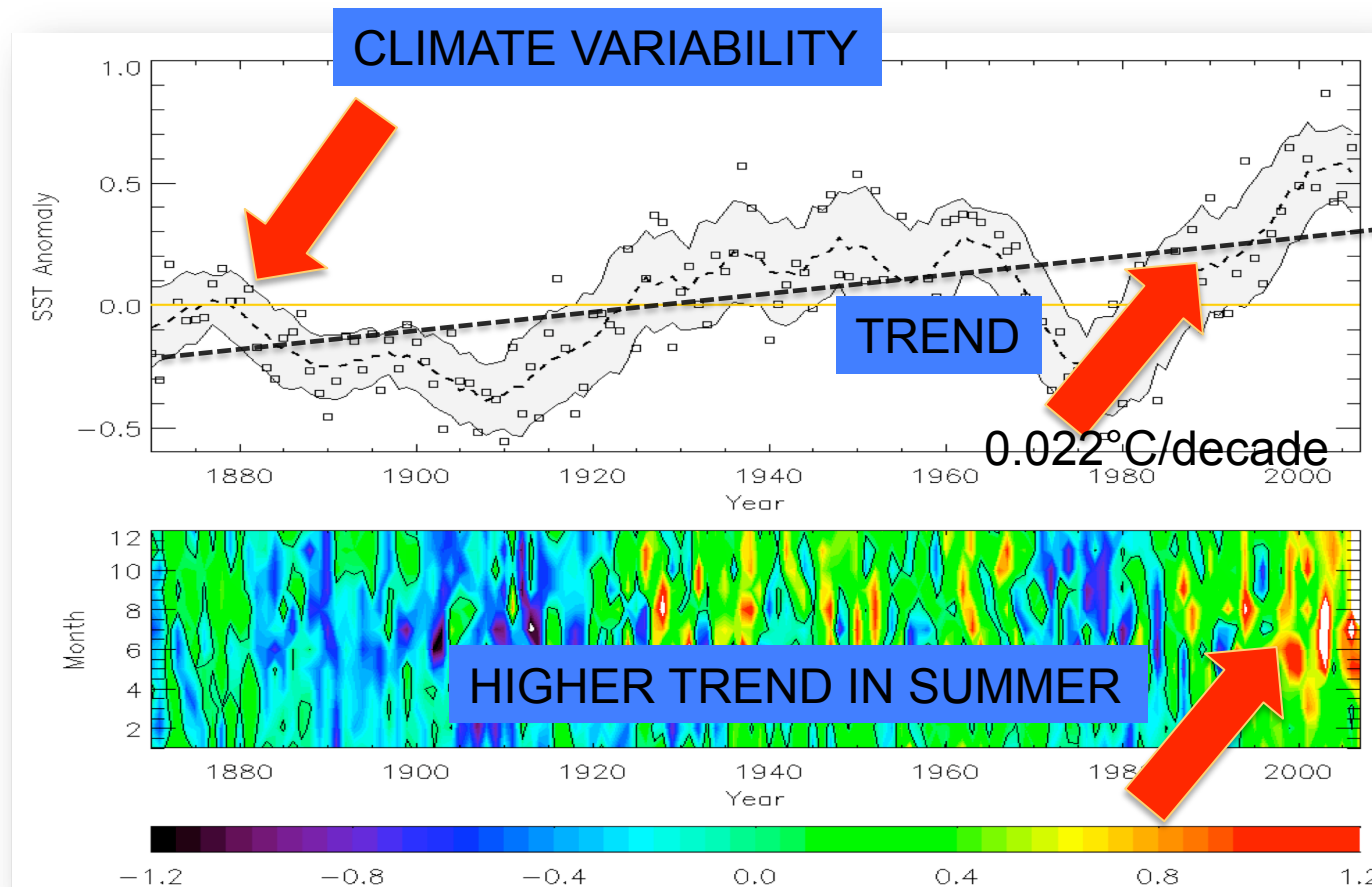
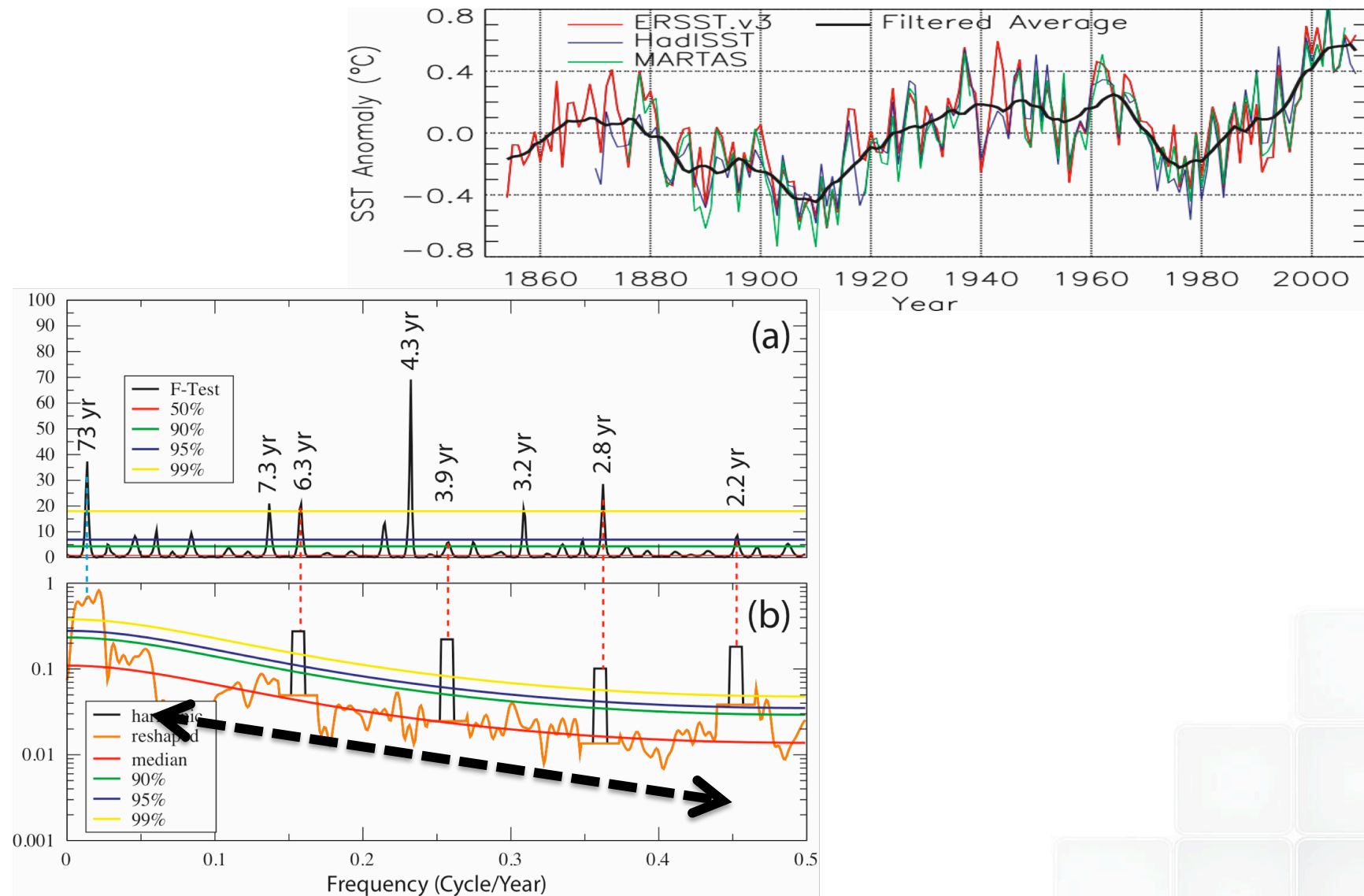
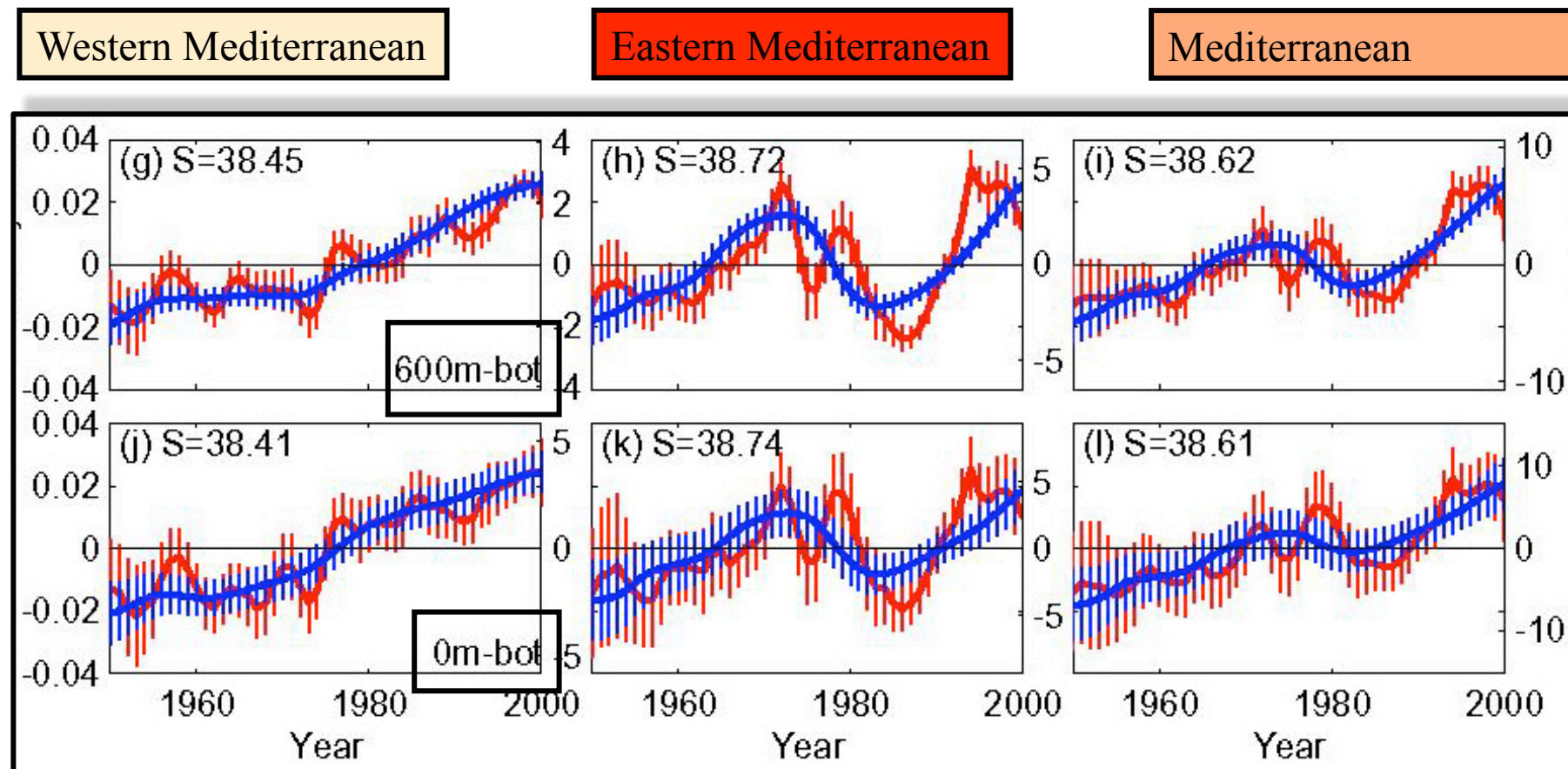


Figure 1. Upper panel SST yearly anomaly. Lower panel SST Monthly anomalies. The black contour line is the zero level

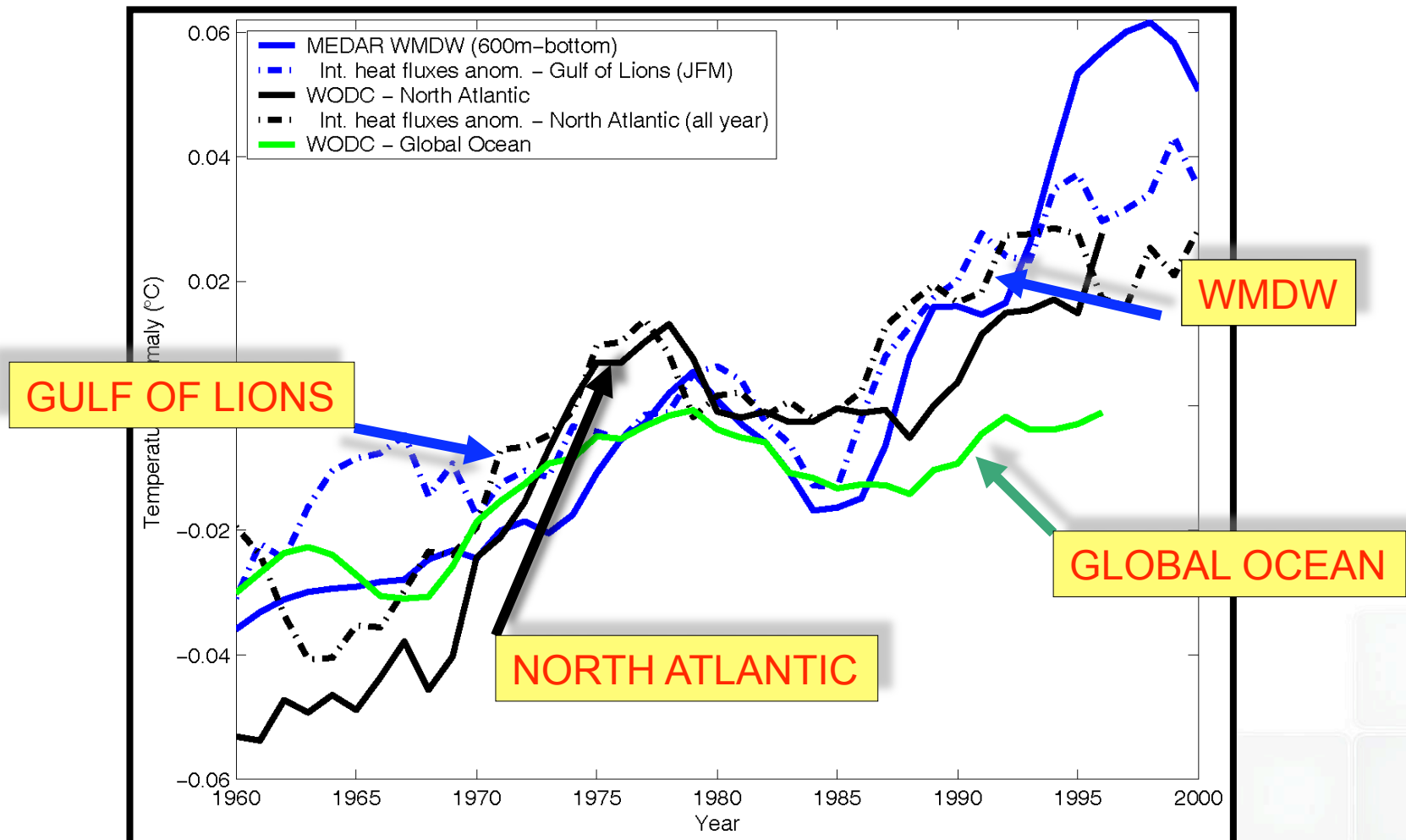
Spectral characteristic



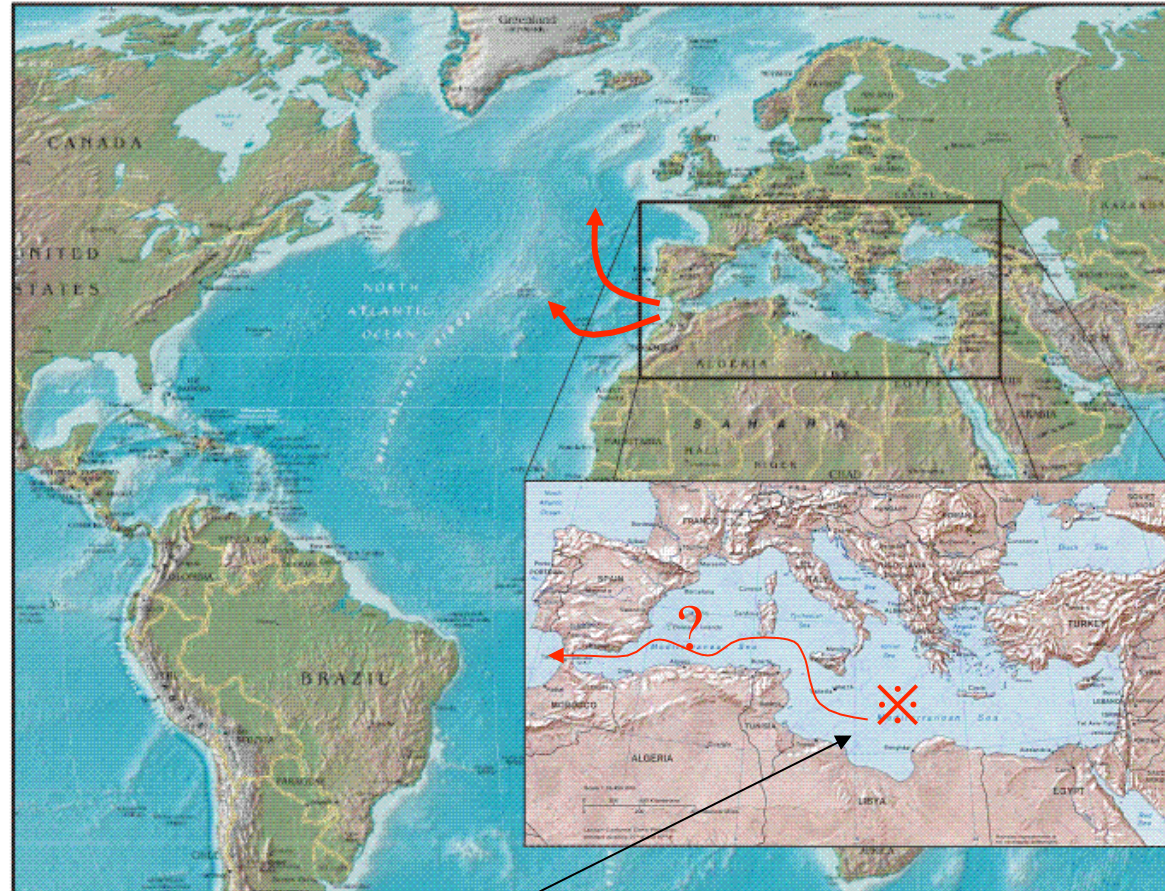
Change of temperature and salinity for the entire water column in the last 50 yrs



Time series of temperature anomalies ($^{\circ}\text{C}$) in the last forty years in the GULF of LIONS

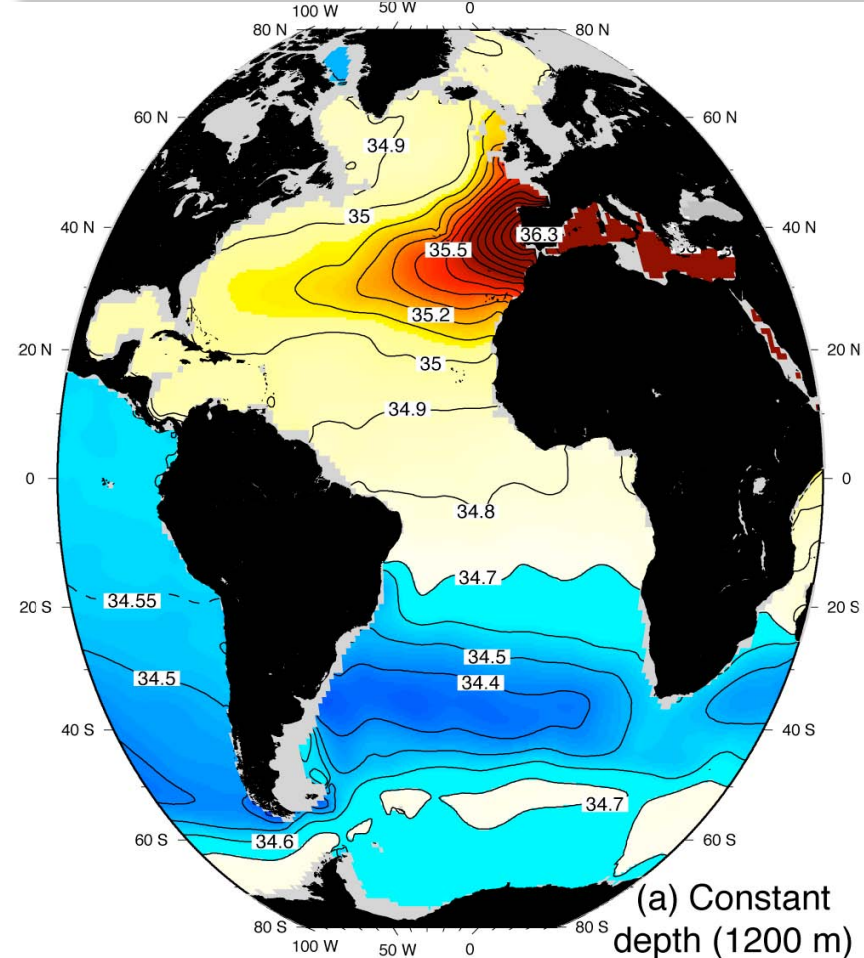
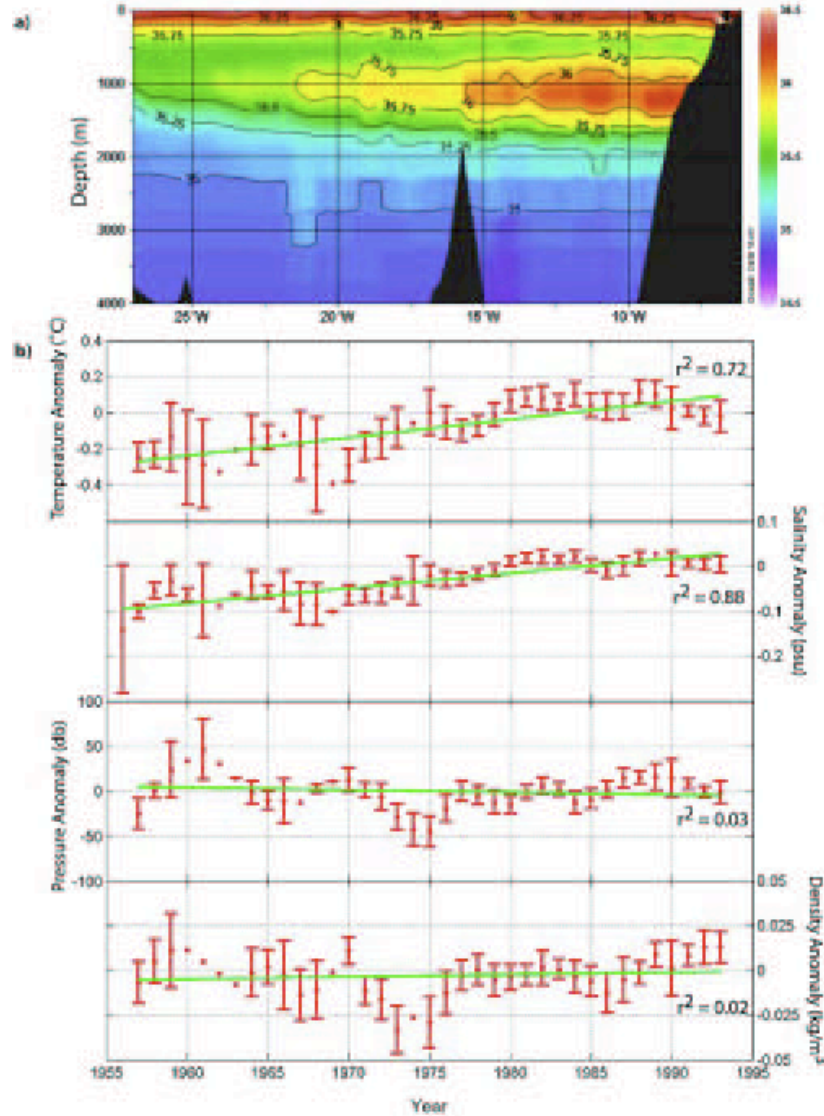


The Mediterranean Sea is an evaporative basin and the Gibraltar strait is a source of intermediate water

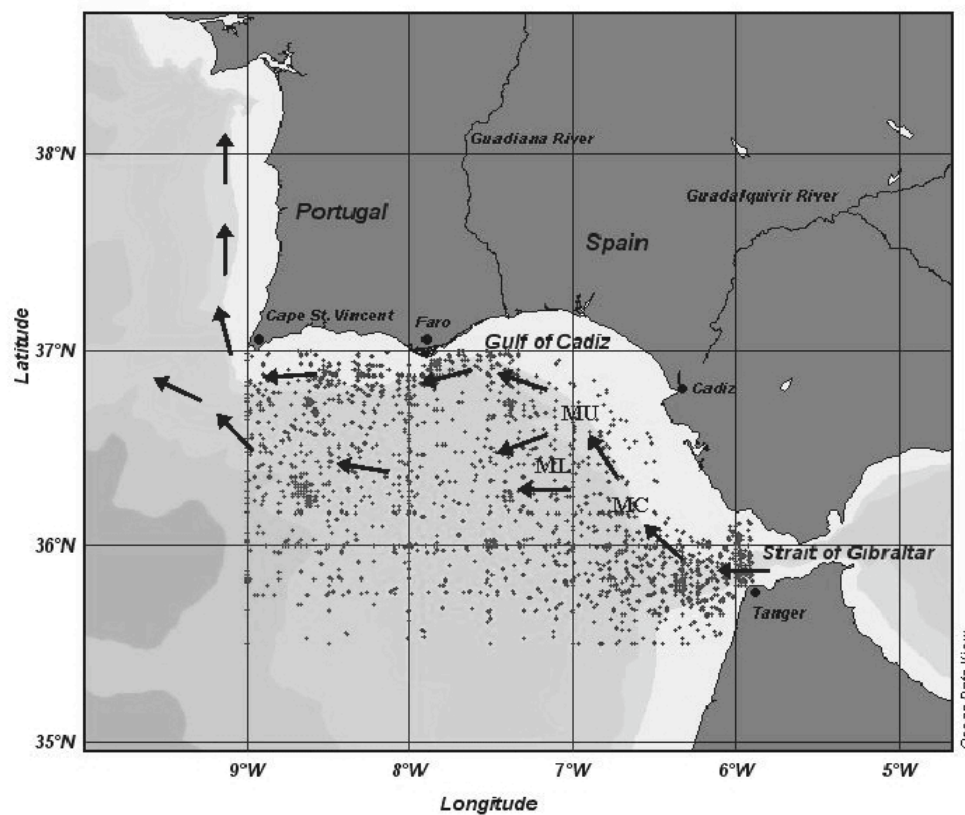


In the 90' have been observed dramatic changes in the deep water formation and in the vertical stratification in the EM. How/when they reflect in the Gibraltar Output ?

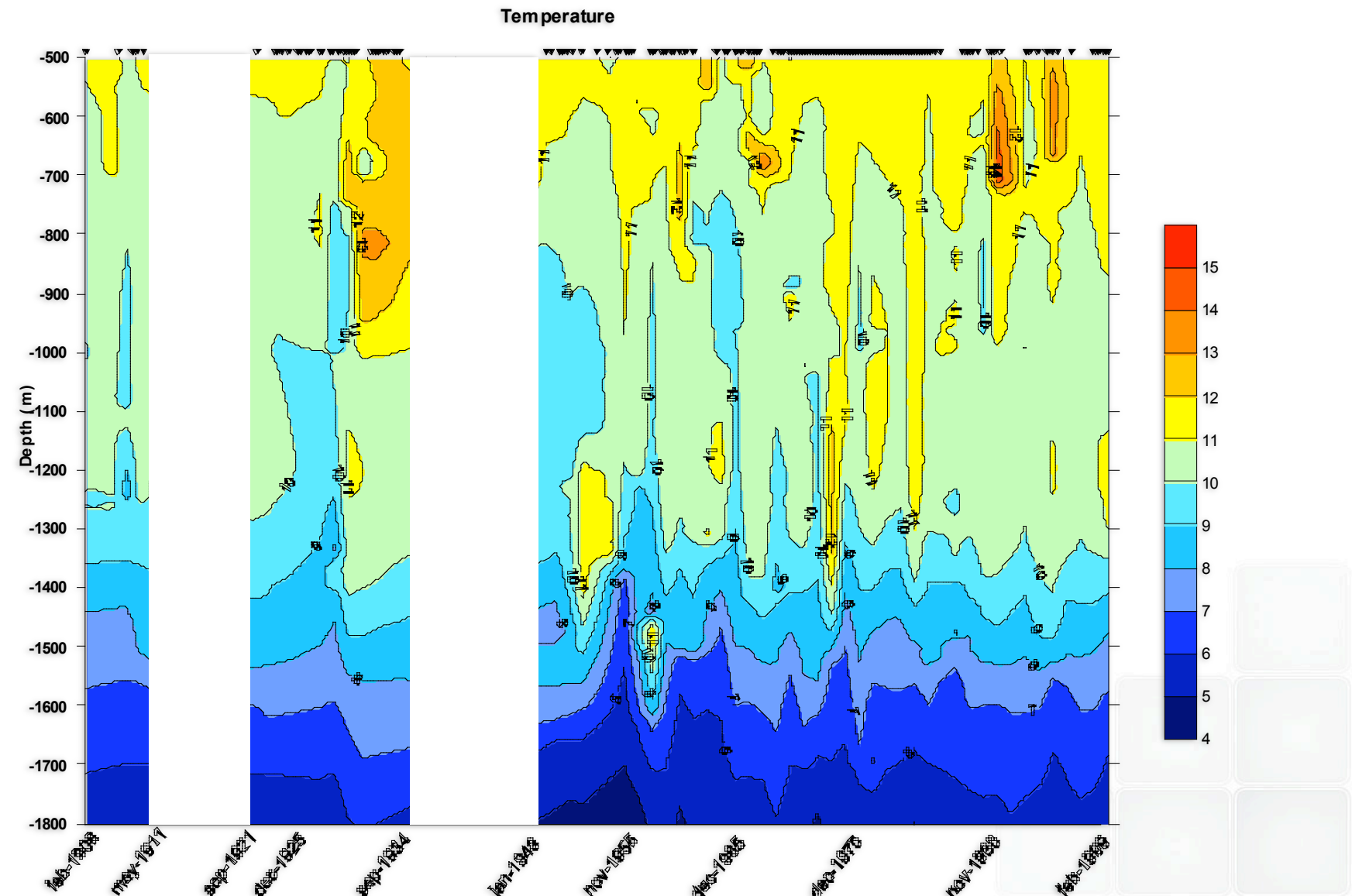
The Mediterranean outflow: source of heat and salt at intermediate depth (1000m)



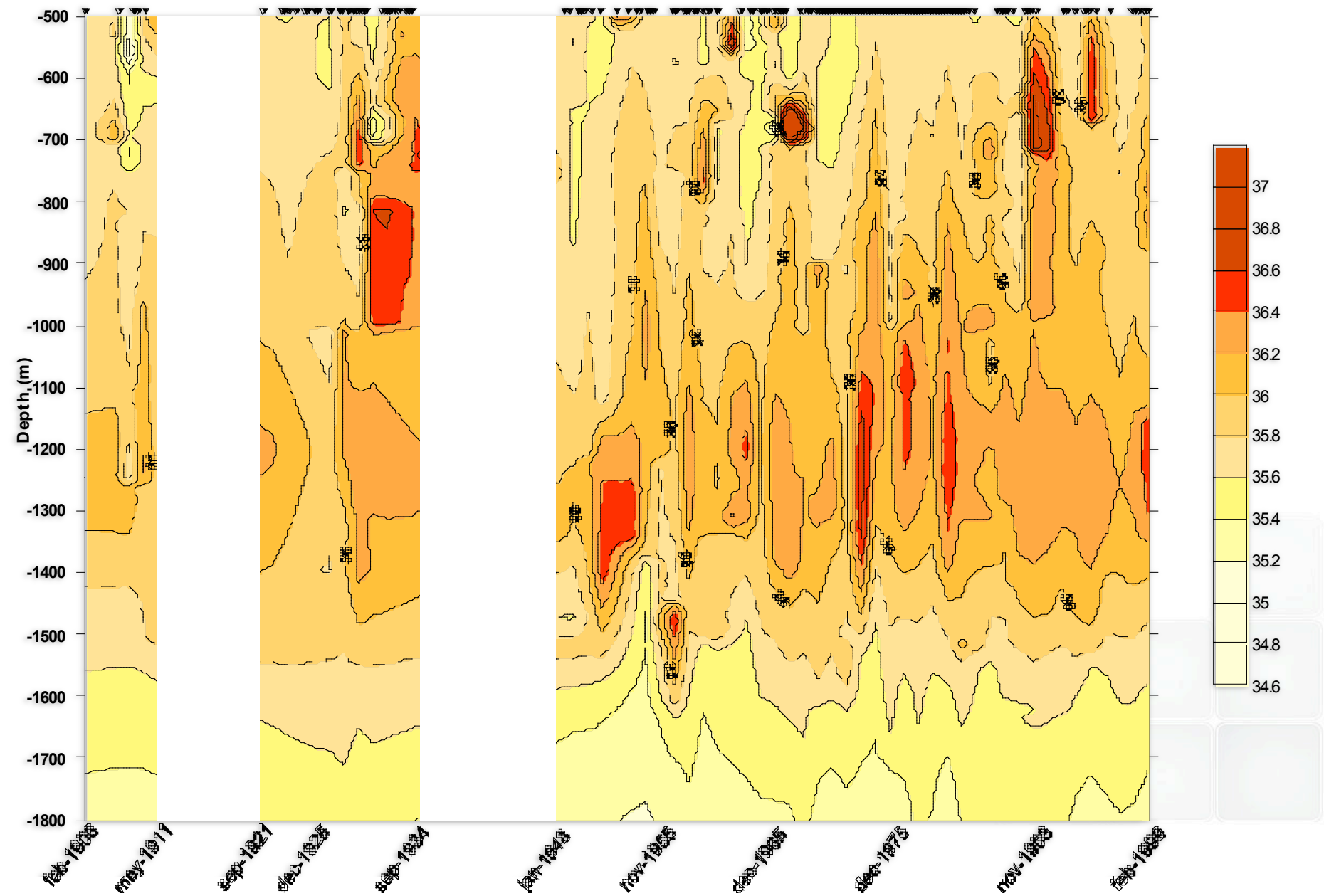
(Potter and Lozier, GRL, 2004 and Fusco, Artale, 2008)



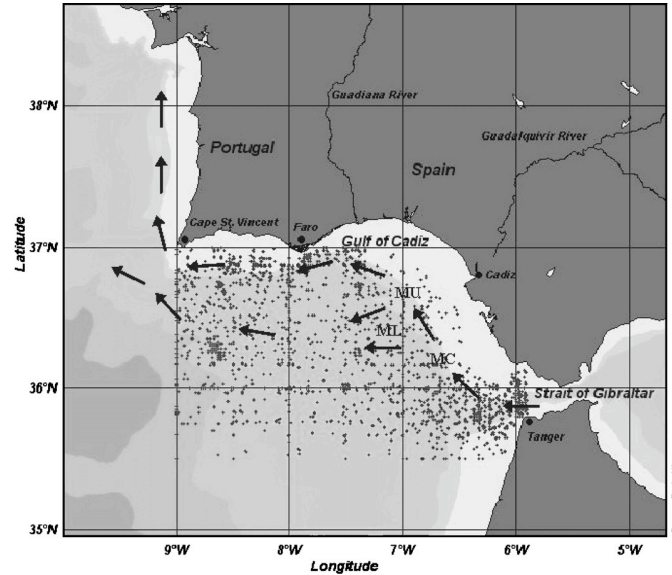
Gulf of Cadiz: selected area, distribution of profiles and principal patterns of the Mediterranean Water (adapted from Mulder et al. 2006): MC (Mediterranean Core water), MU (Mediterranean Upper water) and ML (Mediterranean Lower water).



Salinity

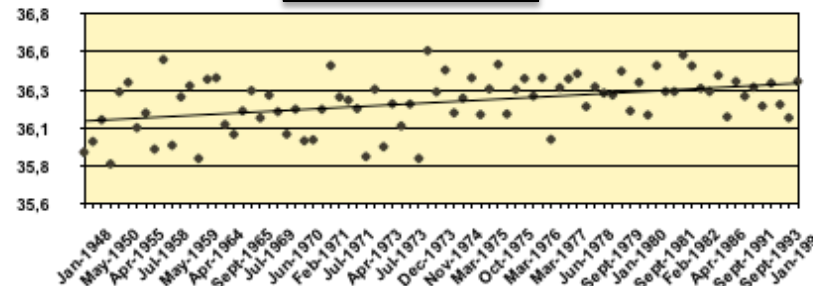


Mediterranean Outflow: source of warming at mid-depth

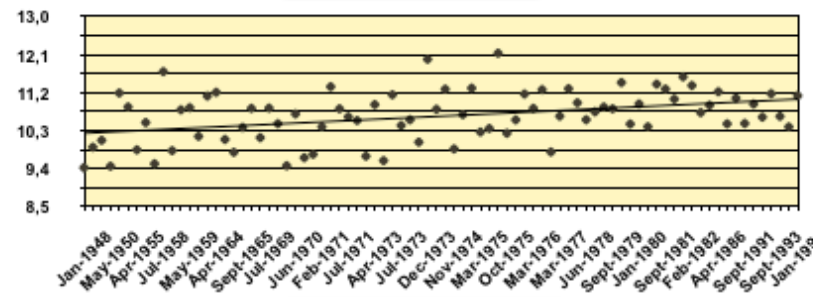


GULF OF CADIZ

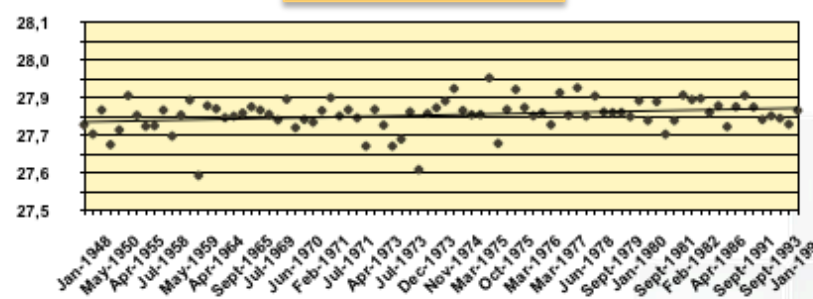
SALINITY



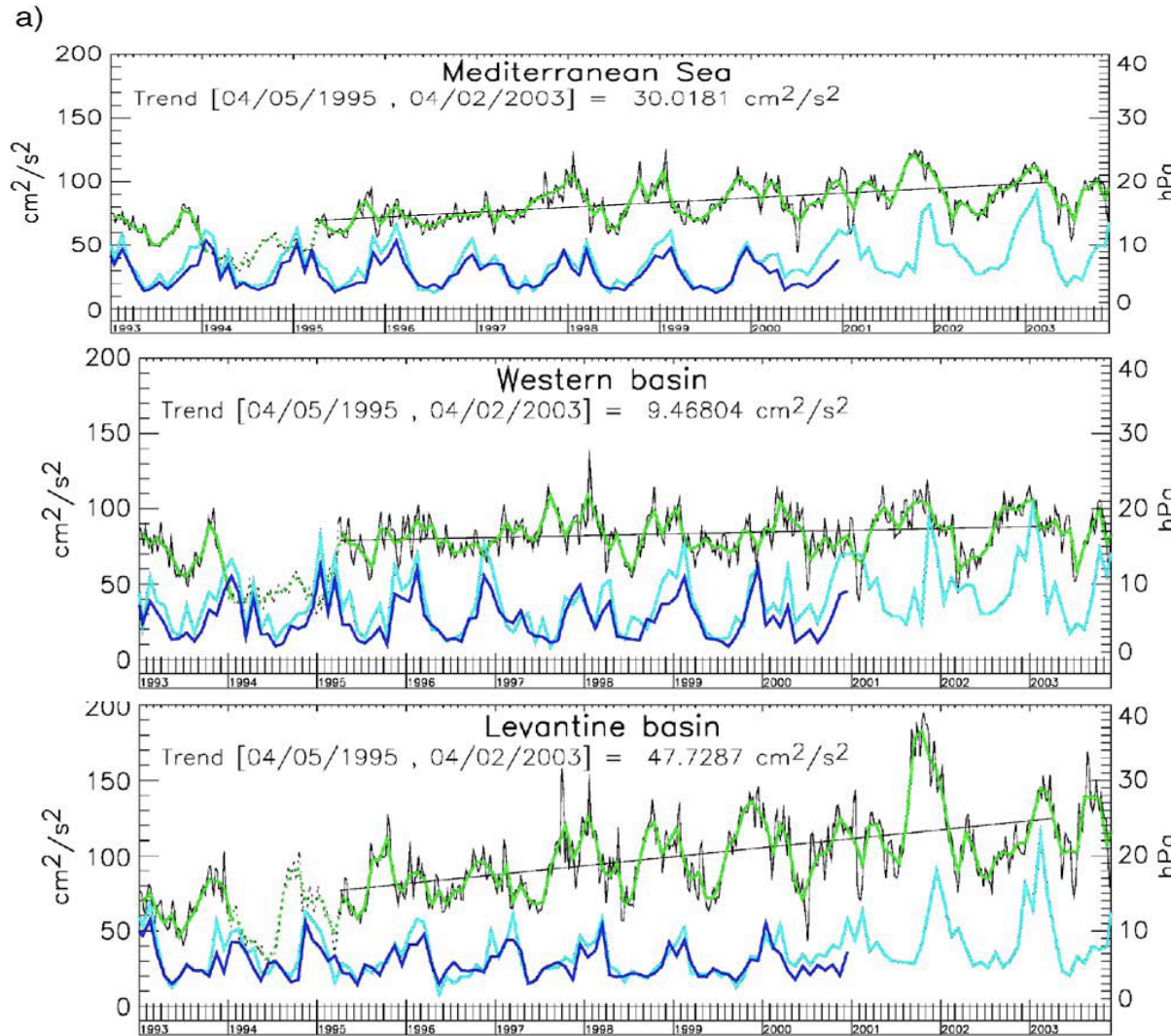
TEMPERATURE



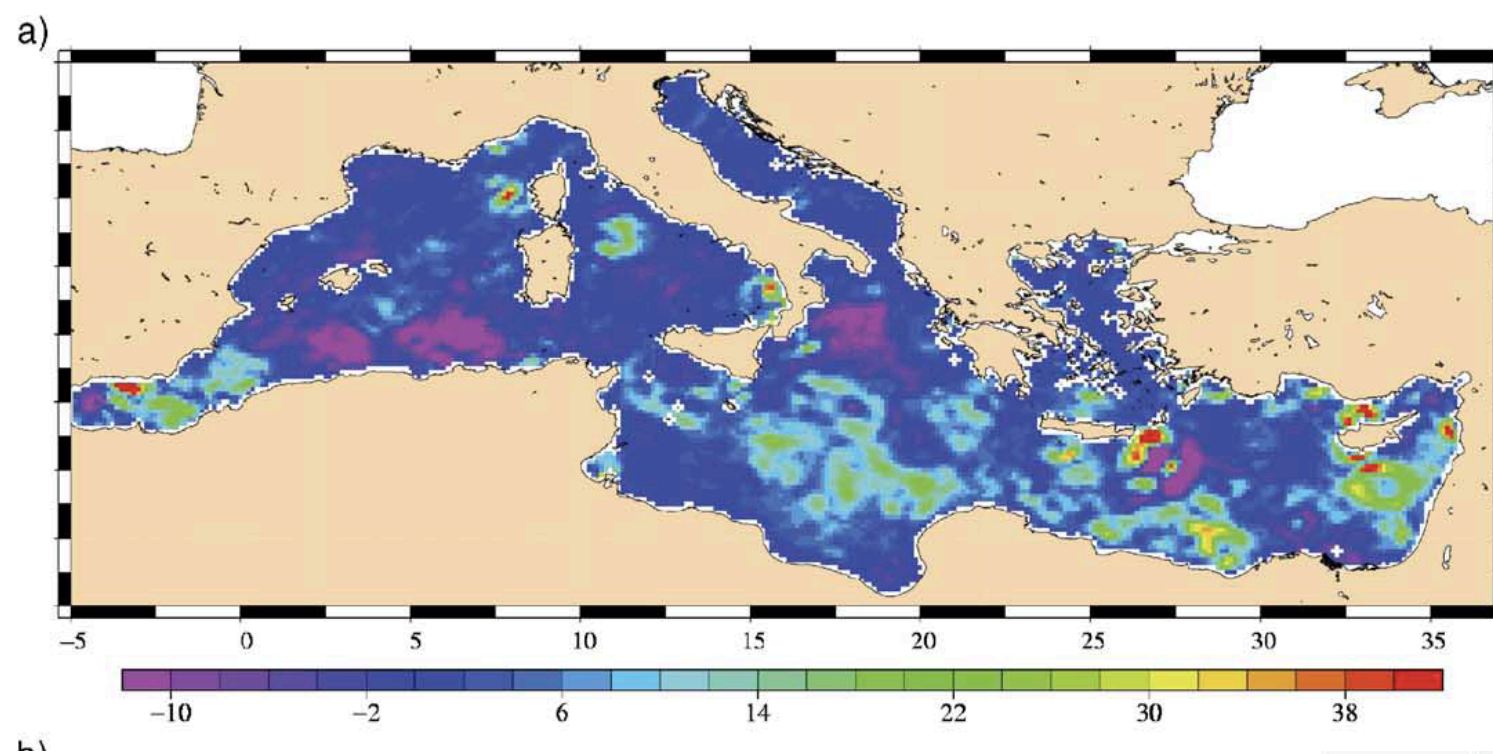
DENSITY



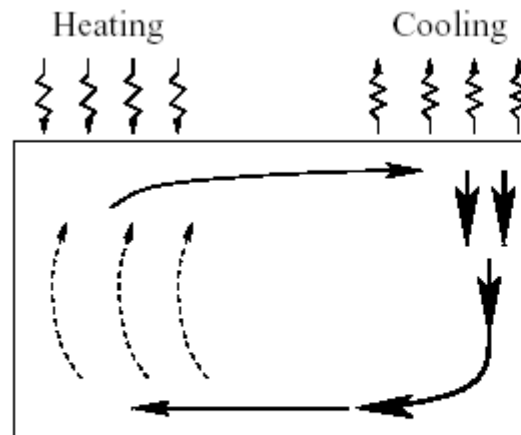
INTERANNUAL VARIABILITY OF THE WIND STRESS



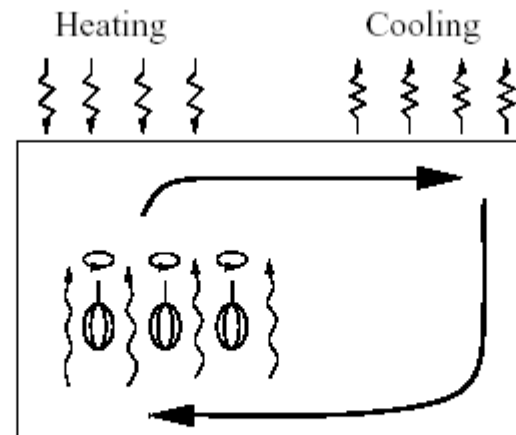
EKE variability, seasonal and interannual variations are predominant components, but mesoscale activity also largely influences EKE variability. The EKE annual cycle study revealed the different behaviour of permanent/recurrent coherent structures



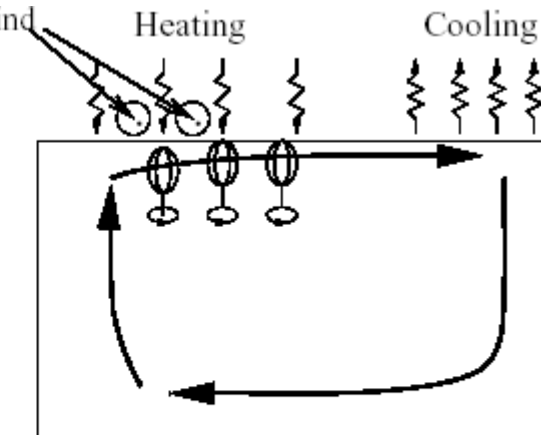
What drives the thermohaline circulation?



a) Pushing by Deepwater Formation

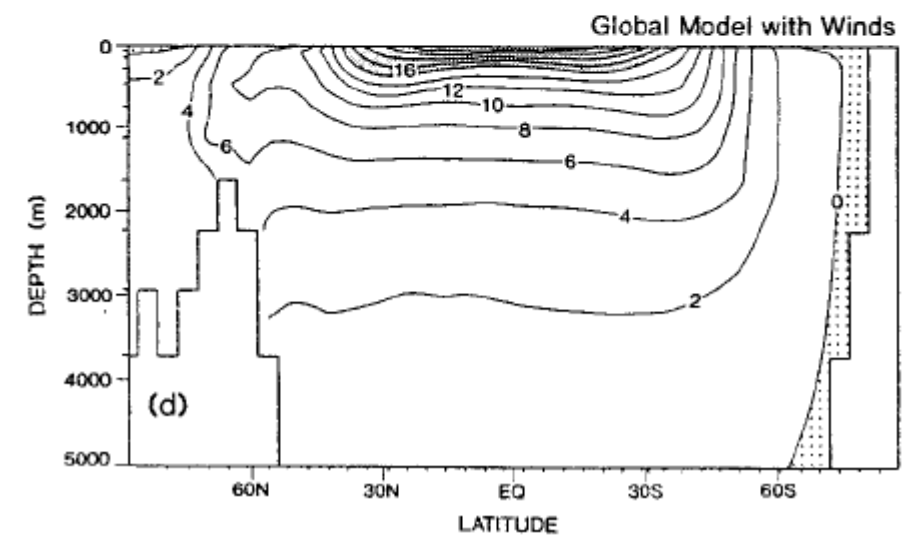
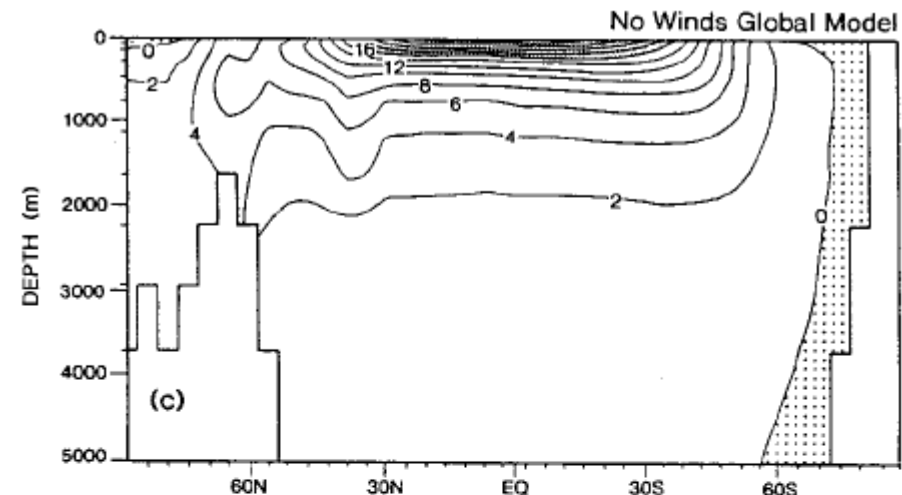
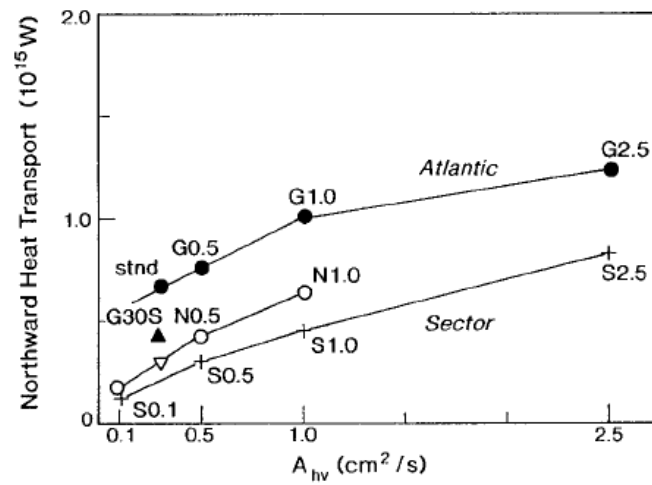
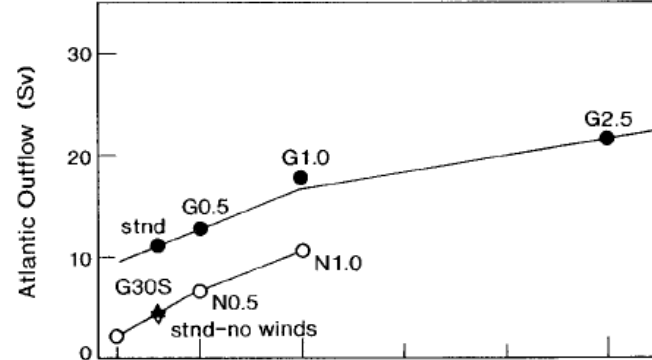


b) Pulling by Deep Mixing

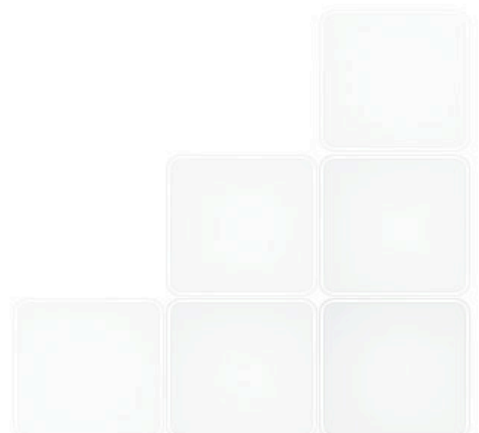


c) Pulling by Wind Stress

Influence of the wind stress on the gyres, vortices and eddies generation and mixing



At mesoscales the ocean is characterized by the presence of coherent vortices, which make it resemble two-dimensional turbulence. Indeed, ocean vortices are known to play a key role in the ocean dynamics due to their effectiveness in moving energy and matter through the ocean and their impact on mixing.



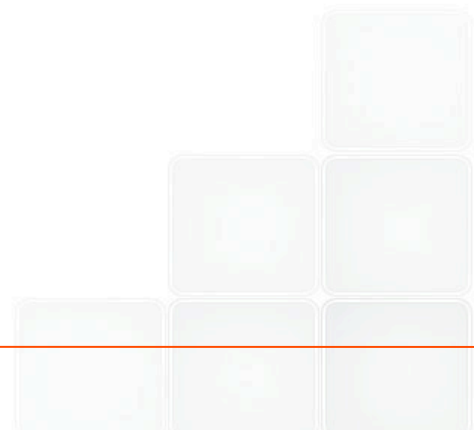
Detection of Coherent structures using a Numerical trajectories in forecasting models



La descrizione del campo di velocità fornita dai modelli operativi (*riferimento Euleriano*) viene utilizzata per calcolare le traiettorie di particelle rilasciate sistematicamente nel dominio di interesse (*riferimento Lagrangiano*)

Il *riferimento Lagrangiano* fornisce informazioni primarie e fondamentali (dove e in quanto tempo va una massa d'acqua) sia nell'ambito dell'oceanografia operativa che nello studio della variabilità climatica;

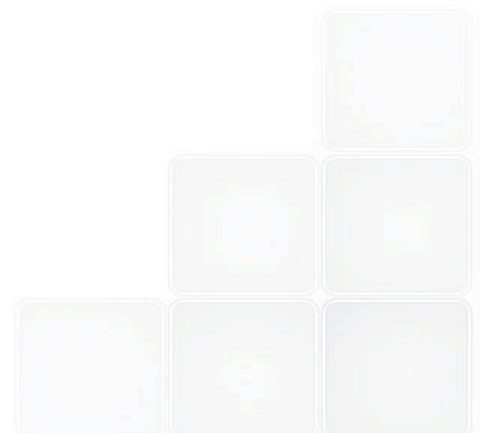
Il *riferimento Lagrangiano* è estremamente sensibile alla variabilità dei campi di velocità euleriani (ne integra nello spazio e nel tempo la variabilità spazio temporale, ed anche gli errori). Campi di velocità Euleriani deterministici possono portare al “*caos Lagrangiano*” (per es. Crisanti et al NC 1991) che si manifesta **anche** attraverso un'estrema sensitività alle condizioni iniziali (particelle rilasciate vicine possono avere traiettorie divergenti).



Strategia di Lavoro, out look della presentazione



- 1) Sono stati adoperati metodi statistici per visualizzare la variabilità stagionale della dispersione prodotta dai modelli MFS, e per effettuare una validazione comparandola con la variabilità stimata da dati di boe derivanti in superficie (Pizzigalli et al JGR 2007, <http://clima.casaccia.enea.it>)
- 2) Sono attualmente usati per definire tecniche di validazione e “prodotti”, da unire all’eventuale “forecast” Lagrangiano, utili ad evidenziare la variabilità della dispersione Lagrangiana (frequenza inerziale, presenza e ruolo delle strutture coerenti [OW e $y=Ta/Tv$] caratteristiche di dispersione relativa – sensibilità condizioni iniziali [FSLE]) .

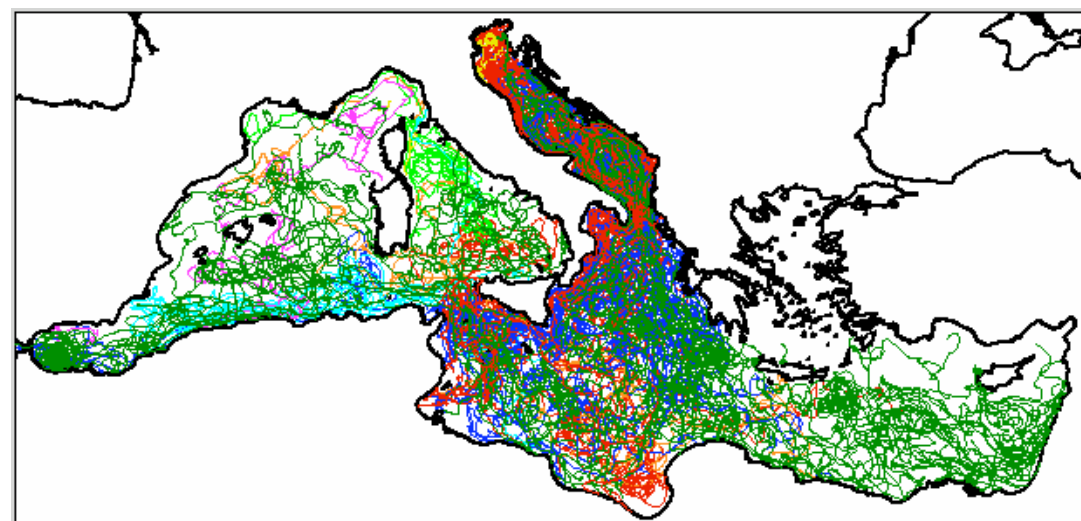


Traiettorie numeriche vs traiettorie di “drifters”



Statistica stagionale della dispersione nel Mediterraneo ottenuta attraverso un sistematico rilascio di particelle in superficie nel modello ‘globale’. Visualizzazione in <http://clima.casaccia.enea.it>

Validazione indiretta: Il “Mediterranean Surface Drifters Data Base” (1986-1999, Poulain 2004), è stato usato per confrontare la variabilità naturale (dati) e numerica (modello globale MFS) della dispersione

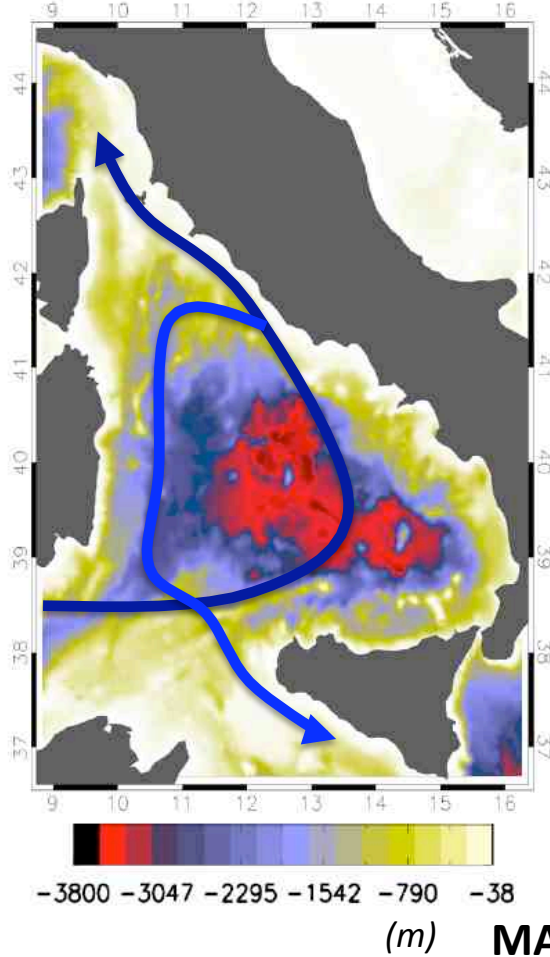


(Pizzigalli et al JGR 2007)

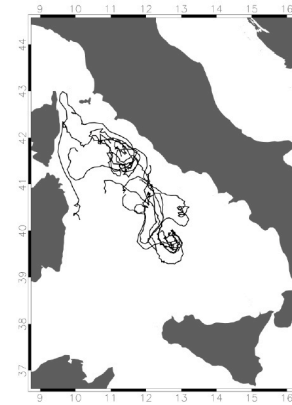
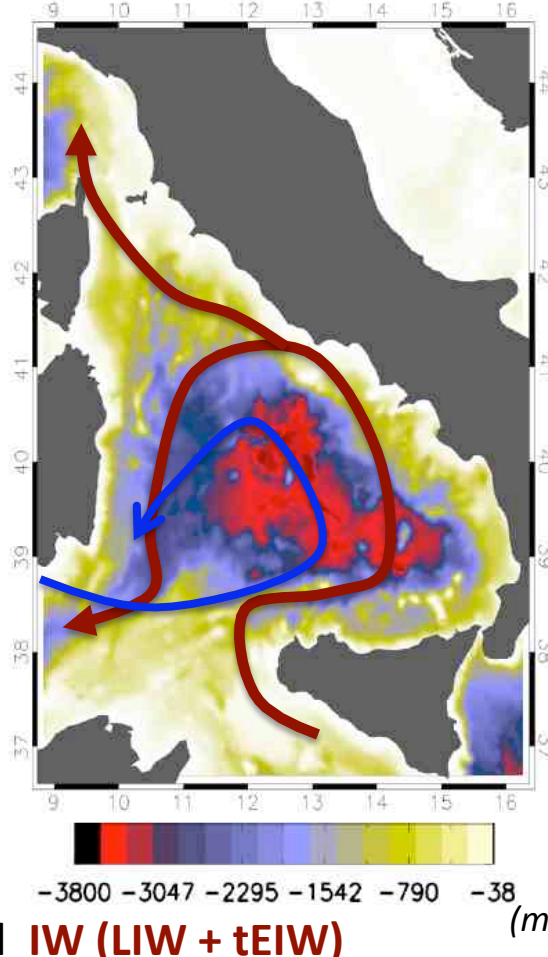
LAGRANGIAN TIME AND LENGTH SCALE IN THE TYRRHENIAN SUB-BASIN



Circolazione superficiale



Circolazione Intermedia e profonda



Scale Lagrangiane
(TEMPO, 1989-1992)

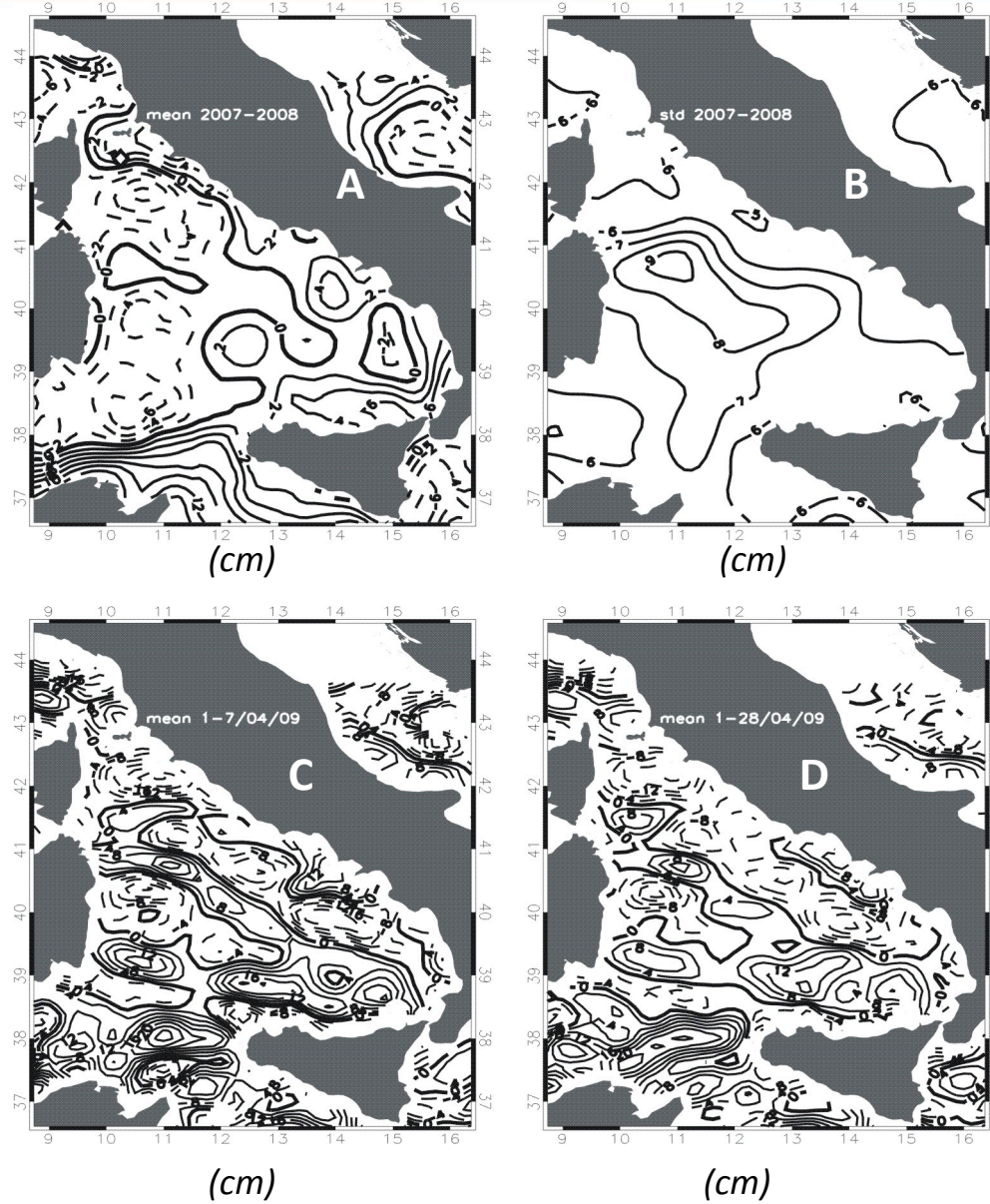
$$T_L \approx 2 \text{ days}$$

$$L_L \approx 25 \text{ Km}$$

$$EKE_L = 270 \text{ cm}^2/\text{sec}^2$$

$$K = 4.7 \times 10^7 \text{ cm}^2/\text{sec}$$

Topografia dinamica, dati AVISO

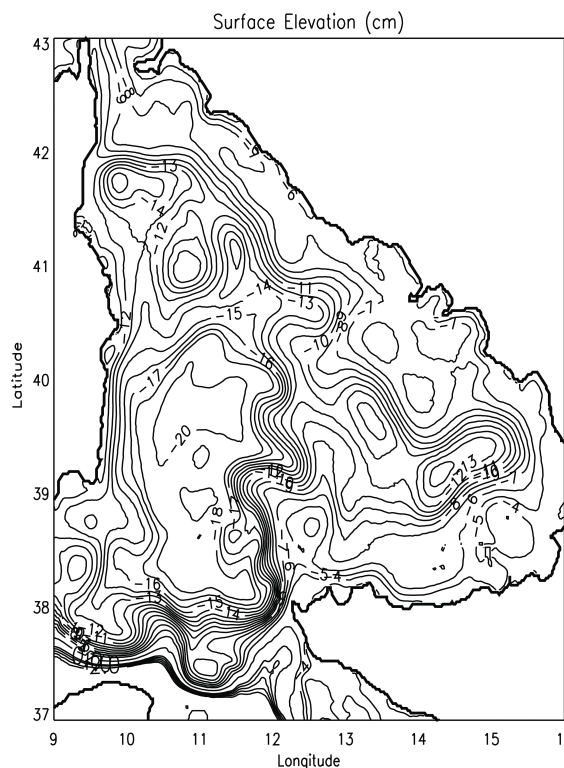


La deviazione standard (B) è più grande della media (A, anni 2007-2008)

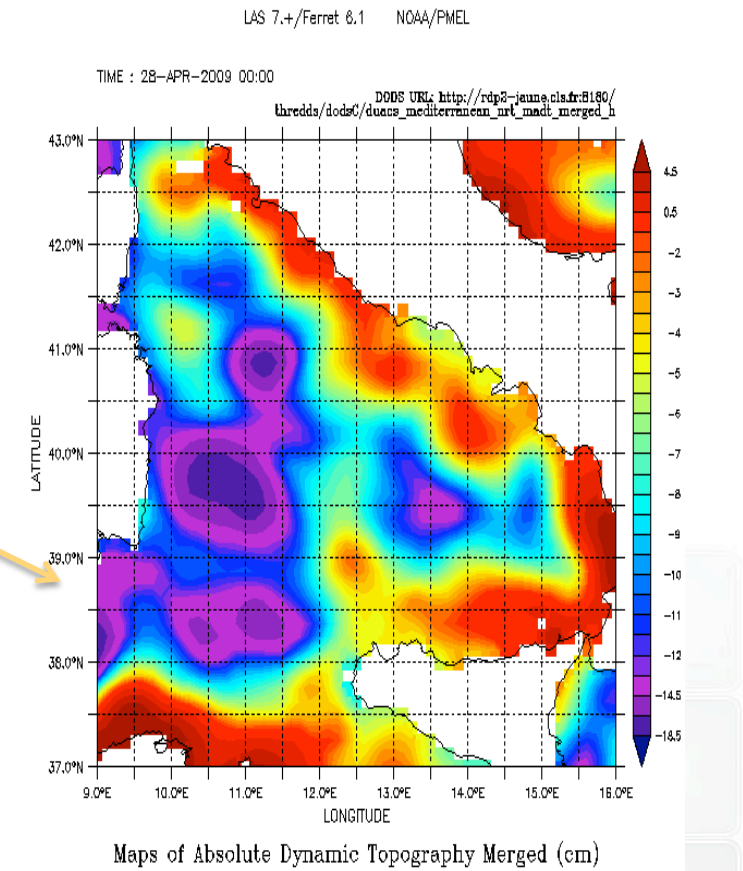
La grande variabilità temporale nel Tirreno è caratterizzata anche dalla presenza di strutture coerenti transienti di scala medio – piccola, (C e D) la cui corretta rappresentazione è fondamentale per il “forecast” Lagrangiano.

Modello operativo Mar Tirreno - ENEA

POM4840: $1/48^\circ \times 1/48^\circ \times 40$ livelli, operativo da Marzo 2009, fornisce “forecast” di 7 giorni ogni giorno. Le condizioni al contorno sono date dal modello globale OPA1671 dell’INGV.



28 Aprile 2009:
confronto (elevazione)
tra “forecast” dati
altimetrici



Algoritmo di integrazione e metodologia



Le traiettorie sono state calcolate usando l'algoritmo Runge-Kutta del II° ordine integrando l'equazione di avvezione senza nessun termine di diffusione.

Le particelle sono considerate traccianti ideali che non influiscono sul campo di velocità e non sono soggette a nessun tipo di trasformazione.

Le particelle sono sistematicamente rilasciate in superficie e vengono integrate considerando il campo di velocità 2D bidimensionale (componente verticale $W=0$, simulazione di oggetti galleggianti) dei modelli operativi del Mar Tirreno POM4840).

Come campo Euleriano viene utilizzato quello di Aprile 2009. Le analisi di decorrelazione vengono effettuate prima su serie di 28 giorni (1-28 Aprile) e poi di 10 giorni (massima estensione dei “forecast”)

Grandezze considerate per caratterizzare il bacino : frequenza inerziale, OW, EKE_L , T_v , T_a , $y=T_a/T_v$, K, FSLE

The quantity $OW = (\text{strain})^2 - (\text{vorticity})^2$

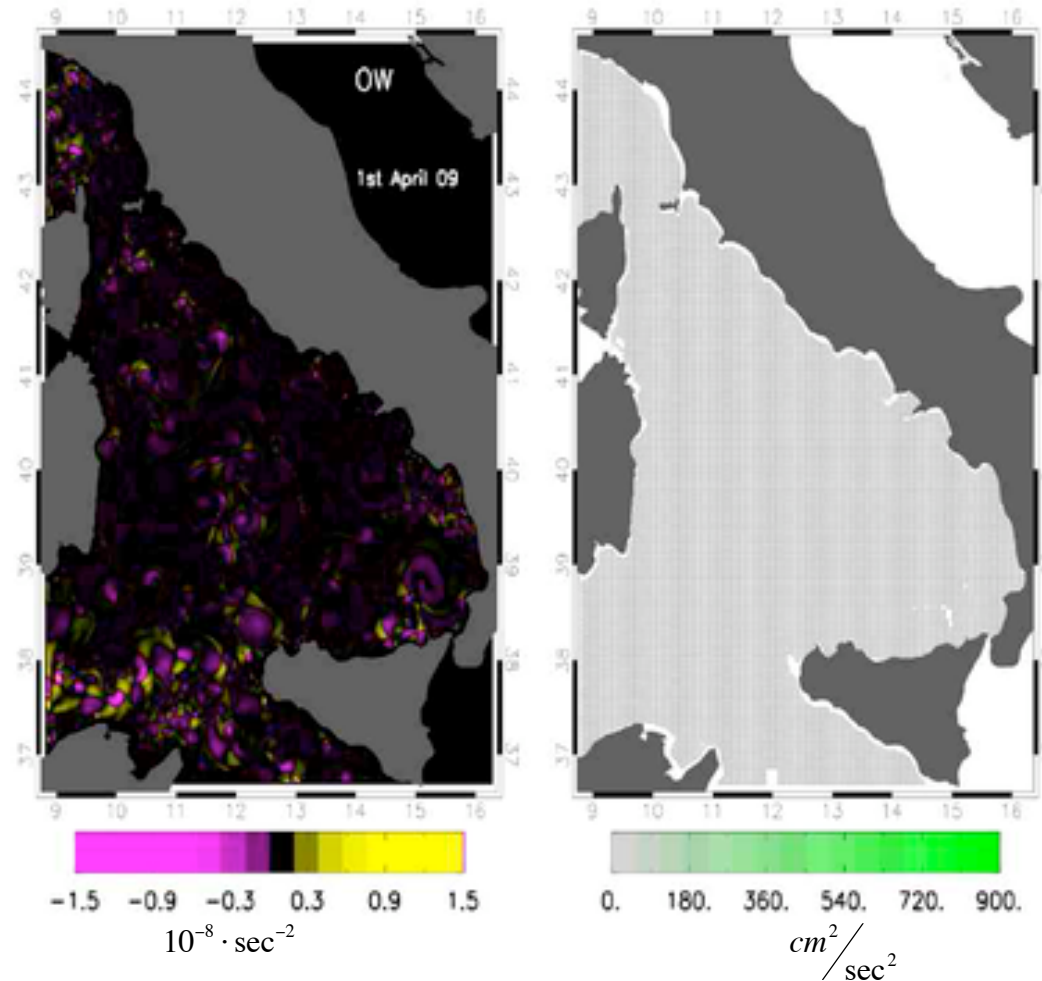


In order to be successful in this approach to the dynamics of the ocean a robust vortex detection algorithm is necessary. A possible choice of such a criterion is one based on the sign of the Okubo-Weiss parameter (Okubo 1970, Weiss 1991), which measures the relative contribution of deformation and vorticity.

Then, a coherent vortex can be defined as the simply connected region with negative values of the Okubo-Weiss parameter. Besides this definition only captures vortex cores, it has been shown that this method is adequate to detect marine eddies in model output. When a vortex, or its core, has been identified it is possible to estimate the individual properties of the vortex such as size, mean kinetic energy and amplitude and then analyze its statistical distribution.

Furthermore, it has been shown that these very coherent vortices are the principal responsible for the non-Gaussian behavior of the Velocity Probability Density Functions having a great impact on the dispersion and mixing processes (Isern-Fontanet et al. 2005b).

67931 particelle numeriche nel Mar Tirreno



67931 sono rilasciate in superficie ($1/48^\circ \times 1/48^\circ$) ed integrate usando i campi di velocità dal 1° al 28 Aprile 2009

$$OW = s_n^2 + s_s^2 - \omega^2$$

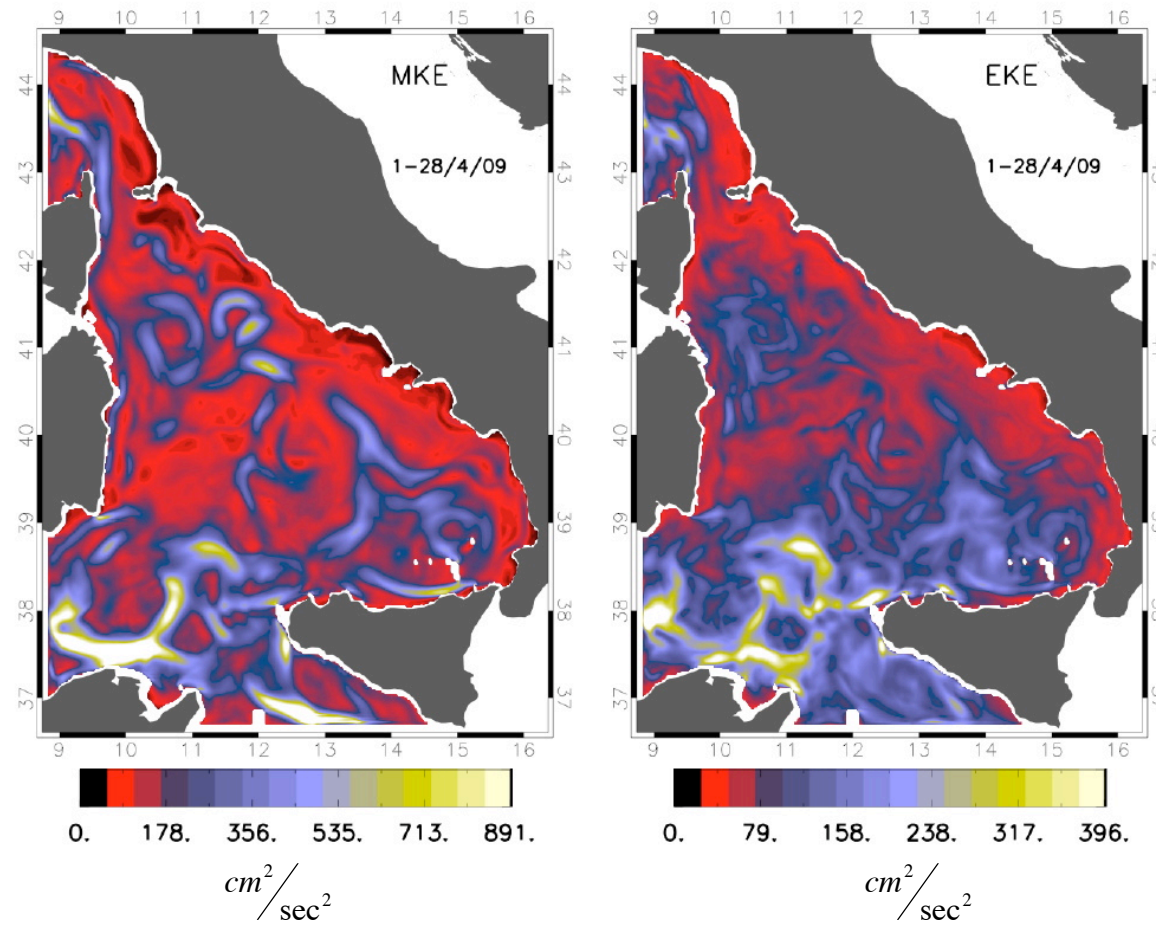
$$\omega = \frac{\partial v}{\partial x} - \frac{\partial u}{\partial y}$$

$$s_n = \frac{\partial u}{\partial x} - \frac{\partial v}{\partial y}$$

$$s_s = \frac{\partial v}{\partial x} + \frac{\partial u}{\partial y}$$

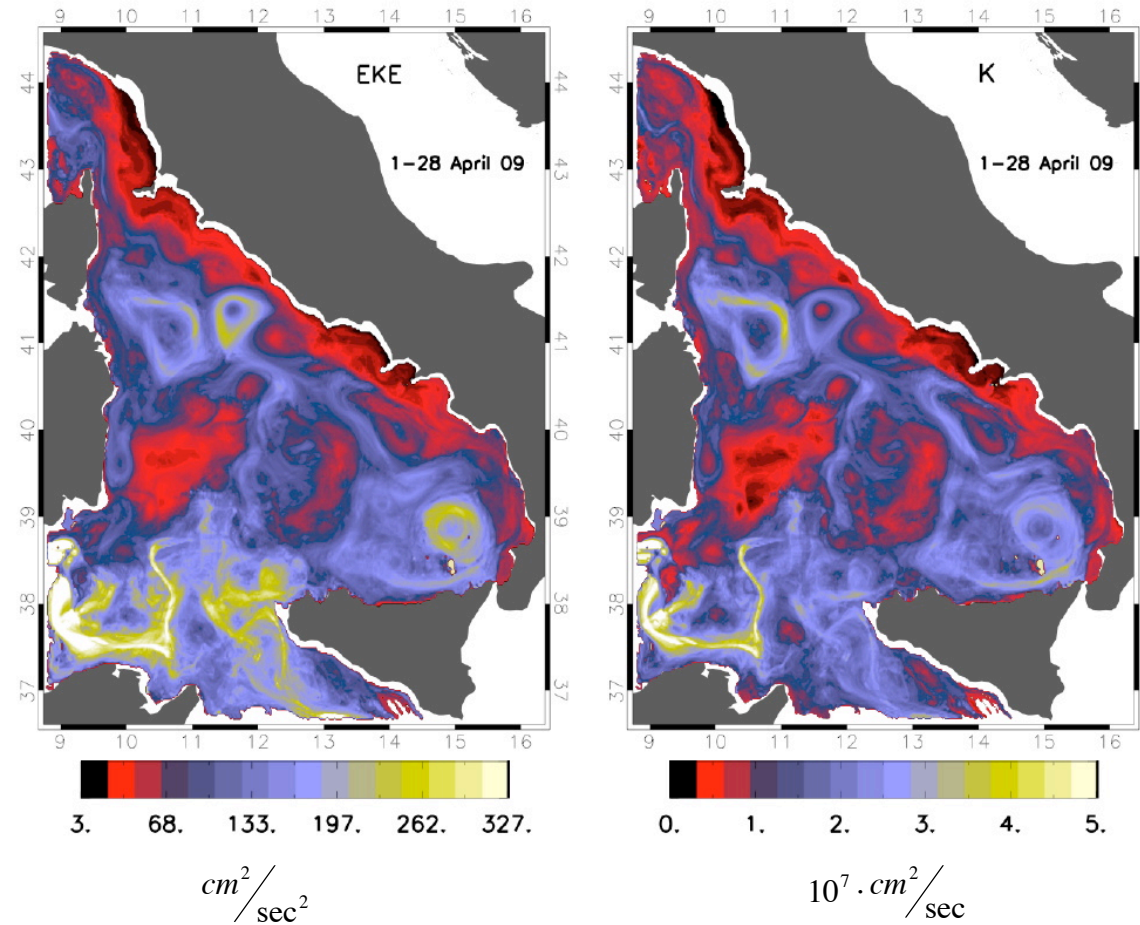
parametro di Okub-Weiss

Energia media e “Eddy Kinetic Energy” Euleriane



28 giorni

“Eddy Kinetic Energy” Lagrangiana e “proxy” del coefficiente di diffusione



$$K = EKE \times T_L$$

dimensionalmente
omogeneo al
coefficiente di
diffusione, ne è
solo un proxy

28 giorni

Finite Size Lyapunov Exponent (FSLE)



Esponente di Lyapunov: tasso di divergenza esponenziale mediato per tempi finiti e per particelle infinitesimalmente vicine al tempo iniziale

FSLE: generalizzazione dell'esponente di Lyapunov per studiare moti non asintotici,
Utile a caratterizzare la dispersione relativa utilizzando dati reali (Artale et al. 1997)

Data una distanza iniziale di separazione δ_0 , una distanza finale di separazione δ_f ,
Per ogni x e t_0 , λ (FSLE) è definito come:

$$\lambda(\vec{x}, t_0, \delta_0, \delta_f) = \frac{1}{\tau} \ln \left(\frac{\delta_f}{\delta_0} \right)$$

dove τ è il tempo in cui viene due particelle inizialmente separate da una distanza δ_0
Raggiungono la distanza di separazione δ_f ,

Integrando avanti nel tempo le linee di grande λ (separazione veloce) definiscono le superfici instabili

Integrando indietro nel tempo, le linee di grande λ (separazione veloce, equivalente a massima convergenza) definiscono le superfici stabili che possono essere interpretate come fronti

Il flusso Lagrangiano è organizzato all'interno di queste superfici, non le attraversa

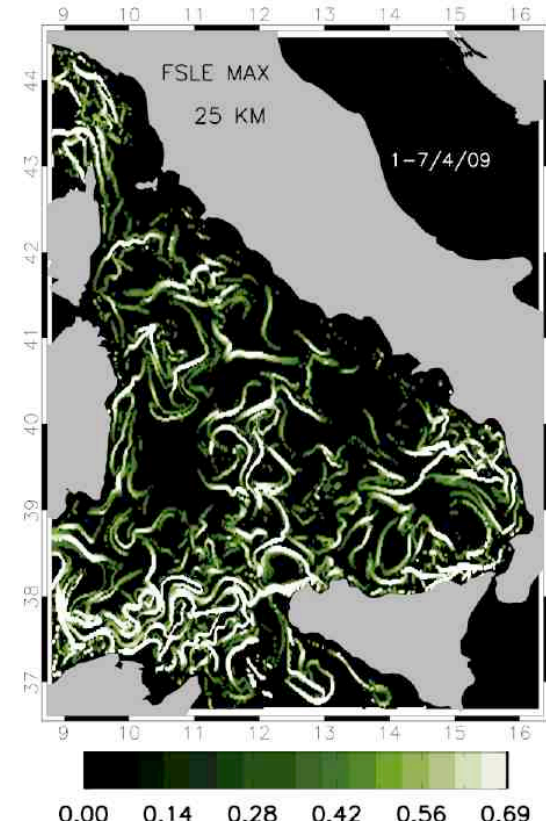
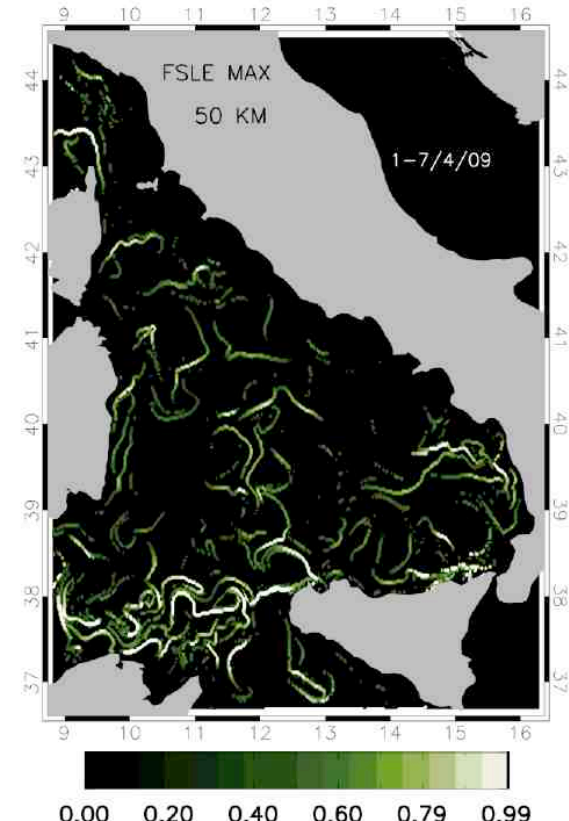
Finite Size Lyapunov Exponent (FSLE)

(integrazione in avanti nel tempo)



$\delta_0 = 1/48^\circ$

$\delta_f = 50 \text{ Km}$



$\delta_0 = 1/48^\circ$

$\delta_f = 25 \text{ Km}$

7 giorni

$$\lambda(\vec{x}, t_0, \delta_0 \delta_f) = \frac{1}{\tau} \ln \left(\frac{\delta_f}{\delta_0} \right)$$

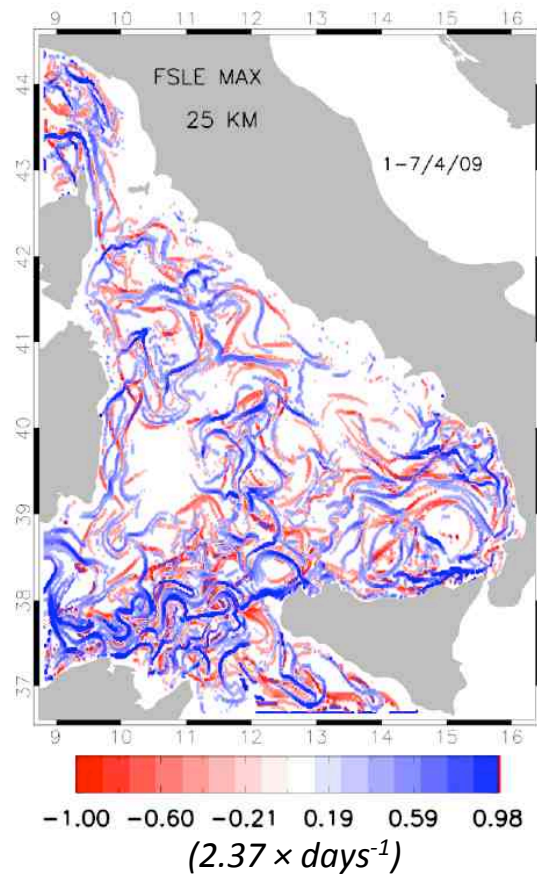
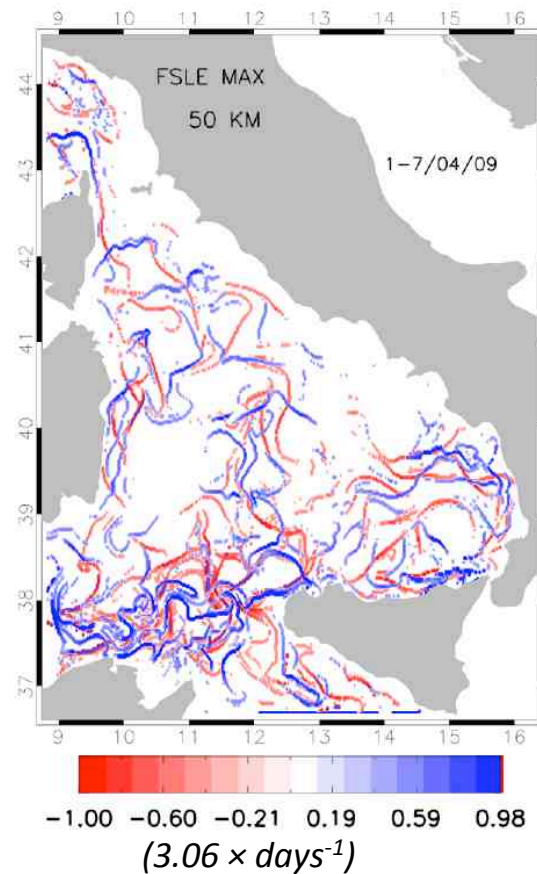
Finite Size Ljapunov Exponent (FSLE)

(integrazione avanti ed indietro nel tempo)

$$\delta_0 = 1/48^\circ$$

$$\delta_f = 50 \text{ Km}$$

Rosso = integrazione
indietro nel tempo,
per convenzione
valori negativi



$$\delta_0 = 1/48^\circ$$

$$\delta_f = 25 \text{ Km}$$

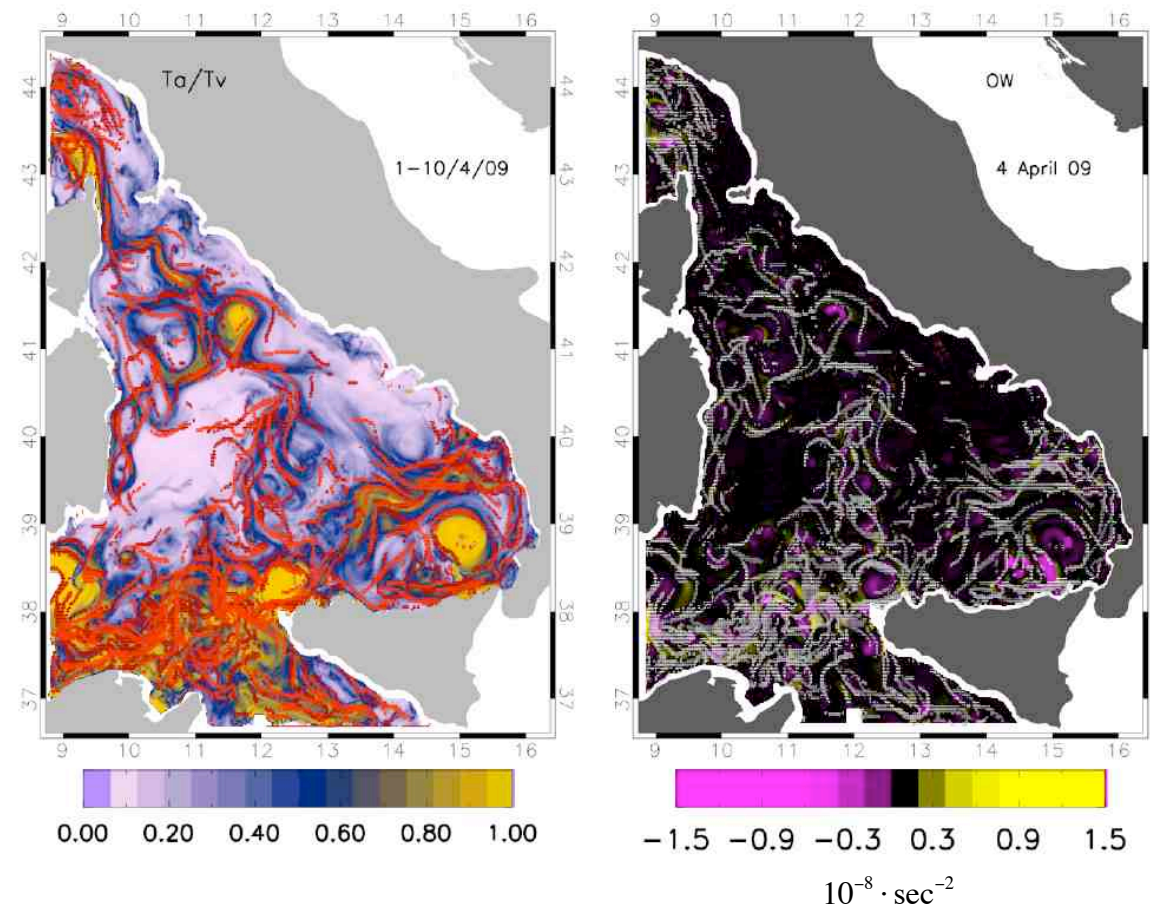
Blu = integrazione
avanti nel tempo,
valori positivi

7 giorni

$$\pm \lambda(\vec{x}, t_0, \delta_0 \delta_f) = \frac{1}{\tau} \ln \left(\frac{\delta_f}{\delta_0} \right)$$

Prodotti su scale temporali caratteristiche del forecast

$$y = \frac{T_a}{T_v} + FSLE$$



Smoothing 12 ore

OW+ FSLE

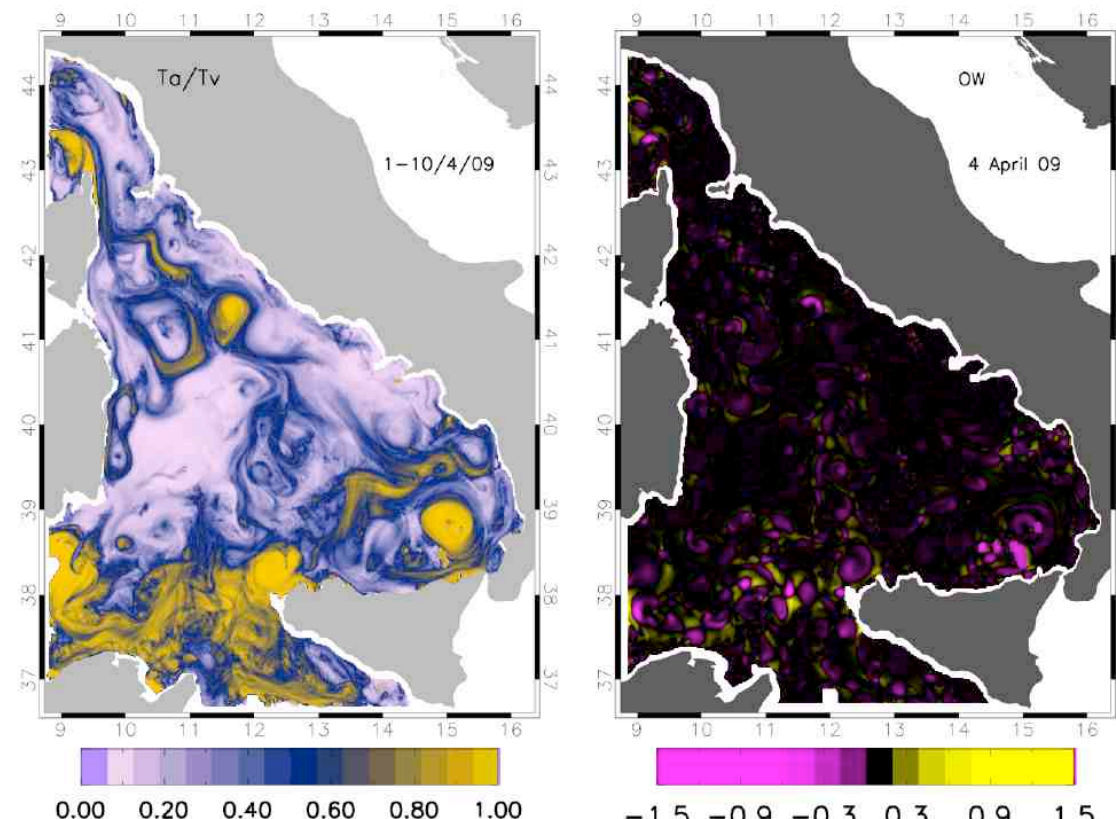
I risultati dalle tre tecniche sono coerenti, le due tecniche
Lagrangiane Definiscono meglio le strutture coerenti

7 e 10 giorni

$T_a/T_v + OW$



$$y = \frac{T_a}{T_v}$$



Smoothing 12 ore

$10^{-8} \cdot \text{sec}^{-2}$

7 e 10 giorni

Sommario e Prospettive

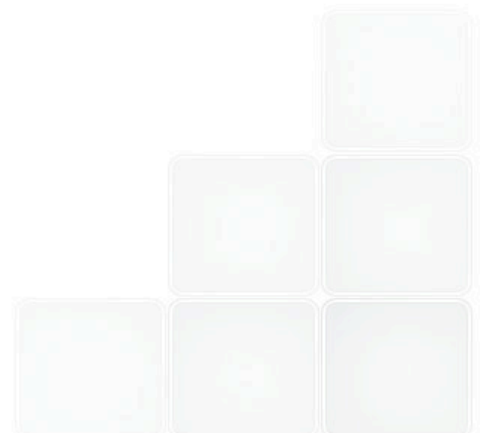


I modelli operativi regionali “devono” rappresentare le strutture coerenti transienti per poter essere di utilità nella previsione della dispersione Lagrangiana. Le tecniche Lagrangiane mostrate in questa presentazione sono utili a definire spazialmente le strutture coerenti. In particolare il metodo del rapporto tra scale di accelerazione e velocità funziona anche sulle scale temporali del “forecast”. E’ così possibile (lavoro in prospettiva) accanto al semplice “forecast” lagrangiano:

- fornire delle mappe sintetiche che individuino le caratteristiche qualitative della dispersione numerica (frequenza inerziale, rapporto tra T_a e T_v) ed individuino i punti critici (numerici) in cui è più grande la dipendenza dalle condizioni iniziali
- costruire un sistema di analisi di dati per la validazione dei modelli, comparando le strutture rappresentate dai modelli con i dati satellitari (altimetro e SST).
- utilizzare i prodotti giornalieri dei “forecast” per costruire una statistica e calcolare le medie di T_a/T_v e FSLE per caratterizzare il bacino a grande scala (zone dove è più probabile avere certe caratteristiche di dispersione)

Abrupt change of the Mediterranean thermohaline circulation: Eastern Mediterranean Transient (EMT)

the western and eastern sub-basins are disconnected at deep levels and their thermohaline circulation are driven by the respective sources. The eastern is a closed cell endowed with multiple equilibria (EMT), in the western sub-basin observational and modelling studies are lacking



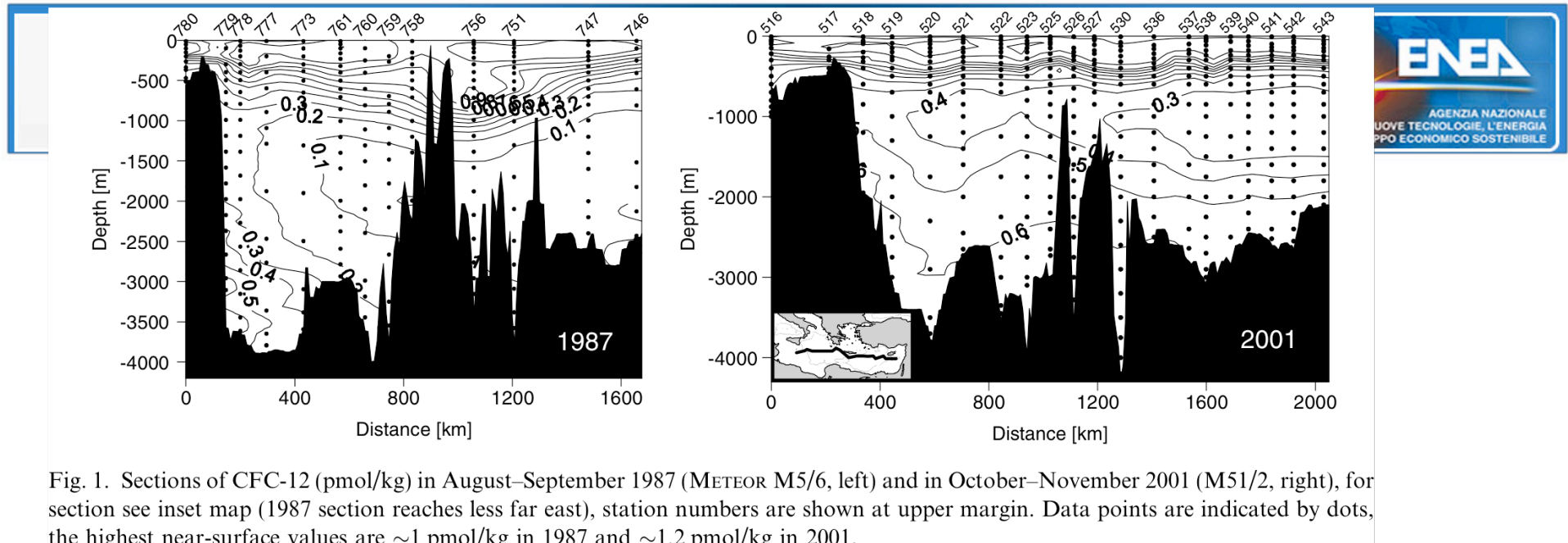


Fig. 1. Sections of CFC-12 (pmol/kg) in August–September 1987 (METEOR M5/6, left) and in October–November 2001 (M51/2, right), for section see inset map (1987 section reaches less far east), station numbers are shown at upper margin. Data points are indicated by dots, the highest near-surface values are ~ 1 pmol/kg in 1987 and ~ 1.2 pmol/kg in 2001.

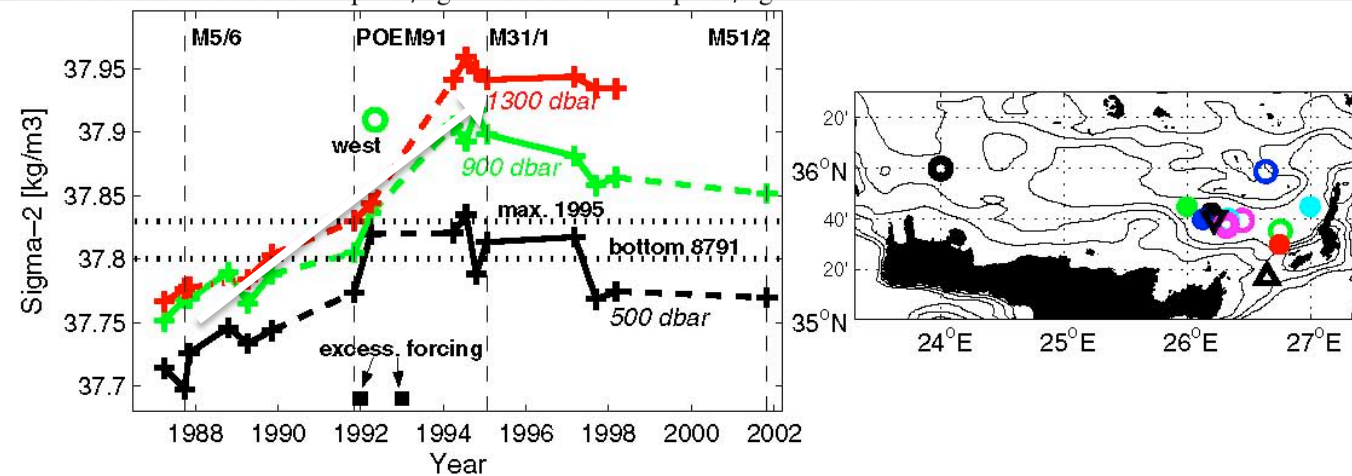


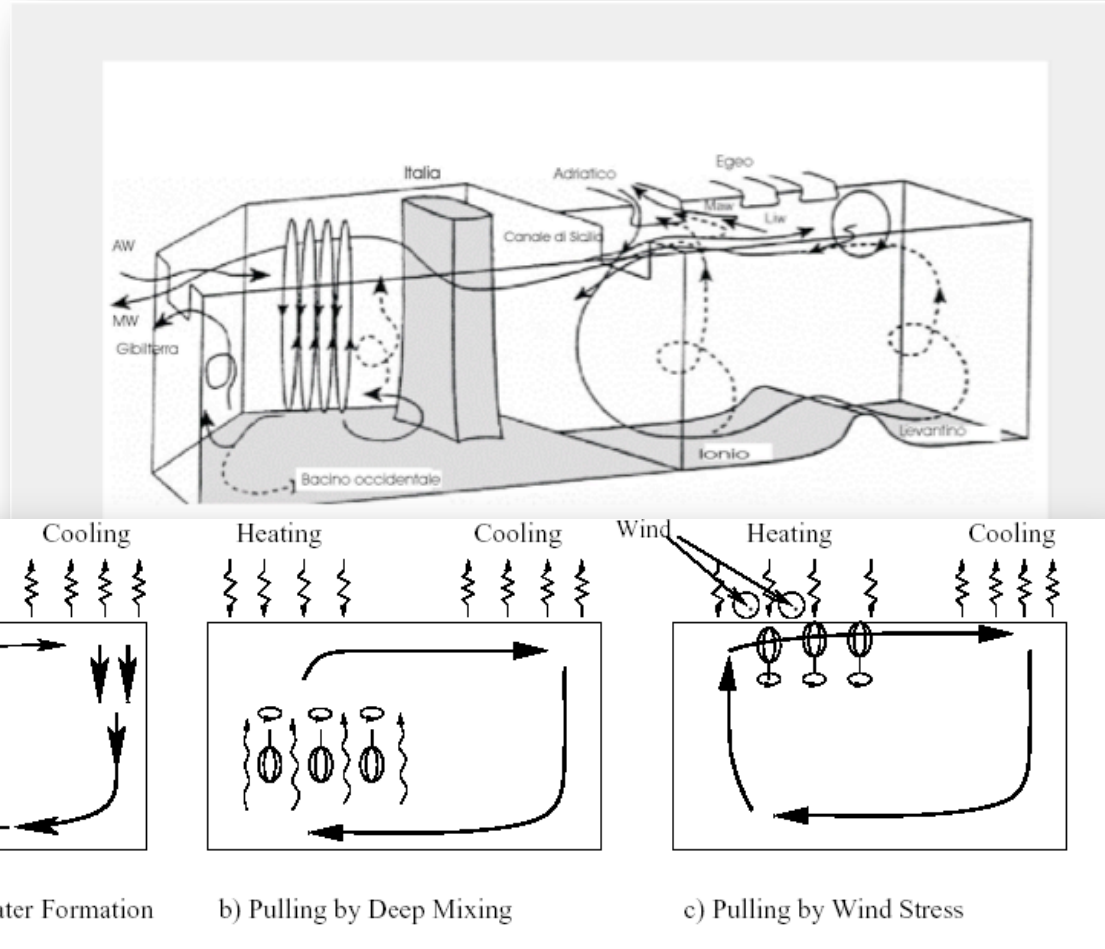
Fig. 10. Density (σ_2) at depths of 500, 900, and 1300 dbar, 1987–2001, for the southeast Aegean stations shown in Fig. 9, and additionally for MATER 1 Sta. msb7 (March 1997) MATER 2 msb7a (September 1997; AEGAEQ, inverted triangle), and for M51/2 534 (9–2001; upright triangle) in the Kasos channel; for positions see adjoined map (coloring as in Fig. 9, thin open symbols: 1987–1989, thicker open symbols: 1991–1992, full symbols: 1994–1998; isolines are 500, 900 and 1300 m). The year marks stand for 1 January of the year. Also shown are the 1992 900 dbar value for the western station included in Fig. 9, and the bottom density in 1987–1991 and the maximum density observed in 1995 outside the Cretan Arc (dotted horizontal lines). Also shown are the periods of four major hydrographic surveys (cf. Figs. 5–7), and of the excess winter forcing according to Josey (2003).

The Mediterranean is an evaporative basin and the Gibraltar strait is a source of intermediate water



In the 90' have been observed dramatic changes in the deep water formation and in the vertical stratification in the EM. How/when they reflect in the Gibraltar Output ?

What drives the thermohaline circulation? (multi-decadale scale)



circolazione termoalina



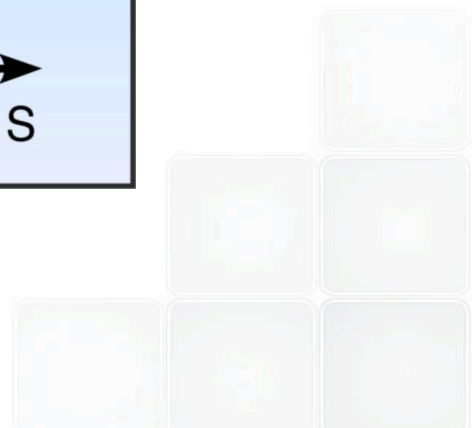
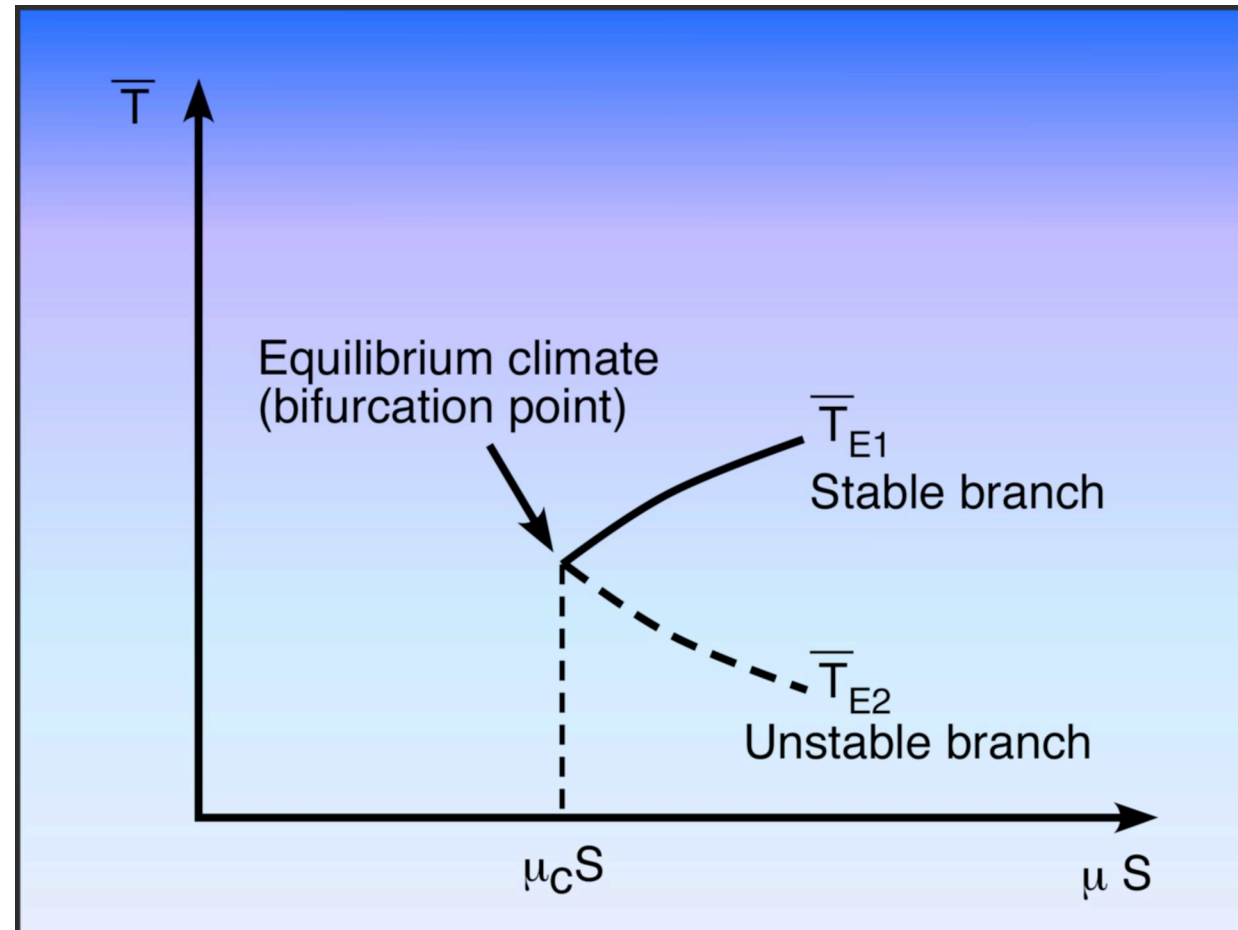
temperature change + temperature advection =
heating/cooling term + diffusion

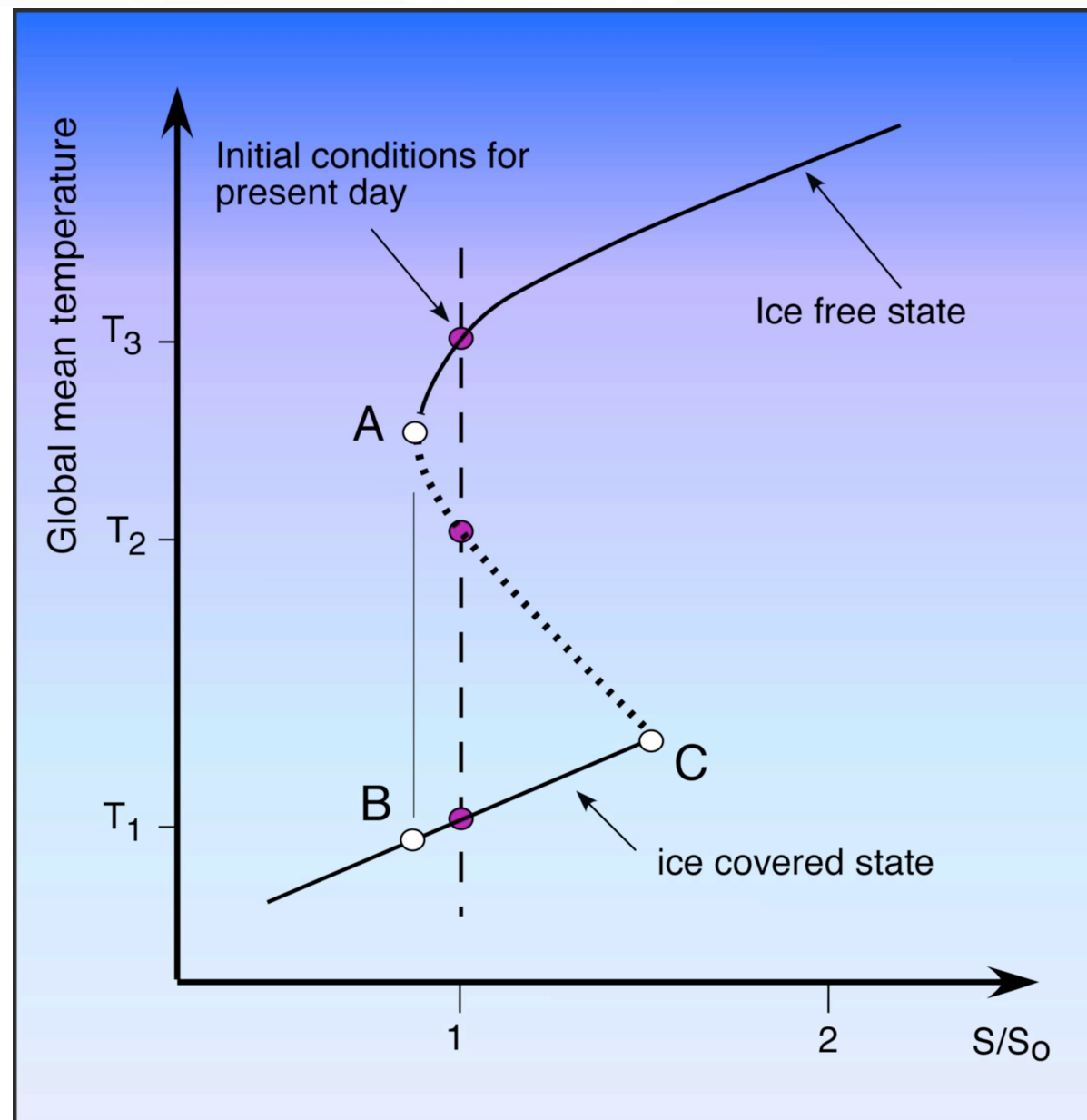
salinity change + salinity advection =
evaporation/precipitation/brine
rejection + diffusion (8.42b)

For the mathematically-oriented reader, these equations are:

$$\frac{\partial T}{\partial t} + u \frac{\partial T}{\partial x} + v \frac{\partial T}{\partial y} + w \frac{\partial T}{\partial z} = Q_H / \rho c_p + \frac{\partial}{\partial x} (\kappa_H \frac{\partial T}{\partial x}) + \frac{\partial}{\partial y} (\kappa_H \frac{\partial T}{\partial y}) + \frac{\partial}{\partial z} (\kappa_V \frac{\partial T}{\partial z}) \quad (8.43a)$$

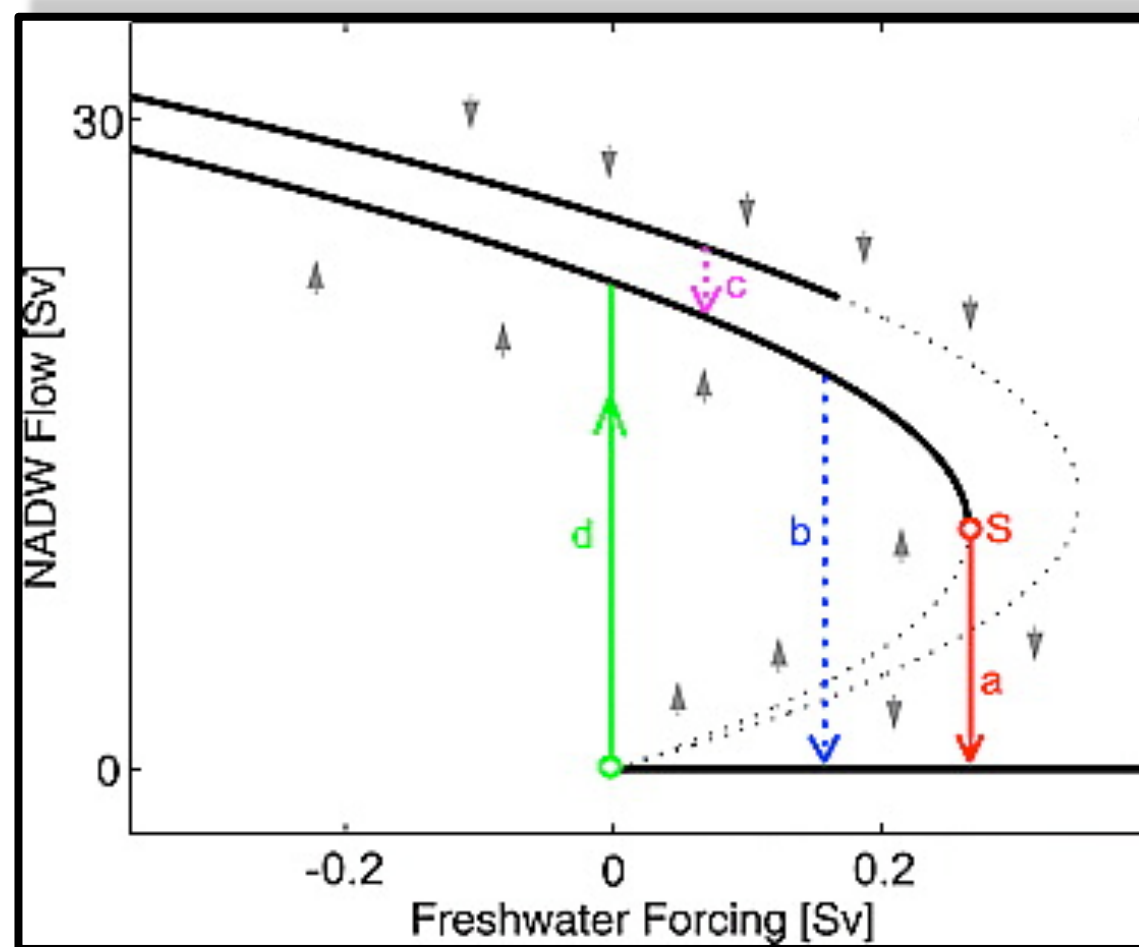
$$\frac{\partial S}{\partial t} + u \frac{\partial S}{\partial x} + v \frac{\partial S}{\partial y} + w \frac{\partial S}{\partial z} = Q_S + \frac{\partial}{\partial x} (\kappa_H \frac{\partial S}{\partial x}) + \frac{\partial}{\partial y} (\kappa_H \frac{\partial S}{\partial y}) + \frac{\partial}{\partial z} (\kappa_V \frac{\partial S}{\partial z}) \quad (8.43b)$$





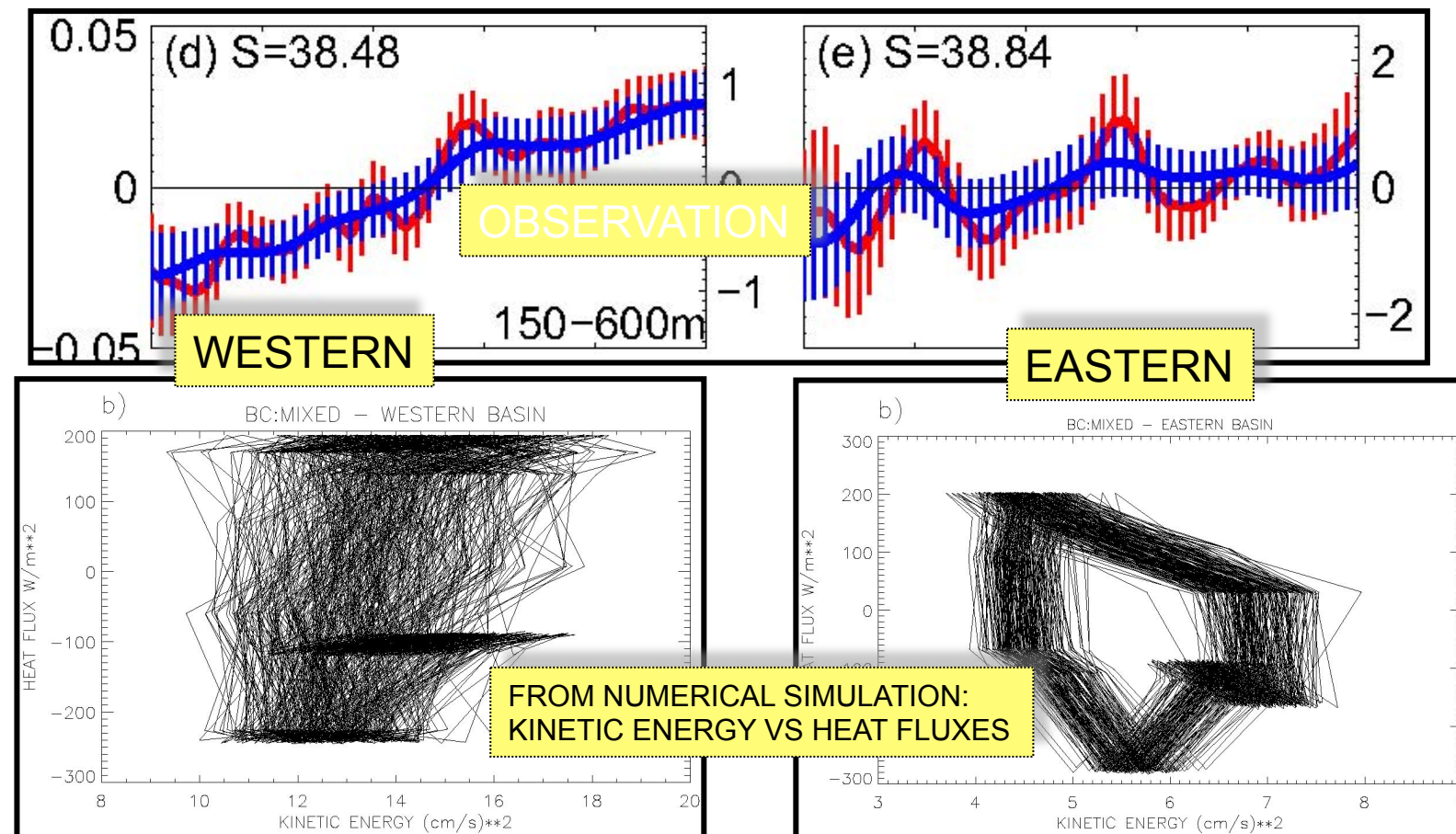
LA RISPOSTA DEL SISTEMA CLIMATICO AI FORZANTI ESTERNI (E.G. SCIOLIMENTO DEI GHIACCIAI) HA UN COMPORTAMENTO NON-LINEARE TIPO *ISTERESI* (ovvero un *giro sulle montagne russe*) OSSIA PER VALORI CRITICI DEI FORZANTI IL SISTEMA

CROLLA PER POI RECUPERARE PER UN PERCORSO DIVERSO DA QUELLO PRECEDENTE

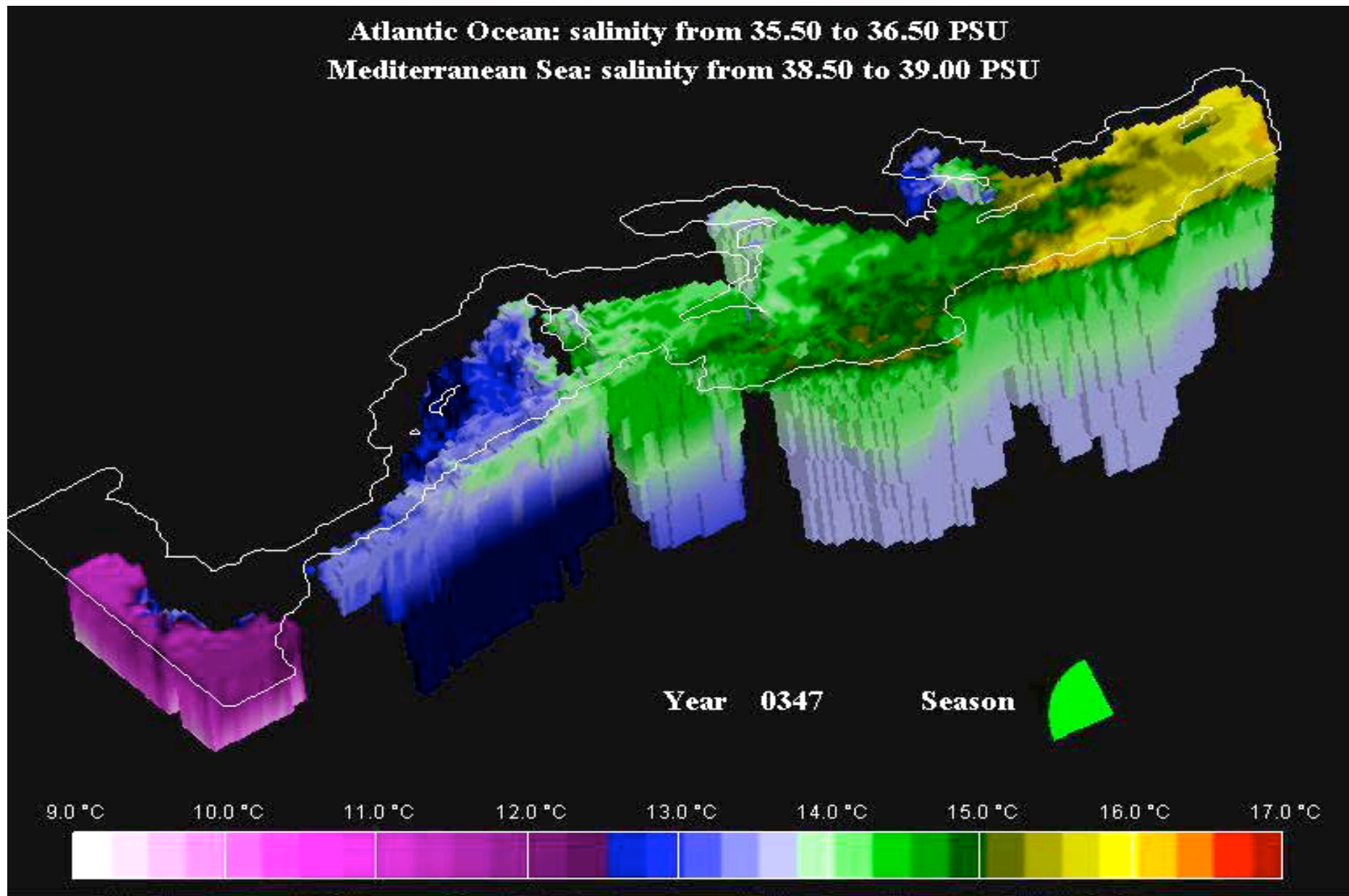


COMPARISON BETWEEN THE TWO SUB-BASINS IN TERMS OF USING NUMERICAL MODELS AND OBSERVATIONS

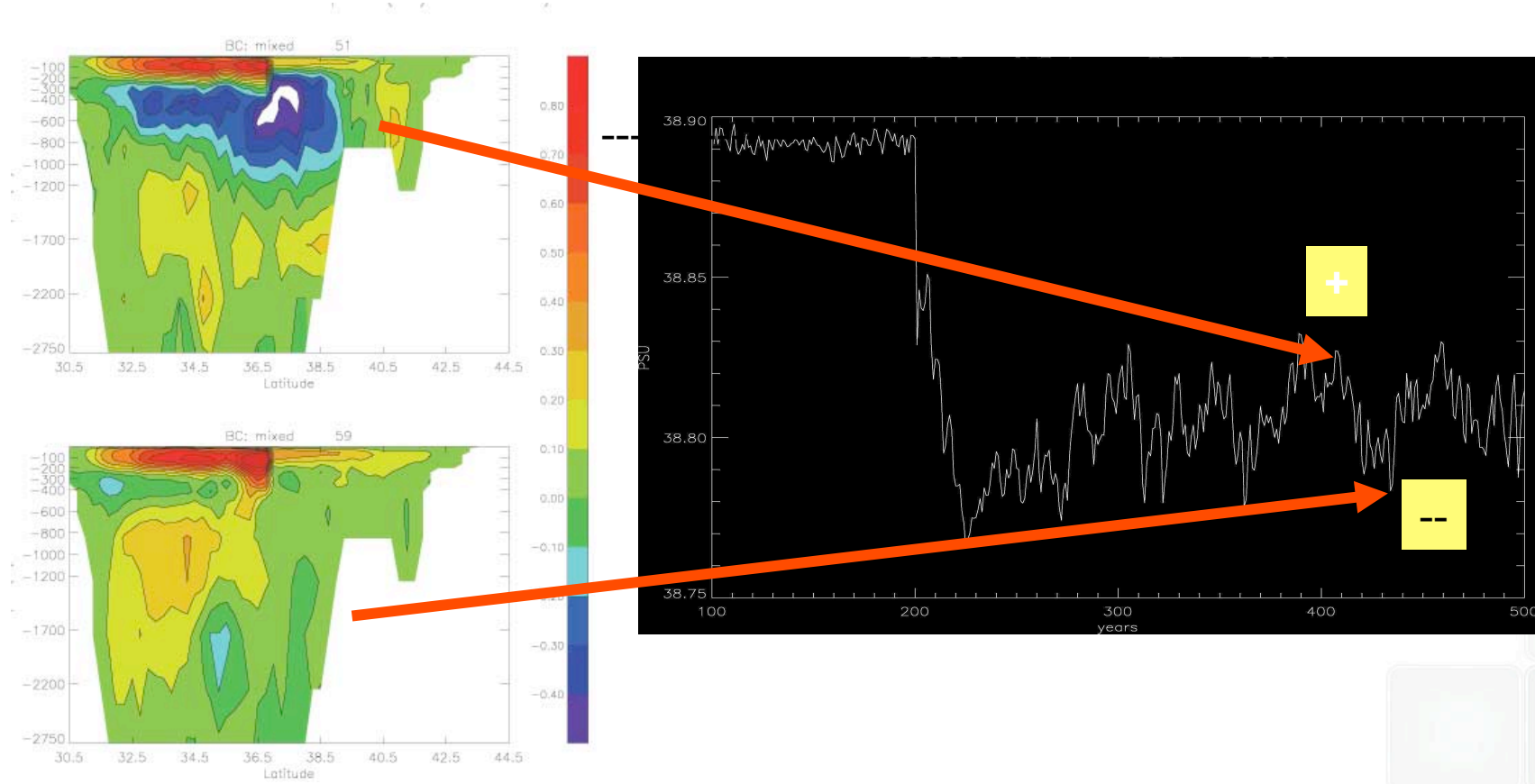
(Pisacane et al. 2006)



Internal variability of the Mediterranean Sea

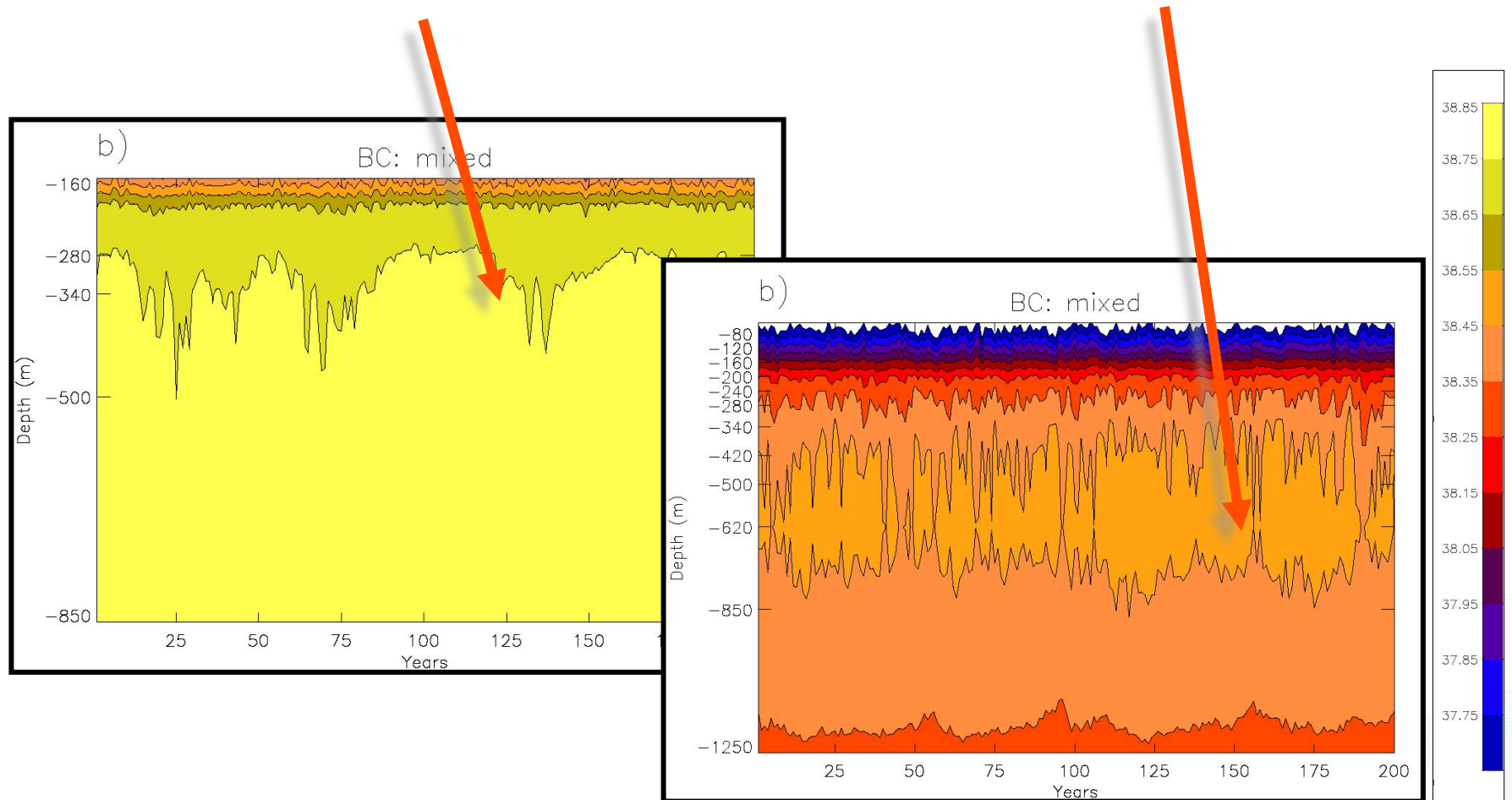


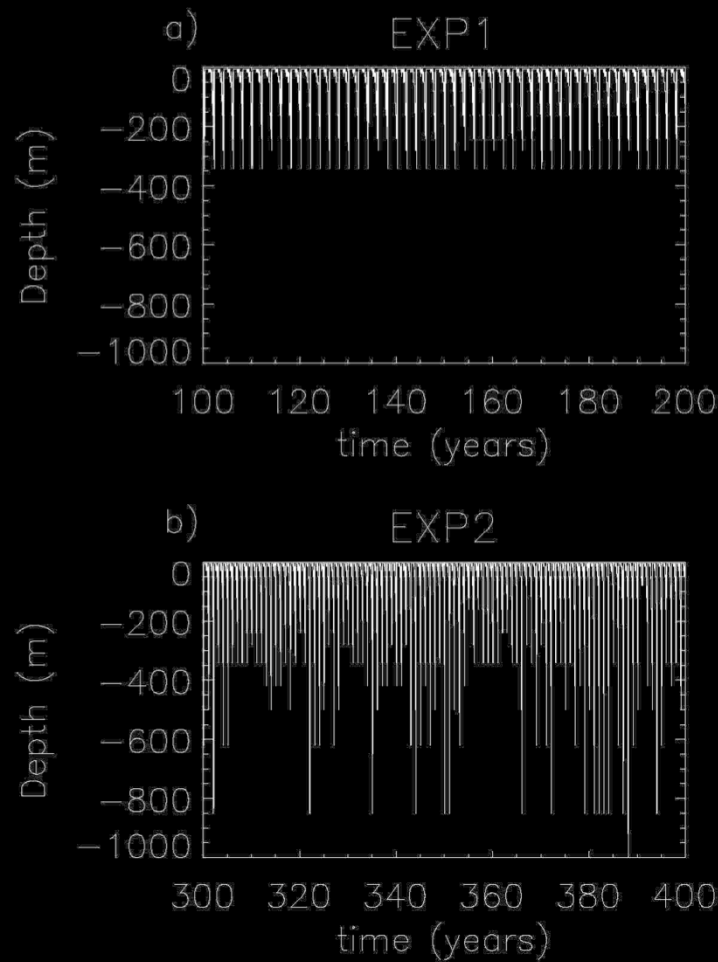
IN THE EASTERN BASIN TWO DIFFERENT REGIMES ARE OBSERVED IN CONNECTION OF THE STRENGTH OF MERIDIONAL OVERTURNING CIRCULATION!



THIS VARIABILITY IS CORRELATED TO SALTY WATER ANOMALIES

IN THE SICILY CHANNEL AND SARDINIA COAST (FROM NUMERICAL SIMULATIONS)





Deep convection in the Gulf of Lyon in the two experiments

The possible explanation of this variability



- the quasi-periodic oscillations in the Eastern Mediterranean sub-basin can be explained by a dynamical response of the ocean flow to a periodic advection of a positive salt anomaly into the convective area which destabilizes the stratification and enhances convection and consequently strong feedback between the convective activity and strength of the EMTHC;
- for the Western Mediterranean sub-basin the features seems coherent with a non-dynamical response of the circulation to the convective processes (local switched “on” or “off” process)



Thanks for your attention !!



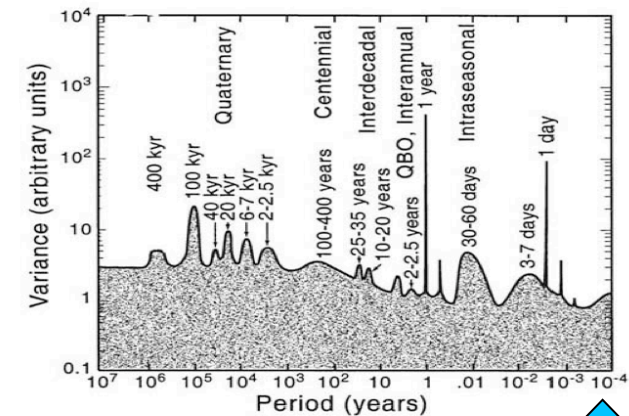
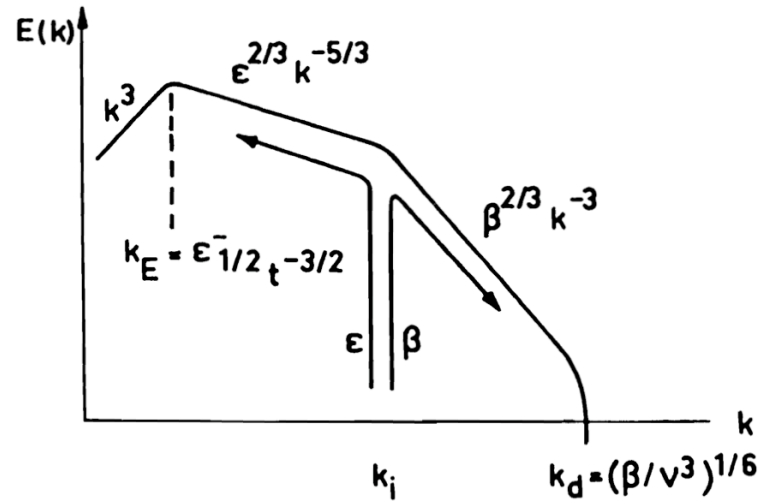


Figure VIII–3: schematic double cascading spectrum of forced two-dimensional turbulence (from Lesieur, 1983)

From 2nd order Lagrangian Stochastic Model (LSM)



$$\frac{du}{dt} = a - \frac{u}{T_v},$$

(Sawford, 1991
Berloff 2003)



$$T_v = \frac{T_L + \sqrt{T_L^2 - 4 \frac{\sigma_U^2}{\sigma_A^2}}}{2}, \quad T_a = \frac{T_L - \sqrt{T_L^2 - 4 \frac{\sigma_U^2}{\sigma_A^2}}}{2}$$

$$\frac{da}{dt} = -\frac{a}{T_a} + K_2 \cdot \frac{dw}{dt}$$

$$T_L = T_v \cdot \left(1 + \frac{T_a}{T_v}\right), \quad \frac{1}{T_a \cdot T_v} = \frac{\sigma_A^2}{\sigma_U^2}$$

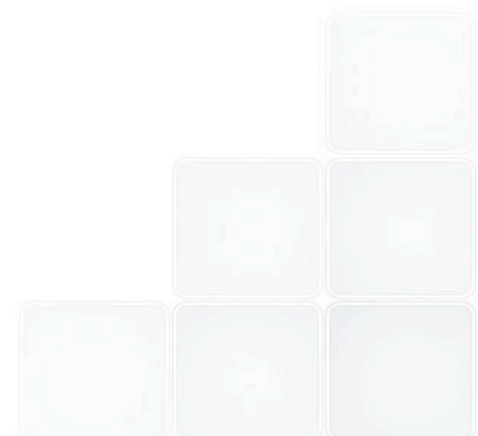
When $T_L^2 < 4 \frac{\sigma_U^2}{\sigma_A^2}$ $T_v, T_a = a \pm ib \in C$ (equivalent to a 2D 1st order LSM,
Reynolds 2002)

For each trajectory we compute T_v, T_a and

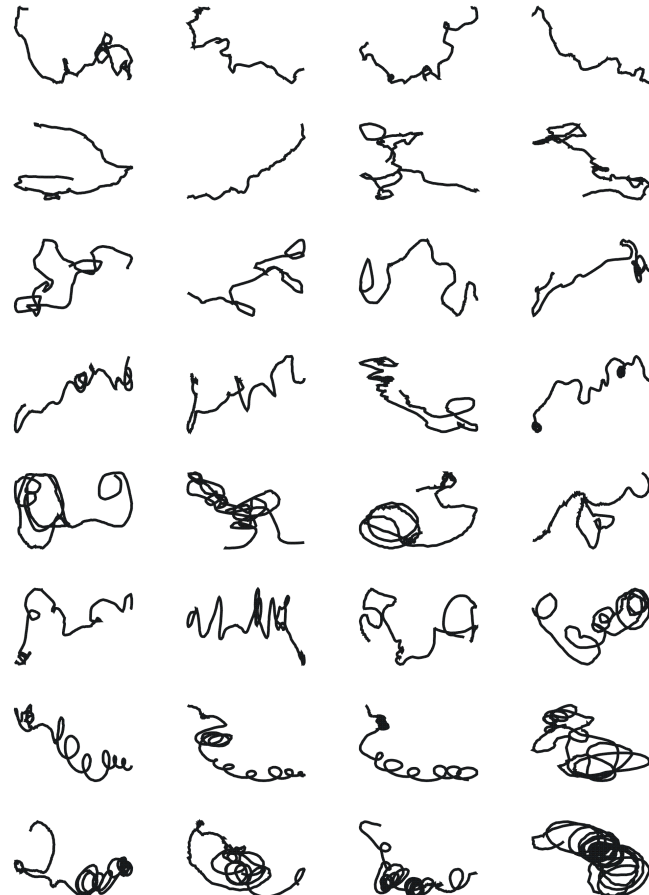
$$y = \frac{T_a}{T_v} \quad \text{when} \quad T_v, T_a \in R$$

$$x = \frac{b}{a} \quad \text{when} \quad T_v, T_a \in C \quad (|y| = 1)$$

For $T_a \rightarrow 0$, the model collapses to a 1st order model



class I $0 < y < 0.2$



class II $0.4 < y < 0.8$

class III $|y|=1, x < 1$ c.c.

class IV $|y|=1, x > 1$ cc '(stable rotation)'

Different weight of classes
In the different datasets



(<http://clima.casaccia.enea.it/staff/rupolo/trajectorybook.html>)

	Class I $y < 0.2$	Class II $0.4 < y < 0.8$	Class III $ y =1, x < 1$	Class IV $ y =1, x > 1$
AF	327, 34%	63, 7%	246, 26%	194, 20%
AD	1922, 80%	89, 4%	147, 6%	26, 1%
PD	5838, 86%	165, 2%	219, 3%	49, < 1%

$$\omega = \frac{\partial v}{\partial x} - \frac{\partial u}{\partial y}$$

$$OW = s_n^2 + s_s^2 - \omega^2$$

$$s_n = \frac{\partial u}{\partial x} - \frac{\partial v}{\partial y}$$

$$s_s = \frac{\partial v}{\partial x} + \frac{\partial u}{\partial y}$$

$$\lambda(\vec{x}, t_0, \delta_0 \delta_f) = \frac{1}{\tau} \ln \left(\frac{\delta_f}{\delta_0} \right)$$

$$\text{cm}^2/\text{sec}^2$$

$$\lambda(\vec{x}, t_0, \delta_0 \delta_f) = \frac{1}{\tau} \ln \left(\frac{\delta_f}{\delta_0} \right)$$

